UNIVERSITY OF CALIFORNIA, MERCED

CELL TYPE-SPECIFIC RNA METABOLISM IN THE *DROSOPHILA* NERVOUS SYSTEM

A DISSERTATION
SUBMITTED TO THE SCHOOOL OF NATURAL SCIENCES
AND THE DIVISION OF GRADUATE STUDIES
OF UNIVERSITY OF CALIFORNIA, MERCED
IN PARTIAL FULFILLMENT OF THE REQUIRMENTS
FOR THE DEGREE OF
DOCTOR OF PHILOSOPHY

by

Mohamed Aboukilila
August 2021

I certify that I have read this dissertation and that, in my opinion, it is fully adequate in scope and quality as a dissertation for the degree of Doctor of Philosophy

_____

(Professor Michael Cleary) Principal Advisor

I certify that I have read this dissertation and that, in my opinion, it is fully adequate in scope and quality as a dissertation for the degree of Doctor of Philosophy

_____

(Professor Aaron Hernday) Committee Chair

I certify that I have read this dissertation and that, in my opinion, it is fully adequate in scope and quality as a dissertation for the degree of Doctor of Philosophy

_____

(Professor Stefan Materna)

Approved for the University of California, Merced Graduate Studies

_____

To Amanda, the Queen of kindness & caring.

Knowledge without action is wastefulness,
and action without knowledge is foolishness.

-Imam Al-Ghazālī

Acknowledgments

I would like to acknowledge the support of my family, friends, colleagues, collaborators, and UC Merced for their continuous support during my PhD journey. First and foremost, I want to sincerely thank my advisor, Professor Michael Cleary. In addition to being the most amazing scientific advisor whose passion for science & style of sharing knowledge with others have shown me the beauty of scientific quest and the strength it brings to us and the generations to come, his genuine personal care & support throughout the turbulent events that took place during my PhD are probably the single most important reason why this work has seen the light of fruition. For that, I shall always be in gratitude to him. I would also like to thank the past & current members of my committee (Prof. Aaron Hernday, Prof. Stefan Materna, Prof. Ramendra Saha, and Prof. Laura Beaster-Jones). To Naoki Hida, Dana Burow, Jade Fee, Josephine Sami, and Rhondene Wint, thank you all from the depth of my heart for giving me the best Merced family anyone could have asked for, both inside and outside the lab. Immense thanks are also due to Professor Robert Spitale and his research group at UC Irvine for their major contributions in both of my research papers. Also, many thanks to the UC Merced Graduate Division and the QSB Graduate Group for their generous support during my graduate career through training grants, fellowships, and travel funds. I would like to send special thanks to Paul Roberts and Jan Zarate for their unwavering support during those last two years.

My special gratitude & thanks to my amazing family. To my mother, the strength of character and sense of commitment you have brought into the lives of me & my siblings have taught us that giving up is never an option. To my dad, your sense of humor is a constant reminder that the best remedy to life's unexpected curveballs is a sincere laugh mixed with a "*kilo*" of love. To my brother, Hossam, and my sister, Nora, the warmth you and your families bring to my heart is a source of renewable hope & strength. Most importantly, to Amanda, my Queen and soulmate, even in your physical absence, you continue to be the driving force of everything that is beautiful & valuable in my life. Your character & your heart are the North Star that my compass always seeks. Till I get to embrace you again, I shall always be true to my promise to you: to be *sincerely* kind & caring and to *always go the extra mile!*

MOHAMED Y. ABOUKILILA

5200 N Lake Rd, SE1, Suite 325, Merced, CA 95343
Telephone: +1 (646) 464 - 7099
Email: mohamed.aboukilila@gmail.com

EDUCATION

2012 – Present — ***Doctor of Philosophy (Ph.D.)*** **Quantitative & Systems Biology**
THE UNIVERSITY OF CALIFORNIA, MERCED

2000 – 2007 — ***Doctor of Medicine (M.D.)***
FACULTY OF MEDICINE, ALEXANDRIA UNIVERSITY

Summer 2006 — ***Summer Medical School,*** **Department of Pulmonology**
UNIVERSITY MEDICAL CENTER OF UTRECHT, THE NETHERLANDS

RESEARCH & TEACHING EXPERIENCE

2012 – Present — **Doctoral Graduate Researcher**, LAB OF DR. MICHAEL CLEARY
QUANTITATIVE AND SYSTEMS BIOLOGY GROUP, UC MERCED
Ph.D. Dissertation: *Cell type-specific RNA metabolism in the Drosophila nervous system*
Helped develop a novel tissue-specific RNA tagging assay (5EC-tagging) using microarrays and RNA-seq to study mRNA synthesis & decay kinetics *in vivo*. Developed a novel next generation sequencing-based approach using 5EC-tagging to model global RNA synthetic & decay kinetics *in vivo*. Lab and project management experience, including launching collaborations and advising junior researchers.

2012 – 2018 — **Teaching Assistant,** BIOLOGICAL SCIENCES, UC MERCED

- BIO 110: The Cell (Prof. Kitazawa & Garcia-Ojeda)
- BIO 170: Advanced Neurobiology (Prof. Michael Cleary)
- BIO 150: Embryos, Genes & Development (Prof. Michael Cleary)

PUBLICATIONS

Fee J, **Aboukilila M**, Cleary M. **(2021)**. Progenitor-derived ribosomal RNA supports protein synthesis in *Drosophila* neurons. July 02, 2021. (***Under Review)***
Preprint available at DOI: 10.22541/au.162523356.62057193/v1

Aboukilila MY, Sami JD, Wang J, England W, Spitale RC, Cleary MD. (**2020**). Identification of novel regulators of dendrite arborization using cell type-specific RNA metabolic labeling. ***PLOS ONE.*** Dec 15(12):e0240386.
doi: 10.1371/journal.pone.0240386

Aboukilila MY*, Hida N*, Burow DA, Paul R, Greenberg MM, Fazio M, Beasley S, Spitale RC, Cleary MD. (**2017**). EC-tagging allows cell type-specific RNA analysis. ***Nucleic Acids Research***. Sep 6;45(15):e138. doi: 10.1093/nar/gkx551 ***co-first authors**

PRESENTATIONS

2018 **Aboukilila M.** & Cleary M. EC-tagging allows cell type-specific RNA analysis. ***QSB Retreat***. Merced, CA, United States (oral presentation)

2017 **Aboukilila M.**, Hida N., Paul R., Greenberg M., & Cleary M. Robust Cell Type-Specific RNA Identification by EC-tagging***. 58th Annual Drosophila Research Conference.*** San Diego, CA, United States (poster presentation)

2014 **Aboukilila M.**, True M., & Cleary M. Expression and function of the mRNA decay factor Smaug during *Drosophila* mushroom body development. ***FASEB, "Post-transcriptional control of gene expression: Mechanisms of mRNA decay"***. Big Sky, MT, United States (poster presentation)

FELLOWSHIPS & AWARDS

2019 Graduate Dean's Dissertation Fellowship, UC Merced
2014 & 2015 & 2017 Summer Research Fellowship, QSB Graduate Group, UC Merced
2014 NSF Travel Award, FASEB Conference
2014 Summer Travel Award, QSB Graduate Group, UC Merced

COMPUTER SKILLS

Operating Systems **UNIX, Windows, Mac**

Languages **R, Python**

Other tools **Galaxy, Seurat, GraphPad Prism, Image J, VectorNTI, SnapGene, Tuxedo Suite, Rsubread, edgeR, DESeq, LaTex, Microsoft Office**

LEADERSHIP ACTIVITIES

2014 – 2016 **Graduate Student Representative**
QSB Educational Policy Committee, UC Merced

Summary of Dissertation

Hight-throughput technologies of functional genomics have revolutionized the dissection of gene expression regulation during development & pathology. However, most of the available genome-wide approaches have traditionally been focusing on the steady-state snapshot of gene expression, which overlooks the dynamic complexity of gene expression regulation that is achieved via different layers of post-transcriptional regulation. Through a set of overlapping processes, post-transcriptional regulation of gene expression achieves an essential spatiotemporal control of protein abundance & functionality, not only through synthesis, but also through localization & decay. The structural & functional architecture of the *Drosophila* central & peripheral nervous systems provide a unique opportunity to model the events & processes of post-transcriptional regulation. While candidate-based studies have revealed important mechanisms of post-transcriptional regulation of gene expression via RNA processing, localization and decay, a more global genome-wide view of such events is still scarce. This is mostly due to the lack of availability of techniques that allows in vivo isolation of cell type-specific RNA for downstream analysis in combination with other approaches addressing the different aspects of post-transcriptional regulation. A method that has been employed to address some of those limitations over the past two decades is called TU-tagging. This method depends on the metabolic tagging of nascent transcripts by a uridine analogue in a cell type-specific manner by exposing UPRT-expressing-cell(s) of interest to 4-thiouracil (4TU). TU-tagging suffers from major specificity limitations due to endogenous pathways of 4-thiouracil (4TU) incorporation. We developed an alternative method, named EC-tagging, to overcome such limitations, which yielded more robust & highly specific isolation of cell type-specific RNA. The sensitivity and specificity of EC-tagging are demonstrated by obtaining cell type-specific gene expression data from intact *Drosophila* larvae, including transcriptome data from a small population of central brain neurons. This has led to the identification of previously uncharacterized *ppk*-expressing neurons in the *Drosophila* mushroom bodies without any need to enrich for such neurons via physical dissection. We also used EC-tagging to profile the transcriptome of the multidendritic (md) sensory neurons of the *Drosophila* peripheral nervous system. Traditionally, it has been a technical challenge to isolate RNA from these neurons without potentially altering gene expression due to their complex morphology and interconnected microenvironments. In addition to the fact that we further confirmed the sensitivity of EC-tagging in purifying cell type-specific RNA, we were able to identify two

genes that encode RNA-binding proteins (RBPs) that play a role in regulating the arborization of dendrites in the multidendritic (md) sensory neurons. Knocking down the poly(A) polymerase Hiiragi and the translation regulator Hephaestus caused significant defects in dendrite arborization. This work provides a technical framework in which combining efficient & specific metabolic tagging of nascent transcripts with high-throughput genomic technologies can be used to profile RNA regulation & metabolism in small subpopulation of cells, including those whose structures render them not amenable to physical isolation.

Contents

List of Tables

List of Figures

Chapter 1

Introduction

The myriad of functions within complex organisms relies on a heterogenous population of highly specialized cells within the many tissues & organs of these organisms. This specialization allows for a more efficient way to respond to overlapping environmental cues in a diverse manner, giving rise to a more adaptive system [1]. Additionally, the dysregulation of many cell type-specific functions & responses is associated with multiple pathologies, especially those related to the nervous system [2], [3]. The normal development & functionality of the multitude of distinct cell types along the spatial and temporal axes require a set of precise cascades of molecular events that are extracted from the information encoded in the organism's genetic code. Such precision, given the vast number of widely variable cellular identities across the same animal, must be dependent on overlapping and interconnected layers of gene expression regulation, especially since all cells possess the same genomic sequence. This is notably important in cells that give rise to different progeny, in terms of identity & function, as a result of asymmetrical and polarized division of the subcellular components & molecular elements among their progeny. A special and extensively studied system with such a quality is the nervous system. Proper development of an organism's nervous system, as a function of the normal proliferation & differentiation of its constituting cells, is crucial for maintaining the animal's homeostatic environment internally as well as externally [4]. Accordingly, dissecting the different events that regulate the development of the highly diverse cellular components of the nervous system represents a unique opportunity of understanding how the different layers of gene expression regulation can yield a plethora of different functions & outcomes.

1.1 *Drosophila melanogaster*: a powerful tool to model neurogenesis and neurodevelopmental disorders

While *Drosophila melanogaster* is widely recognized as an instrumental model organism in studying the molecular and cellular bases of developmental processes of different organs and tissues in metazoan animals, it has particularly become one of the gold-standard model organisms in studying neurogenesis and regulation of the nervous system functionality. This is dependent on the fact that while the fruit

fly's nervous system is a relatively simple one in comparison to more complex metazoan animals, it is still based on a genetic code that is highly conserved across species [5]. This makes it a unique model to study many biological principles that are relevant to human health and disease [6], [7]. Additionally, the genetic and reagent toolkit that is available for the *Drosophila* community is a rather wealthy one that provides multiple experimental approaches to answer a multitude of questions [8].

Neurogenesis in *Drosophila melanogaster*, across all its developmental stages, is a highly choreographed process fulfilling well-characterized spatial patterning and temporal specification axes [9]–[12]. This has laid a strong foundation to study how different molecular events would affect cell fate, identity & function, at the levels of single cells, cell lineages, the organ, and the system [9], [13], [14]. As an example, neural development in the fruit fly takes place in two major waves: the embryonic wave and the larval wave, with a phase of quiescence in-between [15], [16]. The embryonic wave begins with delamination of neural progenitor cells (called "neuroblasts" in the central nervous system or "sensory organ precursor" in the peripheral nervous system) from the neuroectoderm and epidermis. Delamination and acquisition of neural progenitor cell identity depend mainly on Notch signaling interactions between adjacent cells, leading to stem cell-specific expression of pro-neural genes [15]–[17]. Once formed, each neural progenitor cell acquires a specific positional identity along the anterior-posterior, dorsal-ventral and medial-lateral axes. Patterned expression of particular positional genes [18], [19] creates a grid-like system along which each neural progenitor cell is assigned a unique spatial identity. Along with the positional identity, neural progenitor cells also acquire a temporal identity based on the sequential expression of specific transcription factors [20]–[23].

While the embryonic wave of neurogenesis has been the model upon which most cell specification & neuronal circuitry studies have been based historically [24], [25], the larval wave of neurogenesis has provided a lot of insights into how cell lineage is maintained to give rise to specialized and functionally interconnected cell populations [26]–[29]. Regardless of the wave of neurogenesis, neural progenitor cells undergo tightly orchestrated cellular and molecular events that regulate their self-renewal as well as their differentiation into a precise number of different types of neurons and support cells like glia for optimal function [14], [30]–[32]. These differentiated cells are organized into spatially and temporally defined lineages with particular anatomical & functional identities in a process that is dependent on a complicated network of transcriptional switches [15]–[17], [32]–[34]. These

spatial & temporal identities of neural progenitor cells are a fundamental factor in the functional and behavioral repertoire of their progeny, both in the central and the peripheral nervous systems [17], [35], [36]. Such cellular heterogeneity within the nervous system of *Drosophila melanogaster* is increasingly appreciated, especially with the recent advances in applying single-cell sequencing technologies in different *Drosophila* tissues [37]. Supported by an ever-growing set of genetic tools within the fly community [38], [39], this has provided an unprecedented opportunity to investigate the cellular & molecular pathways & networks implicated in the diverse functions and behaviors of the nervous system, both physiologically and pathologically [7], [40]–[48].

1.1.1 Spatiotemporal neurite regulation in *Drosophila* models of nervous system development and diseases

The normal function of a neuron relies on an intricate set of neurites for proper synaptic connections with other neurons and efficient establishment of functional neural circuitry [49]–[54]. Expectedly, neurite dysgenesis represents the main pathophysiological basis of many neurological disorders. For example, axonal degeneration and defects in axonal transport & targeting play major roles in the pathophysiology of nerve injury and neurodegenerative diseases [43], [44], [55], [56]. On the other end, defects in dendrite morphogenesis & synaptic formation have been implicated as being the etiological causes of many neurodevelopmental & neurodegenerative diseases [45], [57]–[61]. Accordingly, dissecting the different cellular & molecular events regulating neurite development in *Drosophila melanogaster* has proven very informative in modeling many human neurological diseases, especially in the context of the *Drosophila* peripheral nervous system and neuromuscular junction [41], [47], [62].

Just as the proneural induction & cell-fate determination phases of neurons undergo tight spatiotemporal regulation, neurites undergo a well-orchestrated developmental program to ensure the preservation of their function, both in space and time, through processes of targeting, extension & pruning [17], [45], [49], [62], [63]. This yields an array of diverse arborization patterns that help determine the type of afferent or efferent input a neuron is capable of processing. Traditionally, studying the molecular mechanisms regulating cell type-specific arborization patterns has largely focused on RNA abundance and relevant transcription factors [17][57][64]–[66]. However, since neurites are relatively distant spatial compartments from the nucleus, transcriptional control may be far upstream of the local

events that regulate outgrowth, branching & pruning of neurites. As a result of that, many research groups have focused their efforts to study the roles of post-transcriptional regulation of gene expression in establishing the local mechanisms necessary to direct neurite development.

1.2 Post-transcriptional regulation of gene expression

The journey of gene expression - starting at the genetic level of DNA and ending with a plethora of functional proteins - requires multiple layers of regulation that would yield a high diversity of cell types and behaviors from a single genome. This would provide the necessary dynamic and tunable flexibility an organism needs to respond to the different extrinsic and intrinsic inputs it receives at any particular point during its development. Many of such regulatory events occur at the level of RNA, both at the transcriptional and posttranscriptional levels, to maintain specified levels of different RNAs at each developmental stage. While high-throughput genomics technologies like microarrays [67], RNA-sequencing [68], and chromatin immunoprecipitation (e.g., ChIP-chip [69]) have established the role of a wide and complex network of *cis*-regulatory elements and transcription factors in regulating different aspects of development in many metazoans, differential transcription alone fails to consider the role of post-transcriptional regulation in determining gene expression levels. Following transcription, RNAs are regulated at multiple points during their lifetime. Such post-transcriptional regulatory steps are critical for certain developmental processes including establishment of body axes [70], [71]. This begins in the nucleus where mRNAs undergo selective capping, polyadenylation, splicing, base modification, sequence editing, and directed transport from the nucleus [72]–[78]. Once exported to the cytoplasm, not all mRNAs will undergo translation, as many are sequestered away from the translation machinery in a non-translating pool [79], [80]. In the cytoplasm, multiple pathways - including RNA decay, microRNAs (miRNAs), RNA interference (RNAi) - have been well-characterized [81], [82]. Additionally, directed localization of RNA in restricted subcellular domains is commonly observed, especially during early embryonic development in metazoans [72] and in situations where rapid response to a localized signal requiring time- and place-specific protein synthesis is needed [83].

While the above-mentioned layers of post-transcriptional regulation are mediated by both RNA-RNA and/or RNA-protein interactions at different sub-cellular compartments, RNA-binding proteins (RBPs), in particular, play a central role in regulating RNA metabolism. RBPs have been extensively reported to play many regulatory aspects of RNA splicing, 5′ and 3′ processing, modification, transport,

localization, translation, and stability [84]–[90]. RBPs, collectively, constitute about >5% of the eukaryotic proteome [91]. In order to perform their regulatory functions, RBPs form ribonucleoprotein (RNP) complexes with single-stranded or double-stranded RNA, either through recognizing a specific sequence and/or structure [92]–[94] or through unconventional binding modes [95]. RBPs possess different domains that allow them to recognize their target transcripts [90]. While RBPs have been extensively associated with regulatory roles via their interaction with mRNAs [88], [96], [97], recent work has demonstrated the importance of interactions between RBPs and various types of non-coding RNA such as microRNAs, small nucleolar RNAs, piRNA, and long-non-coding RNA [98]–[105]. By binding to their targets, RBPs can provide coordinated regulation of sets of functionally related RNAs. Formation of ribonucleoprotein (RNP) complexes act to regulate a wide range of essential cellular functions, through regulating transcription and post-transcriptional gene regulation [85], [106]–[108]. For example, regulated transcripts are often associated with cytoplasmic RNPs that can regulate translation (e.g., stress granules) [109]–[111], degradation [112], or both (e.g., RNA processing (P)-bodies) [80]. It is important to note that RBP-based dysregulation of many RNAs has been implicated in many pathologies such as cardiovascular diseases, neurodegenerative abnormalities, immunological diseases, and cancer [89], [106], [113]–[116]. Given the pivotal importance of RBPs in posttranscriptional regulation, defining and predicting RBP interactions has been a major research focus [117]–[120]. Accordingly, transcriptome-wide RNA target sets have been identified for many RBPs across multiple organisms, which has helped to elucidate RBP roles in numerous regulatory processes [120]–[122].

1.2.1 Post-transcriptional regulation of gene expression during neurogenesis

Polarized cells with high structural & functional diversity like neurons rely heavily on post-transcriptional regulation processes to achieve healthy development. As neurons differentiate and the neuronal circuitry is established, several RNAs undergo many posttranscriptional changes to expand the variety of functional proteins produced [123]–[126]. Being one of the main pathways regulating post-transcriptional gene expression in the nervous system, alternative splicing of pre-mRNAs into an array of different mature mRNAs via the removal of introns and the linking of exons together has been the center of extensive research [127]. Alternative splicing is a tightly regulated process. Alternatively spliced exons and their flanking introns contain short nucleotide sequences called “*cis*-regulatory motifs”.

These motifs are recognized in a sequence-specific manner by a class of RBPs known as "*trans*-regulatory splicing factors". On binding their target *cis*-regulatory motifs, *trans*-regulatory splicing factors either facilitate or inhibit the assembly of the spliceosome on the exon promoting its inclusion or exclusion [123]. Tissue-dependent alternative splicing events are particularly relevant in the context of neurogenesis, synaptic interactions, and the establishment of the neuronal network. They are regulated by distinct classes of nervous system-specific factors that tend to be conserved across metazoan animals [128]–[131]. One of the most interesting & unique examples of how alternative splicing plays a major function in the nervous system is Dscam. In *Drosophila*, Dscam provides a prime example of the generation of thousands of alternative isoforms by splicing. Dscam is a transmembrane protein that regulates neural circuit development mainly through self-avoidance. While heterophilic adhesion between different Dscam1 isoforms allows neuronal interaction, homophilic adhesion of the same isoform promotes repulsion [132]–[134]. The mechanism allowing single cells to express particular Dscam isoforms that are similar or different from their neighboring neurons is thought to be based on a probabilistic manner [135]. Accordingly, different patterns of Dscam protein members lay the foundation for unique neuronal circuits by promoting either adhesion or repulsion [136]–[138].

Another form of post-transcriptional regulation that is prevalent during neural development is the regulation of mRNA stability [139]. Modulation of mRNA stability allows for precise regulation of protein abundance and localization [140], [141]. This is particularly valuable during neural development, where control of mRNA stability and localization have been found to play pivotal roles in cell fate determination and neuron structure [142]–[145]. Fine-tuning of mRNA stability is achieved with spatial & temporal specificity through tissue-specific expression of *trans*-acting RBPs, non-coding RNAs (ncRNAs), and *cis*-acting elements in target mRNAs [145]–[147]. For example, the Hu/ELAV (Hu antigen/embryonic lethal, abnormal vision) family of *trans*-acting RBPs plays essential roles in neuronal development, differentiation, neurogenesis, dendritic maturation, neural plasticity, and synaptic transmission by regulating the processing, localization, stability, and translation of target mRNAs [148]–[150]. This family of RBPs bind to their target transcripts via highly conserved RNA-recognition motifs (RRMs) that preferentially bind to poly(A) or AR-containing regions of target mRNAs. While ELAV RBPs mediate the stability of their target mRNAs in the nervous system by expressing neural-specific 3'UTR isoforms [151], [152], Hu RBPs can either increase the stability of some mRNAs by competing with decay factors such as AU-binding factor 1 (AUF1) or decrease the stability of other mRNAs through a microRNA-dependent pathway [146].

RNA modifications represent an additional layer of spatiotemporal post-transcriptional regulation of gene expression [153]. This field has garnered much attention recently, especially in the context of nervous system development and neurodevelopmental & neuropsychiatric disorders. RNA modifications fine-tune gene expression by regulating multiple steps of mRNA processing such as splicing, export, stability, degradation, and translation [154]. While over 150 distinct RNA modifications have been modified, N^6-methyladenosine (m^6A) is highly enriched in the mammalian nervous system [155], [156]. A method known as methylated RNA immunoprecipitation sequencing (MeRIP-seq) has revealed that m^6A is prevalent in the brain transcriptome, with a special bias towards transcripts of neuronal coding and non-coding genes [155], [157]. Furthermore, the profiles of those m^6A-containing transcripts revealed yet another layer of spatiotemporal regulation of neuronal genes across different brain regions and developmental stages [156], [158]. Mechanistically, m^6A modification has been implicated in splicing, stability, localization, and translation of target mRNAs via recruiting or repelling specific RBPs or through inducing structural changes in target transcripts, which would subsequently modulate the accessibility of RBPs on the transcripts [159]. These regulatory mechanisms serve important physiological functions in the nervous system, including neurodevelopment [158], [160], [161] and synaptic plasticity [162], [163], as well as in addiction [164], [165], neural injury [166], and stress response.

1.2.2 Role of post-transcriptional regulation of gene expression in neurite development

Post-transcriptional regulation processes have proven critical for precise spatiotemporal protein abundance and localization which is crucial for spatial and temporal modulation of neuronal branching and dendrite morphogenesis [167]–[175]. Regulation of mRNA stability was found to play a crucial role in axon guidance [176], synaptic formation [177], plasticity [178], [179], and function [180], [181]. For example, some micro-RNAs were shown to regulate branching morphogenesis. In *C. elegans*, *lin-4* miR and its target mRNA encoding the transcription factor LIN-14 modulate axonal branching, while, in mammals, *miR-9*, *miR-124*, and *miR-16* alter dendritic branching by functioning upstream of signaling pathways such as the MAPK/ERK pathway [182]–[185]. On the other hand, alternative splicing factors, such as Caper and Rbfox1, have been implicated in regulating branching [186], [187]. Caper negatively regulates branching of class IV dendritic arborization neurons in *Drosophila* by directly or indirectly regulating the expression of over 500 genes. Regulation of mRNA translation, especially locally in the axon or the

dendrite, also affects arborization [174], [188], [189]. For example, local protein synthesis within dendrites is required for activity-dependent synaptic refinement and strengthening [170], [171]. In *Drosophila*, the extensively studied translational repressors Nanos (Nos) and Pumilio (Pum) repress the expression of the pro-apoptotic gene *head involution defective* (*hid*) [168], [190]. This helps maintain a balance between outgrowth and retraction of dendrites. In contrast, when Hid is upregulated, non-apoptotic caspase activation leads to dendritic arbor pruning. To achieve its regulatory functions, Nanos needs to be localized to the axon processes & dendrites. This strict spatial expression of the protein is achieved by localizing the *nos* mRNA at such destinations. Indeed, it was found that *nos* mRNA is localized not only in the cell body but also in RNPs distributed along the dendrite and axon processes of *Drosophila* class IV dendritic arborization neurons in a process mediated by recognition of sequences in the 3′ UTR of the transcript. This is achieved through interaction with the dynein machinery and the Rump & Osk RNA-binding proteins [191]. Similar to the *nos* mRNA, an unbiased genome-wide screen identified 55 new candidate transcripts that localize specifically to dendrites of *Drosophila* class IV dendritic arborization neurons [192]. Further validation identified that mRNA of 18 of those genes is transported specifically to dendrites for local translation and regulation of branching.

Other examples of RNA-binding proteins that regulate neurite branching via additional post-transcriptional processes are Imp and YTHDF1. Imp was found to be localized to specific RNPs that move actively via microtubule-dependent transport within axons undergoing remodeling [193]. During larval development and pupal metamorphosis in *Drosophila*, mushroom body axonal branches undergo selective pruning, which, subsequently, regrow to form adult-specific branches. During the regrowth phase of the γ neurites in the *Drosophila* mushroom body (which is important in olfactory learning & memory), Imp selectively associates with the 3′UTR of *chickadee* (*chic*) mRNA which localizes to the growing γ neurites to facilitate the remodeling of axons that have been pruned [72]. On the other hand, YTHDF1 (one of the cytoplasmic readers of N^6-methyladenosine (m^6A)) is required for axonal, dendritic and spine development. One mechanism involves a direct interaction between YTHDF1 and Fmr1 (the *Drosophila* homolog of Fragile X Mental Retardation RNA-binding Protein (FMRP)). This interaction inhibits the translation of key transcripts involved in axonal growth regulation in the larval neuromuscular junctions as well as in the adult mushroom bodies [194]. Another mechanism entails the enrichment of m^6A-containing transcripts and YTHDF1 in RNA granules associated with microtubule plus-end. These granules contain extensive networks of mRNAs organized by autism risk gene

Adenomatous Polyposis Coli (*APC*). Disrupting m^6A signals by knocking down the methyltransferase METTL14 or YTHDF1, or by overexpressing autism or schizophrenia-associated missense mutations in METTL14, reduced expression of APC granules and tubulin, which, in turn, disrupted microtubule assembly and function. This has yielded drastically reduced axonal length & branching, as well as severely disrupted dendritic growth [195].

1.2.3 Role of post-transcriptional regulation of gene expression in neurological diseases and neurite dysgenesis

As detailed above, post-transcriptional regulation of gene expression provides an essential layer of control for the development and function of polarized cells like neurons. This is particularly important for the relatively distant sub-cellular locations (like axon terminals) where translationally silent mRNAs are required to be transported to for local translation activation in order to achieve the necessary physiological structural & functional development. Naturally, dysregulation of RNA and protein synthesis has been described in many neurological disorders.

Abnormal alternative splicing events, for example, have been associated with a growing number of neurological diseases, like autism, schizophrenia, Parkinson's disease, and spino-muscular atrophy (SMA) [196], [197]. In these disorders, splicing defects have been well characterized. For example, in spino-muscular atrophy (SMA), which results from a loss-of-function mutation of the *spinal motor neuron-1* (*SMN1*) gene, the severity of the illness is correlated with exon7 inclusion in the *SMN2* mRNA since this would impact the extent at which the paralog *SMN2* gene could compensate for the loss of *SMN1* gene. Aberrant regulation of mRNA decay is also associated with neurodegenerative and developmental disorders like Alzheimer's disease [198], [199], Amyotrophic Lateral Sclerosis [200], and Fragile-X syndrome [201]. In Alzheimer's disease, misregulation of certain neural microRNAs has been linked to amyloid beta [202]–[204] and tau [205], [206] pathologies. On the other hand, the non-sense mediated decay (NMD) pathway is important in regulating the expression of certain RNA-binding proteins (RBPs) implicated in the pathophysiology of Amyotrophic Lateral Sclerosis [207], [208]. Fragile-X syndrome, which is the most common form of inherited mental retardation, is also rooted in dysregulation of RNA stability [209]. Fragile-X mental retardation protein (FMRP) is a well-studied RNA-binding protein that regulates synaptic localization, translation, and stability of specific mRNAs [210], [211]. Dysregulation of FMRP-directed RNA decay is the main etiology for Fragile-X syndrome [209]. In addition

to their implications in neurological diseases via regulating alternative splicing & RNA stability, RNA-binding proteins provide the etiological bases for many neurological disorders by regulating other aspects of post-transcriptional regulation of gene expression [55], [212], [213]. For example, GLE1, an evolutionarily conserved RNA-binding protein that acts as an mRNA export factor, is mutated in Lethal Congenital Contracture Syndrome 1 (LCCS1) [214]. RNA-binding proteins associated with mRNA localization and local translation have been implicated in spino-muscular atrophy (SMA), Fragile-X syndrome, and Parkinson's disease [215], [216]. Finally, alterations in RNA modifications also influence the progression of several neurologic disorders. The mechanistic underpinning of how some RNA modifications (like m^6A, m^1A, inosine, m^5C, and pseudouridine) and their associated enzymatic machinery regulate different neurological pathologies (including acute brain injuries, nerve damage, chronic neurodegeneration, and neuropsychiatric disorders) is being increasingly evaluated and established (as reviewed in [154], [217], [218]). Similarly, post-transcriptional regulation of gene expression has been found to be the main regulatory step responsible for several neurological disorders that are specifically characterized by neurite dysgenesis. Indeed, inappropriate mRNA regulation and altered rates of protein synthesis have been described in a number of neurological disorders (e.g., Down syndrome, Rett syndrome, Fragile-X syndrome, and phenylketonuria) where neuronal arborization is affected [219]–[221].

As evident, such an intercalating network of post-transcription regulatory steps requires an in-depth understanding, especially since it would aid in the development of therapeutic agents for the associated disorders [55]. Neuronal cells, especially because of their architecture that is based on functionally distinctive spatial compartments that are distant from the nucleus (like axons, dendrites, and synapses), provide such a unique platform to study the mechanistic intricacies of post-transcription regulation. While genome-wide attempts have been made to dissect the different aspects of post-transcriptional regulation in many models, including the nervous system, the approaches used by these studies have not achieved *in vivo* global analyses due to technical limitations.

1.3 Tools to identify distinct cell types through their unique gene expression signature

Tools capable of capturing gene activity changes between different cell types have become a cornerstone in the fields of cellular & developmental biology since they let us understand how gene expression regulation impacts cellular diversity.

While distinct cell types were historically identified based on tools differentiating cellular morphology and expression of specific genes, such tools had many limitations mainly because not all cell types have readily identified endogenous markers. This means that many cell types would be overlooked altogether or, at the very best, a group of unique cellular identities would end up being lumped together under one cell type due to the low resolution of such methods. To overcome this main constraint, high-throughput gene expression and functional genomics technologies, like microarrays, RNA-sequencing (RNA-seq), and chromatin immunoprecipitation (e.g., ChIP-chip and ChIP-seq), have become the gold standard in establishing an ever-growing network of gene expression regulatory elements that would ultimately give rise to molecular signatures that are highly specific to each cell type with a high resolution.

Concluded with mRNA translation and protein assembly & modifications that would yield particular functions in the right place and at the right time, gene expression regulation is carried out at multiple points that start with gene activation & transcription and passes through different events of post-transcriptional regulatory steps. These various layers of regulation have been shown to play major roles in organismal development, cellular processes & functions, as well as many pathological conditions. Different cell type-specific tools have been employed to measure gene expression at each one of these points. These tools, which differ on the specific gene regulatory step they report on, can be employed either separately or in combination, to further deepen our understanding of the molecular mechanisms that multicellular organisms utilize to adapt to changing environments. For example, different methods exist to profile and quantify nuclear RNAs, non-coding RNAs, ribosome-bound mRNAs, or global mRNAs. There are also multiple tools to profile different chromatin states or binding of different regulatory proteins such as transcription factors and RNA-binding proteins (RBPs) to the genome or the different molecules of the transcriptome, respectively [222]. This level of detailed information, particularly if gathered under *in vivo* conditions, should provide for a more robust and refined quantitative systems-level understanding of how cell type-specific gene expression regulation works, both physiologically & pathologically.

Since the main distinguishing feature of any method used to study cell type-specific gene expression is how a particular cell(s) of interest is isolated from within a complex tissue or a whole animal, the choice of any particular approach(es) during experimental design depends on a number of factors: (1) the biological question(s) being addressed by the experiment, which will dictate the choice of an appropriate control(s) as well as the particular stage of gene expression to be

profiled; (2) the different limitations of the biological material to be collected (for example, usage of a model organism versus human tissue, abundance of isolated material from cell(s) of interest, and ease of chemical and/or physical manipulation of cell(s) of interest); and (3) availability of the necessary equipment & resources to achieve robust profiling of gene expression from the collected material.

1.3.1 Labeling of cell(s) of interest for purification of cell type-specific material

To facilitate extracting a particular cell population(s) from within a tissue or a whole organism for subsequent isolation of cell type-specific features for gene expression analysis, the initial step entails labeling the cell type(s) of interest with high specificity and sensitivity. Regardless of the intended target of the isolation procedure (e.g., whole cells, nuclei or specific protein complexes) or the specific feature to be profiled (e.g., DNA, RNA or protein moieties), there are currently two main approaches used to label the targeted cell type(s): (1) expressing a transgene encoding a protein that would, in turn, aid in cell type-specific imaging techniques, physical separation of cell(s) of interest or biochemical tagging of a particular feature(s) within such cell(s) [222], [223]; or (2) labeling of endogenous cell type-specific markers.

Generally speaking, in order to make use of transgene-based approaches, genome editing tools (with organism-dependent varying degree of efficiency) are used to integrate specific transgenes into the genome of model organisms. Subsequently, such transgenes are expressed in a cell type-specific manner using a binary system such as the Gal4/UAS or the Cre/Lox systems [224]–[230]. In short, a transcription factor (like Gal4) would be encoded using one transgene under the control of a tissue or cell type-specific promoter. The transcription factor, in turn, would activate the expression of another transgene (the gene of interest) by binding to a specific binding site (like the UAS in case of the Gal4/UAS system [231]). Alternatively, more recent genome-editing technologies, such as CRISPR/Cas9 and TALENs, allow for direct cell type-specific expression of specific labeling proteins without the need for any binary systems [232], [233]. In addition to overcoming the limitation of possibly producing some undesired phenotypes that could be associated with the expression of some transgenes, the approaches relying on labeling of endogenous markers, like immunolabeling against endogenous proteins for example, are usually more practical for human tissues & other organisms whose genomes are not as tractable. That said, such approaches have their own

limitations, mainly that not every single cell type has a readily identified endogenous maker(s) as well as the fact that many of the processing steps associated with these techniques can render certain analyses very difficult (e.g., RNA analysis using immunostaining approaches could be unfeasible due to degradation of RNA molecules).

1.3.2 Importance of isolating cell type-specific RNA for gene expression analysis

Transcriptome profiling provides valuable information about the identity, function, and state of a particular cell type(s). Unlike the static view that whole-genome profiling provides, examination of the transcriptome allows assessment of dynamic changes in gene expression in response to various stimuli [234]. Different active signaling pathways, metabolic functions, and other cellular processes can be inferred from the analysis of a cell's transcriptome. Additionally, transcriptomic analysis permits identification of unique transcripts such as rare transcripts, alternative splicing variants, fusion genes, and single-nucleotide polymorphisms (SNPs) [235]. Moreover, since a full transcriptome profile should include data on all coding and non-coding RNAs, incorporating such data in an integrative analysis with chromatin landscape and *cis*-regulatory elements should reveal how gene expression regulation takes place through overlapping layers to define distinct functional & developmental profiles of different cell types [236]–[241]. Accordingly, coupling cell type-specific RNA purification and high-throughput transcriptome profiling has become an essential item in any biologist's toolbox.

1.3.3 Methods of isolation of cell type-specific RNA

With multiple methods being available for cell type-specific RNA isolation, each method comes with its own set of strengths and weaknesses that will, in turn, affect the type of collected information. There are two main categories under which cell type-specific RNA purification tools can be grouped: (1) tools based on physical isolation; and (2) tools based on biochemical tagging. Physical isolation can be performed at different levels: whole cells, nuclei, or other specific subcellular compartments. As stated above, the choice of any particular physical isolation approach mainly depends on the question(s) being addressed by the experiment in addition to the availability of experimental resources. For example, whole-cell physical isolation approaches are useful to collect an averaged overview of a cell's

steady-state RNA profile given the fact different transcripts localize to different parts of the cell. On the other hand, analysis of RNA isolated from the nucleus provides a more robust understanding of transcriptional activity of individual genes, especially since it is more biased towards measuring newly synthesized transcripts. Physical isolation can also be used to profile RNA in specific cellular compartments like dendrites, growth cones and other subcellular domains. Physical isolation of cells for subsequent whole-cell RNA analysis is typically performed through fluorescence-activated capture cell sorting (FACS) [245], [246], or laser-capture microdissection (LCM) [247], [248]. Similar approaches are utilized for physical isolation of nuclei like INTACT [249], [250] and fluorescence-activated nuclear sorting (FNAS) [251]. Each one of these approaches has its own advantages and disadvantages, which must be considered in order to choose the most relevant transcriptomic analysis for the question at hand [222]. While physical isolation-based transcriptomic profiling has established a valuable level of insight into gene expression regulation in complex biological systems, especially since they can capture both coding and noncoding RNAs, such tools possess some major drawbacks that limit their utility and the quality of data & inferences derived from the experiments based on them. The main concern associated with physical isolation approaches is the fact that abandoning sample integrity and removing cells from their physiological microenvironment could induce changes in normal gene expression regulation [223], [252], [253]. Additionally, isolation of unwanted cell types, contamination by non-specific RNA from lysed cells, low amount of starting material due to increased sample loss, and the need for specialized equipment are among the big technical limitations of physical isolation methods [222], [254], [255].

Accordingly, the alternative strategy of purifying cell type-specific RNA using tools that rely on biochemical tagging & capture has become favorable in certain experimental designs. Contrary to physical isolation-based methods, biochemical tagging tools provide the advantage of allowing for efficient isolation of cell type-specific material from small population(s) of cells under *in vivo* conditions with a relatively high yield. With a constantly growing repertoire of methods that rely on biochemical tagging to capture cell type-specific RNA, choosing the right method to answer the biological question at hand becomes critical, especially since each method comes with its own set of strengths & weaknesses. For example, two methods, named Tandem Ribosome Affinity Purification (TRAP) and RiboTag, utilize tagged ribosomal proteins expressed in a cell type of interest mainly to capture mRNAs undergoing translation [256], [257]. A major disadvantage of both of these methods is how they fail to purify non-coding RNAs, whose functions are becoming increasingly appreciated in development and disease. Another method that makes

use of biochemical tagging is poly(A)-binding protein tagging [258]. In this method, a FLAG-tagged PAB1 is expressed in the cell type(s) of interest, followed by cross-linking the sample and affinity purifying FLAG-PAB1 with FLAG antibody. While this method possesses a slight advantage over TRAP & RiboTag since it allows for the isolation of some non-coding RNAs that contain poly(A) tails, it still fails to isolate most of the non-coding pool of RNAs. To partially circumvent this issue, another biochemical tagging technique, named miRAP, was established to isolate cell type-specific micro-RNAs [259]. Even though this technique provides insight into how micro-RNAs regulate different physiological & pathological processes in a cell type-specific manner, its repertoire of isolated non-coding RNAs is still limited. Additionally, since all the above-mentioned four biochemical tagging-based techniques rely on purifying RNAs from cell lysate mixtures, they are susceptible to post-lysis re-association of RNA complexes [260], [261], which could lead to false interpretation that some RNAs are associated with the cell(s) of interest when, in fact, they are not. Furthermore, none of the biochemical tagging-based techniques described above reports on nascent RNAs, and, accordingly, they fail to address RNA expression dynamics. While some bioinformatics pipelines have been established to gain some insight into RNA kinetics from data derived from steady-state RNA expression [262], they lack the depth and resolution provided by techniques that focus on nascent RNAs. To address this gap in information that is collected from total RNA tagging methods, biochemical tagging approaches that would allow for physical isolation-free cell type-specific enrichment of nascent transcripts under *in vivo* conditions were needed.

The answer to such a quest was found in biosynthetic RNA metabolic labeling methods. In addition to covering the above-mentioned weaknesses, biosynthetic RNA metabolic labeling approaches also provide temporal control, which allows us to study RNA metabolism at specific developmental windows. The road to cell type-specific RNA metabolic labeling was paved by the usage of modified nucleotide analogues (e.g., 4-thio-uridine (4SU), 5-Bromo-uridine (5BrU), and 5-ethynyl-uridine (5EU)) to isolate nascent transcripts in a non-cell type-specific manner. These analogues provided the means to study RNA transcription & decay kinetics [263], especially in the context of global cellular response to stimuli, stress and signaling. To achieve cell type-specific RNA metabolic labeling, some key elements need to be present: (1) an enzyme that is capable of metabolizing a non-toxic inert metabolic intermediate (usually an inert nucleoside analogue) into a non-toxic active metabolic intermediate (usually a nucleotide analogue) that can be incorporated into the nascent RNA; (2) a tool to achieve cell type-specific expression of such an enzyme (usually achieved through genetically encoded pairs of *trans*

and *cis*-acting elements); (3) the means to expose the animal or tissue that include the cell(s) of interest to the inert metabolic intermediate; and (4) an optimized chemical toolkit to enrich for the tagged RNAs. The first widely used technique that fulfilled such elements was TU-tagging [264]. In TU-tagging, 4-thio-uracil (4TU) is metabolized into 4-thio-uridine (4SU) through the activity of a uracil salvage enzyme from *Toxoplasma gondii* called uracil phosphoribosyltransferase (*Tg*UPRT). The cell type-specificity of TU-tagging can be achieved by expressing *Tg*UPRT in a cell type-specific manner while exposing the cells of interest to non-toxic concentrations of 4-thio-uracil (4TU). While TU-tagging has proven useful in studying cell type-specific gene expression in many systems [265]–[271], its specificity is limited due to detectable non-specific RNA labeling with 4-thio-uracil (4TU) by UPRT-independent pathways (e.g., uracil can be converted to uridine monophosphate by orotate phosphoribosyltransferase as a part of de novo pyrimidine synthesis or through the sequential activity of uridine phosphorylase and uridine kinase) [223]. Additionally, endogenous UPRT activity has been identified in certain species, which further reduces the specificity of TU-tagging. For example, in *Drosophila*, a UPRT homolog, named Krisha, was identified [272]. The resulting background labeling of RNA with TU-tagging usually necessitates tissue dissection following exposure to 4-thio-uracil (4TU) to improve the signal to noise ratio [223].

1.4 Objective of the study

As described above, dissecting the different layers of post-transcriptional regulation of gene expression is of great importance in order to identify more factors that can be used to establish new biomarkers as well as possible therapeutic targets for the diseases caused by dysregulation of such regulatory steps. The *Drosophila* nervous system, with particular attention to spatial domains like dendrites and axon terminals, provides a unique model to study the role of post-transcriptional regulation in processes that are highly dependent on RNA processing & metabolism, like neuronal arborization. For example, dendritic arborization (da) neurons in the *Drosophila* peripheral nervous system (PNS) have been recently used in several studies as a model for studying dendritic morphogenesis. A specific subset of such neurons, *Drosophila* class IV da neurons, possess specific functions in nociception and light avoidance [273], [274]. These functions are achieved through a characteristic tree of dendritic arbors that cover most of the larval epidermis following a tightly regulated spatial pattern [29]. Such characteristics provide an excellent platform to study the different molecular mechanisms regulating the structural & functional development of those neurons and their neurites, including those

involved in post-transcriptional regulation. While many attempts have been made to study the role of post-transcriptional gene regulation in dendritic morphogenesis, the approaches used by these studies have not achieved global analyses since they mainly relied on target-specific approaches using RNAi [275], [276]. At a more global genome-wide level, isolating cell type-specific RNA from the *Drosophila* peripheral nervous system (PNS) has always proven technically challenging. Traditionally, it was done using physical isolation methods like laser capture microdissection [277] and fluorescence-based cell sorting techniques [278], whose limitations were discussed in some detail above. While biosynthetic RNA labeling methods (like TU-tagging) could be used for the same purpose, the available methods have disadvantages mainly related to their specificity, sensitivity, and the quality & type of RNA analysis they could allow [272], [279]. Hence, my project aims to establish a novel & robust method of *in vivo* cell type-specific RNA metabolic labeling that would overcome the issue of non-specific background RNA labeling and to apply this method in profiling the transcriptome of the *Drosophila* peripheral nervous system (PNS), which would, in turn, provide the necessary foundation for dissecting the different mechanistic events of post-transcriptional regulation in the peripheral nervous system (PNS). The specific aims of this project are:

Aim 1: Establish a new *in vivo* biosynthetic RNA labeling technique that allows cell type-specific RNA analyses with high sensitivity and specificity in *Drosophila*

Aim 2: Profile & characterize the transcriptome of the *Drosophila* peripheral nervous system (PNS) using physical isolation-free approach

Chapter 2

EC-tagging allows cell type-specific RNA analysis

** The following has been reproduced from the following publication in Nucleic Acids Research: **Aboukilila M. Y.***, Hida N.*, Burow D. A., Paul R., Greenberg M. M., Fazio M., Beasley S., Spitale R. C., and Cleary M. D. (2017). EC-tagging allows cell type-specific RNA analysis. ***Nucleic Acids Research***. Sep 6;45(15):e138. doi: 10.1093/nar/gkx551 (*co-first authors) [280]

2.1 Abstract

Purification of cell type specific RNAs remains a significant challenge. One solution involves biosynthetic tagging of target RNAs. RNA tagging via incorporation of 4-thiouracil (4TU) in cells expressing transgenic uracil phosphoribosyltransferase (UPRT), a method known as TU-tagging, has been used in multiple systems but can have limited specificity due to endogenous pathways of 4-thiouracil (4TU) incorporation. In this chapter, an alternative method is described which requires the activity of two enzymes: cytosine deaminase (CD) and UPRT. The sequential activity of these enzymes converts 5-ethynylcytosine (5EC) to 5-ethynyluridine monophosphate that is subsequently incorporated into nascent RNAs. The ethynyl group allows efficient detection and purification of tagged RNAs. The data supports that “EC-tagging” occurs in tissue culture cells and *Drosophila* engineered to express CD and UPRT. Additional control can be achieved through a split-CD approach in which functional CD is reconstituted from independently expressed fragments. The sensitivity and specificity of EC-tagging are demonstrated by obtaining cell type-specific gene expression data from intact *Drosophila* larvae, including transcriptome data from a small population of central brain neurons. EC-tagging provides several advantages over existing techniques and should be broadly useful for investigating the role of differential RNA expression in cell identity, physiology, and pathology.

2.2 Introduction

Cell type-specific transcription is an essential determinant of cell fate and function. While techniques that quantify mRNAs (RNA-seq, microarrays) allow

investigation of gene expression, the quality and type of information obtained may be limited by the method of RNA purification. Ideally, cell type-specific RNA should be obtained under *in vivo* conditions, with no physical alteration of tissues. Additionally, analysis of newly transcribed mRNA is often more informative than analysis of bulk mRNA: newly transcribed mRNA can be used to determine synthesis and decay rates [281], [282] and reveal rare transcripts [282]. Techniques for obtaining cell type-specific mRNA generally fall into two categories: physical isolation or tagging and capture of RNAs [222]. Methods of physical isolation (fluorescence-activated cell sorting [277], laser-capture microdissection [278], INTACT [250]) disrupt the cell's environment and may affect mRNA transcription or decay. Methods of RNA tagging and capture often use mRNA-binding proteins that allow purification of bulk poly(A) mRNAs [283] or translating mRNAs [284], but do not enrich for newly transcribed mRNAs and miss noncoding RNAs [222].

TU-tagging is a cell type-specific RNA tagging method that allows analysis of newly transcribed RNAs [264], [285] and has the potential to purify noncoding RNAs [286]. TU-tagging relies on cell type-specific expression of uracil phosphoribosyltransferase (UPRT) to convert a modified uracil, 4-thiouracil (4TU), into 4-thiouridine monophosphate that is subsequently incorporated into nascent RNAs. TU-tagging has been used to study cell type-specific gene expression in *Drosophila* [265], [266], zebrafish [267], [268], mammalian tissue culture cells [269], and mice [270], [271]. TU-tagging has also been used to measure cell type-specific mRNA decay in *Drosophila* embryos [126]. While this technique has proven useful in many systems, the specificity of TU-tagging is limited in some cases. UPRT activity is primarily found in bacteria, fungi and protozoans but metazoan cells may salvage uracil via alternative pathways (potentially through the sequential activity of uridine phosphorylase and uridine kinase) [279] and an endogenous UPRT was recently identified in *Drosophila* [272]. Another limitation of TU-tagging is the relative inefficiency of RNA purification based on disulfide bond formation, although optimized methods have been described [287]. In contrast to thiol-containing nucleosides, other orthogonal handles may be more robust for RNA enrichment [288], [289]. The need for novel approaches for cell type-specific biosynthetic RNA tagging necessitates expanding the chemical toolkit and manipulating alternative metabolic pathways, all while achieving stringent cell type-specificity.

The cytosine deaminase (CD) enzyme is unique to bacteria and yeast: animals lack cytosine deaminase activity [290]. Cytosine deaminase converts the ribonucleobase cytosine into uracil and the combined activity of CD and UPRT results in conversion of cytosine into uridine monophosphate. The CD-UPRT pathway has

been used in suicide gene approaches where mammalian cells expressing CD and UPRT convert 5-fluorocytosine (5FC) into the cytotoxic nucleotide 5-fluorouridine monophosphate (5FUdMP) [291]. 5FUdMP toxicity is primarily caused by inhibition of thymidylate synthetase and impaired DNA synthesis, although 5-fluorouridine triphosphate is also incorporated into tRNA and may interfere with tRNA aminoacylation [292]. While 5FUdMP is cytotoxic, the nucleoside 5-ethynyluridine (5EUd) is an RNA polymerase substrate that is generally well-tolerated by cells [293] (toxicity is only observed after prolonged exposure [294]). Additionally, the ethynyl group of 5EUd allows efficient click chemistry-based labeling and purification of RNA [295]. We reasoned that the modified nucleobase 5-ethynylcytosine (5EC) might be useful for RNA tagging: if 5EC is a CD substrate (allowing production of 5-ethynyluracil) and 5-ethynyluracil is a UPRT substrate (allowing production of 5-ethynyluridine monophosphate (5EUdMP), then 5EC could allow cell type-specific RNA tagging via the CD-UPRT pathway. Here, we describe RNA tagging via the combination of 5EC exposure and cell type-specific expression of CD and UPRT. We call this technique “EC-tagging” and demonstrate the specificity and sensitivity of EC-tagging by obtaining cell type-specific transcriptome data from distinct cell populations in *Drosophila*.

2.3 Results

2.3.1 EC-tagging in cell lines

5-ethynylcytosine (5EC) was synthesized and characterized (as described in section 2.5.1 below). The pathway of 5EC conversion to 5EUdMP (5-ethynyluridine monophosphate) by CD and UPRT is summarized in (Figure 2.1A). To test RNA tagging via this pathway, we expressed a CD-UPRT fusion gene (CD:UPRT) in human SH-SY5Y neuroblastoma cells. CD:UPRT expression conferred 5EC dose-dependent RNA tagging and no RNA tagging was detected in cells lacking CD:UPRT (Figure 2.1B and Figure A.1). We also tested CD and UPRT individually or in combination and found that optimal RNA tagging occurs in cells expressing CD and UPRT (Figure 2.1C). No RNA tagging occurred in cells expressing mCherry-UPRT while relatively weak RNA tagging occurred in cells expressing GFP-CD. These results revealed that SH-SY5Y cells can convert the nucleobase 5-ethynyluracil (5EU) produced by CD to 5EUdMP (likely via UPRT-independent pathways [279]) and confirmed that conversion of 5EC to 5EU is a necessary first step in EC-tagging. These results also demonstrated that conversion of 5EU to 5EUdMP is augmented by transgenic UPRT expression.

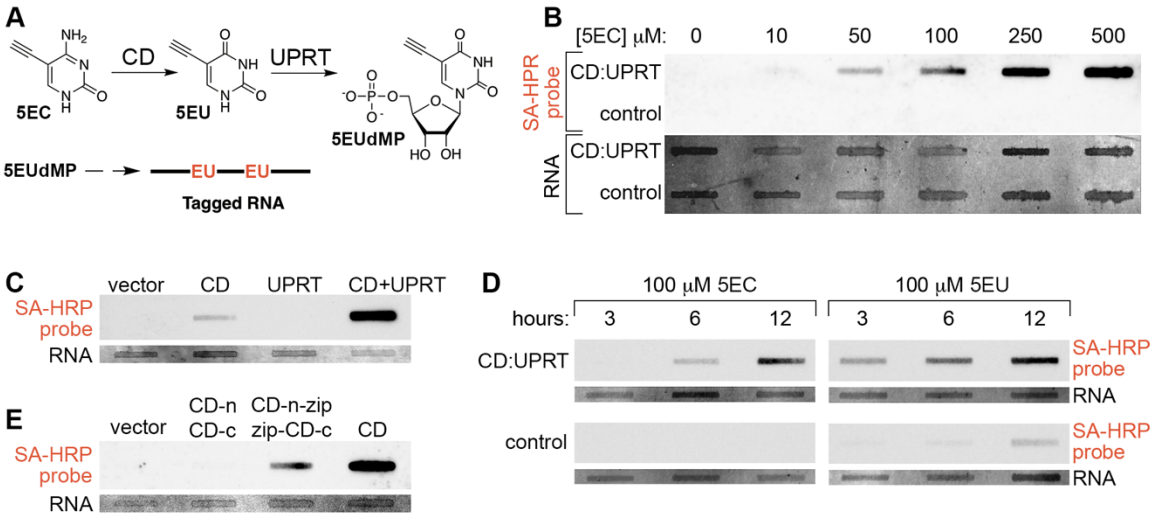

Figure 2.1: RNA tagging via combined CD expression, UPRT expression, and 5EC delivery. (A) Pathway of 5EC conversion to 5EUdMP (5-ethynyluridinemonophosphate). 5EUdMP is phosphorylated by nucleoside kinases to form 5EUdTP (dashed arrow) prior to incorporation into nascent RNA. (B) 5EC dose-dependent RNA tagging. CD:UPRT+ SH-SY5Y cells and control SH-SY5Y cells were exposed to the indicated concentration of 5EC for six hours prior to RNA extraction, biotinylation and slot-blot probing with streptavidin-HRP (SA-HRP). The "RNA" panel shows total RNA based on methylene blue staining and the top "SA-HRP probe" panel shows the streptavidin-HRP signal specific for RNA containing biotinylated 5-ethynyluridine nucleotides. (C) Optimal EC-tagging in cells expressing CD and UPRT. SH-SY5Y cells were transfected with empty vector, a vector expressing CD, a vector expressing UPRT, or a combination of CD and UPRT expressing vectors. Cells were exposed to 500 μM 5EC for six hours. (D) 5EC-tagging versus 5EU-tagging. CD:UPRT+ HeLa cells and control HeLa cells were exposed to 5EC or 5EU for the indicated time. (E) RNA tagging via "split CD". UPRT(+) SH-SY5Y cells were transfected with empty vector, vectors expressing N-terminal and C-terminal CD fragments lacking leucine zipper domains (CD-n, CD-c), vectors expressing N-terminal and C-terminal CD fragments with complementary leucine zipper domains (CD-n-zip, zip-CD-c), or a vector expressing full-length CD.

We next compared RNA tagging by 5EC (the CD-UPRT pathway) and 5EU (the UPRT pathway) in control and CD:UPRT(+) HeLa cells (Figure 2.1D). Robust CD:UPRT-dependent RNA tagging was observed for both nucleobases. 5EU RNA tagging was more rapid, possibly due to the single enzymatic step required for 5EU conversion to 5EUdMP as opposed to the two steps required for 5EC conversion

to 5EUdMP. No RNA tagging occurred in CD:UPRT(-) cells exposed to 5EC while relatively weak RNA tagging occurred in CD:UPRT(-) cells exposed to 5EU, similar to the RNA tagging observed in CD(+) SH-SY5Y cells treated with 5EC. We also tested if CD:UPRT(+) cells exposed to 5EC excrete 5EU, since uracil excretion has been described in cultured fibroblasts [296]. CD:UPRT(+) HeLa cells were exposed to 5EC for two hours and cell-free media was transferred to CD:UPRT(-) HeLa cells. Exposure to conditioned media caused relatively weak RNA tagging in CD:UPRT(-) cells compared to robust RNA tagging in CD:UPRT(+) cells (Figure A.2), suggesting that 5EU (or possibly 5-ethynyluridine) is excreted from CD:UPRT(+) cells. From these comparisons of 5EC RNA tagging and 5EU RNA tagging, we conclude that RNA tagging via 5EC and CD-UPRT is much more sensitive and stringent. EC-tagging achieves cell type-specificity even when 5EU may be shared between CD:UPRT(+) and CD:UPRT(-) cells, although the relative contribution of RNA tagging via 5EC and excreted 5EU should be considered in such mixed cell culture experiments.

Previously described RNA tagging and purification methods rely on cell type-specific expression of a transgene (such as UPRT [285] or an epitope-tagged ribosomal protein [284]) and the resolution of tagging is therefore largely determined by the specificity of the enhancer used to drive transgene expression. EC-tagging has the potential to provide greater resolution via combinatorial control of CD and UPRT expression. The experiments described above suggest that CD may be the primary determinant of specificity due to the ability of UPRT-negative cells to incorporate 5EU into RNA. We therefore sought a method of placing CD under combinatorial control. Split protein systems have been used to restrict various activities to specific cell types, including targeted reconstitution of the Gal4 transcription factor in *Drosophila* [297]. Work in yeast has shown that functional CD can be reconstituted from N-terminal and C-terminal fragments fused to complementary leucine zipper domains [298]. We used similar leucine zipper-CD fusions and expressed the complementary fragments in UPRT(+) SH-SY5Y cells (Figure 2.1E). Co-expression of the leucine zipper-CD fragments enabled EC-tagging, while co-expression of CD fragments lacking the leucine zippers did not enable EC-tagging. These results establish an experimental platform that may be used to fine-tune EC-tagging specificity via combinatorial control of split CD expression.

To be useful for RNA analysis, EC-tagging should have minimal effects on cell physiology and gene expression. To assay toxicity in tissue culture cells, we measured the viability of control cells and CD:UPRT(+) cells exposed to 5EC over 72 hours. CD:UPRT(+) cells cultured in 100 μM 5EC had no loss of viability and

CD:UPRT(+) cells cultured in 500 µM 5EC were unaffected over 48 hours followed by a decline in viability to approximately 60% of controls by 72 hours (Figure 2.2A). The toxic compound 5-fluorocytosine (5FC) had a markedly different effect on viability: 100 µM 5FC caused approximately 50% loss of viability by 48 hours (Figure 2.2A). To test if EC-tagging alters gene expression, we compared RNA from CD:UPRT(+) cells exposed to 500 µM 5EC for six hours to RNA from untreated control cells. The mRNA profiles of control and CD:UPRT(+) cells were nearly identical (Figure A.3). Only 148 genes had reproducible differences in transcript abundance. We performed gene ontology (GO) analysis to determine if these minor changes were indicative of altered cell physiology but did not find any significant GO category enrichment. We interpret these results as evidence that EC-tagging does not significantly alter cell physiology or gene expression.

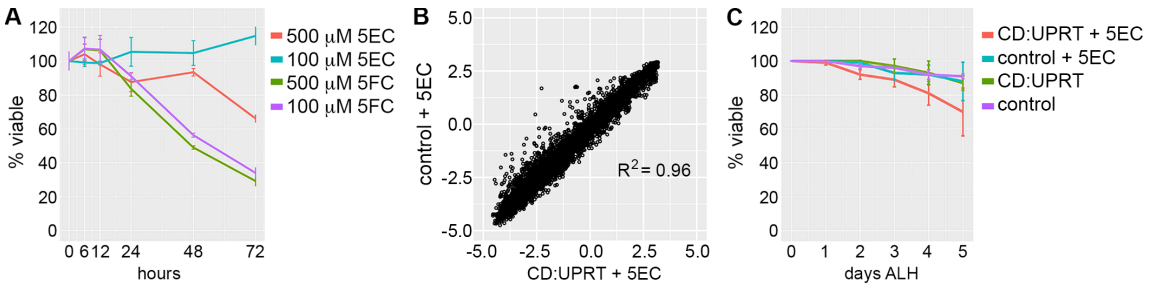

Figure 2.2: Analysis of EC-tagging effects on viability and gene expression.
(A) Viability of CD:UPRT(+) cells exposed to 5EC or 5FC, relative to untreated CD:UPRT(-) control cells. (B) Gene expression in ubiquitous CD:UPRT larvae fed 1.0 mM 5EC for 24 hours (CD:UPRT + 5EC) compared to CD:UPRT-negative larvae fed 1.0 mM 5EC for 24 hours (control + 5EC). Expression levels for 7,434 individual genes are plotted as the $\log_2$ of the gene-specific signal / mean microarray signal for all genes. (C) Viability of ubiquitous CD:UPRT larvae and CD:UPRT(-) larvae with or without continuous 500 µM 5EC feeding, relative to day zero. ALH = after larval hatching.

2.3.2 EC-tagging in *Drosophila*

To apply EC-tagging in an animal model, we made *UAS-CD:UPRT* transgenic *Drosophila* to allow targeted expression of CD:UPRT when combined with cell type-specific Gal4 lines [231]. We first tested the effects of EC-tagging on *Drosophila* development using *Act5C-Gal4* to ubiquitously express CD:UPRT. Ubiquitous CD:UPRT larvae and negative control larvae were fed 500 µM 5EC from the

time of hatching. No morbidity or mortality was observed over the first 24 hours of development. The viability of ubiquitous CD:UPRT larvae gradually began to decline after 24 hours and reached 70% of controls by five days after larval hatching (Figure 2.2C). Ubiquitous CD:UPRT larvae continuously fed 5EC transitioned between larval instars with normal timing (based on size and morphological characteristics) but did not develop beyond the late third instar (L3) stage. Ubiquitous CD:UPRT larvae reared in the absence of 5EC developed normally, indicating that expression of the enzyme does not affect development. To test if EC-tagging alters gene expression in *Drosophila*, we compared RNA from L3 larvae that ubiquitously express CD:UPRT (*da-Gal4* > *CD:UPRT*) and control larvae (no CD:UPRT) that were fed 1.0 mM 5EC for 24 hours. Gene expression between the EC-tagged and control larvae was nearly identical (Figure 2.2B). Only 159 genes had reproducible changes in gene expression of 2-fold or more (9 genes with increased expression, 150 genes with decreased expression). Gene ontology analysis did not reveal any functional relationships among these genes, suggesting that their altered expression is not indicative of a specific response to EC-tagging. We conclude that EC-tagging for periods as long as 24 hours does not adversely affect gene expression in Drosophila larvae.

We tested EC-based RNA tagging in larvae by expressing CD:UPRT broadly in the nervous system and imaginal discs using *GMR12B08-Gal4* [299], [300]. *GMR12B08 > CD:UPRT* larvae and *UAS-CD:UPRT* larvae (without any Gal4 activation of CD:UPRT expression) were fed 5EC for 24 hours. As a positive control, *UAS-CD:UPRT* larvae were fed 5-ethynyluridine (5EUd) for 24 hours. 5EUd is incorporated into RNA in all cells independent of CD or UPRT expression. RNA blots revealed strong RNA tagging in 5EUd-fed larvae, relatively weaker RNA tagging in *GMR12B08 > CD:UPRT* larvae (as expected, since fewer cells are capable of incorporating the RNA tag) and no RNA tagging in negative control larvae (Figure 2.3A). Next, we tested dose-dependent EC-tagging in a small population of neurons, using *TH-Gal4* to express CD:UPRT in approximately 75 dopaminergic neurons of the central nervous system (CNS) [301]. 5EC dose-dependent RNA tagging occurred in *TH-Gal4 > UAS-CD:UPRT* larvae and no tagging was detected in negative control larvae, even after feeding high doses of 5EC (Figure 2.3B). Additionally, we observed time-dependent RNA tagging in larvae, with EU-RNA detected after 30 minutes in 5EUd-fed larvae and after 3 hours in 5EC-fed larvae that express CD:UPRT in a small population of mushroom body neurons (*MB247-Gal4* [302] > *UAS-CD:UPRT*) (Figure A.4).

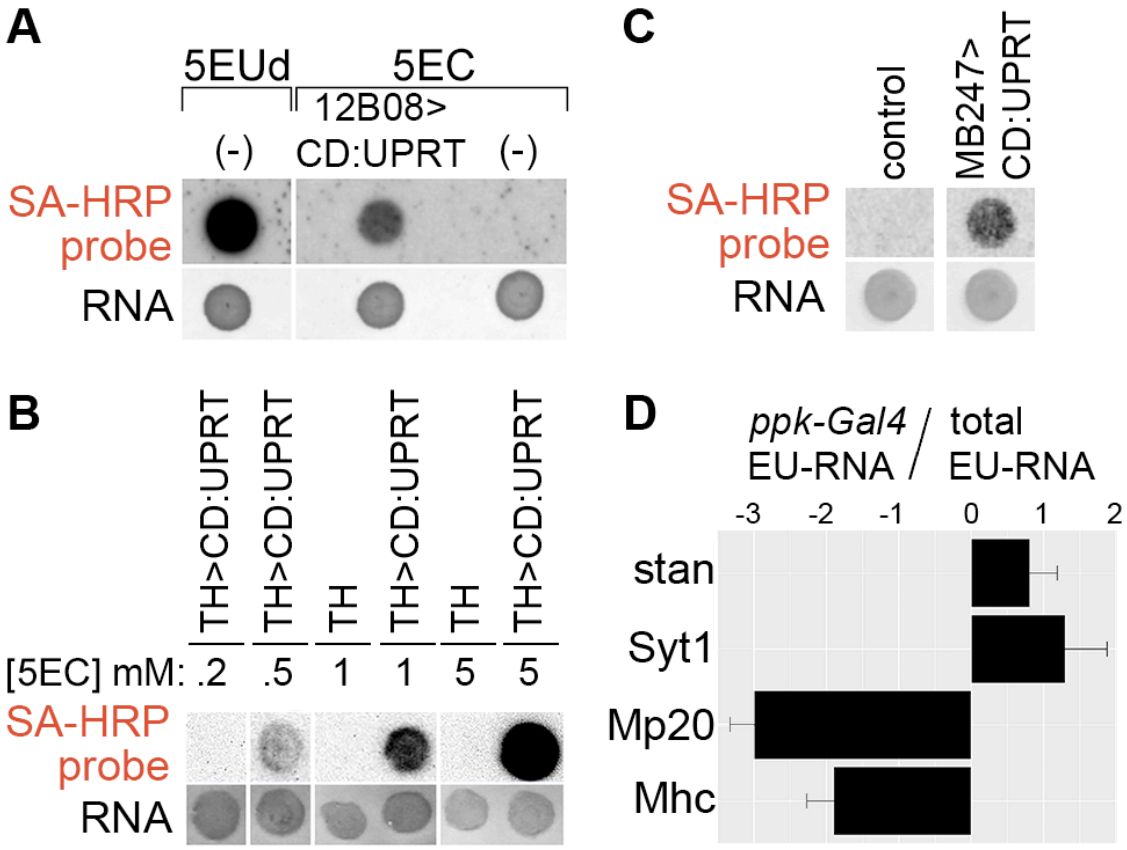

Figure 2.3: EC-tagging in *Drosophila*. (A) EC-tagging in larvae. CD:UPRT(-) larvae were fed either 500 μM 5EUd (positive control for RNA tagging) or 500 μM 5EC (negative control for RNA tagging) for 24 hours. Larvae expressing CD:UPRT under control of *GMR12B08-Gal4* were fed 500 μM 5EC for 24 hours. Total RNA was analyzed by dot blot and the "RNA" and "SA-HRP" panels are as described for Figure 2.1. (B) 5EC dose-dependent EC-tagging in larval dopaminergic neurons. Larvae expressing CD:UPRT under control of *TH-Gal4* or *TH-Gal4* larvae alone (no CD:UPRT) were fed the indicated concentration of 5EC for 6 hours. (C) EC-tagging in adult brains. Adult flies expressing CD:UPRT under control of *MB247-Gal4* driver or control flies (*UAS-CD:UPRT* alone) were fed 1.0 mM 5EC for 16 hours prior to RNA extraction from whole flies. (D) Cell type-specific mRNA enrichment from larval peripheral nervous system neurons. Larvae expressing CD:UPRT under control of *ppk-Gal4* were fed 500 μM 5EC ("EC-tag" sample) and matched larvae were fed 500 μM 5EUd ("total" sample). mRNA abundance for the indicated genes was measured by RT-qPCR. Data are the average and standard error of the mean from two biological replicates (separate 5EC feeding, RNA purification, and RT-qPCR analysis).

In addition to EC-tagging in larval stages, we found that 5EC feeding resulted in robust RNA tagging in adult flies with *MB247-Gal4* expressing CD:UPRT primarily in mushroom body neurons of the brain [302] (Figure 2.3C) and in embryos with *string-Gal4* (*GMR32C12*) expressing CD:UPRT primarily in the developing nervous system (Figure A.5). To further test the specificity and sensitivity of EC-tagging, we used *ppk-Gal4* to express CD:UPRT in a very small subset of larval peripheral nervous system cells [303]. *Ppk > CD:UPRT* L3 larvae were fed 5EC for 24 hours prior to carcass dissection and RNA extraction. Carcass dissection provided a defined tissue population composed of known cell types: the rare CD:UPRT(+) neurons (*ppk-Gal4* is expressed in only three multidendritic neurons per hemisegment) and a large excess of CD:UPRT(-) cells including muscle (30 muscle fibers per hemisegment), oenocytes, and epidermis. To obtain reference tagged RNA from all cells, we fed larvae 5EUd for 24 hours prior to performing the same carcass RNA extraction. Purified RNA containing the 5-ethynyluridine tag (EU-RNA) from *ppk > CD:UPRT* larvae and 5EUd-fed larvae was compared using reverse transcription – quantitative PCR (RT-qPCR) for two neural-specific transcripts, *Synaptotagmin 1* (*Syt1*) & *starry night* (*stan*), and two muscle-specific transcripts, *Myosin heavy chain* (*Mhc*) & *Muscle protein 20* (*Mp20*). These genes were selected because their cell type-specific expression is well known and their mRNA abundance in L3 carcasses has been measured by the modENCODE Anatomy RNA-seq Project [304]. The modENCODE RNA-seq data (linear values, scaled to maximum expression level) show that in L3 carcasses, the neural-specific transcripts are present at low levels (expression values of 11 (*Syt1*) and 24 (*stan*)) and the muscle-specific transcripts are present at very high levels (expression values of 218 (*Mhc*) and 582 (*Mp20*). In our EC-tagging experiments, *Syt1* and *stan* were enriched in the *ppk > CD:UPRT* EU-RNA while *Mhc* and *Mp20* were depleted from the *ppk > CD:UPRT* EU-RNA (Figure 2.3D). The ability to enrich mRNAs transcribed in a small number of target neurons and deplete much more abundant mRNAs transcribed in non-target cells suggested that EC-tagging is sensitive and cell type-specific, prompting us to further test EC-tagging using transcriptome-wide measurements.

2.3.3 Cell type-specific transcriptome analysis

To evaluate the use of EC-tagging in transcriptome analysis, we compared EU-RNA purified from *GMR12B08 > CD:UPRT* larvae to EU-RNA purified from larvae fed 5EUd. We refer to RNA purified from *GMR12B08 > CD:UPRT* larvae as 12B08 EU-RNA and RNA purified from the 5EUd-fed sample as whole larvae EU-RNA (Figure 2.4A). Independently processed biological replicates were prepared for

each condition and used to compare 12B08 EU-RNA and whole larvae EU-RNA by microarray analysis. As expected, microarray signals between biological replicates correlated well, while correlations between 12B08 EU-RNA and 5EUd samples were much lower (Figure A.6). We first used 12B08 EU-RNA and whole larvae EU-RNA microarray data to test for any correlation between the efficiency of EU-RNA purification and the number of uridines per mRNA. Transcripts with more uridines are expected to incorporate more EU residues and this could favor their purification relative to transcripts with fewer uridines. We did not find any correlation between uridine number and mRNA yields (Figure A.7), suggesting that all mRNAs are equally likely to incorporate the minimum number of EU tags required for efficient biotinylation and purification.

Comparison of 12B08 EU-RNA and whole larvae EU-RNA identified 1,279 mRNAs enriched two-fold or more in 12B08 EU-RNA and 405 mRNAs depleted two-fold or more in 12B08 EU-RNA. We performed GO analysis and found significant overrepresentation of categories associated with *GMR12B08*-positive tissues (nervous system and imaginal discs) among the enriched genes and significant overrepresentation of categories associated with *GMR12B0*8-negative tissues (epidermis and digestive system) among the depleted genes (Figure 2.4B). GO categories depleted in 12B08 EU-RNA also include categories associated with mitochondrial activity. We previously observed decreased abundance of mitochondria-associated mRNAs in the embryonic nervous system [126] and this may reflect the unique mitochondrial homeostasis needs of neurons [305]. Next, we compared 12B08 EC-tagging results to data obtained by sequencing RNA from dissected larval tissues, as reported in the modENCODE Anatomy RNA-seq database [304]. Of the 1,279 mRNAs enriched two-fold or more by 12B08 EC-tagging, we identified 609 genes with corresponding RNA-seq counts above the “very low expression” threshold (Flybase annotation) in at least one of the following tissues: central nervous system (CNS), imaginal discs, and carcass (composed of muscle, epidermis, oenocytes and peripheral neurons). We used these RNA-seq data to calculate CNS / carcass and imaginal disc / carcass ratios and found that 524 genes (86%) were enriched 1.5-fold or more in the CNS or imaginal discs according to the modENCODE data (Figure 2.4C). Examples of EC-tagging versus modENCODE RNA-seq data are shown for expected enriched CNS genes in the “axon guidance” category and expected depleted digestive system genes in the “small molecule metabolism” category in Figure 2.4D. These comparisons of EC-tagging and modENCODE data suggest that EC-tagging is similarly effective at identifying cell type-specific mRNAs without the need for any tissue dissection.

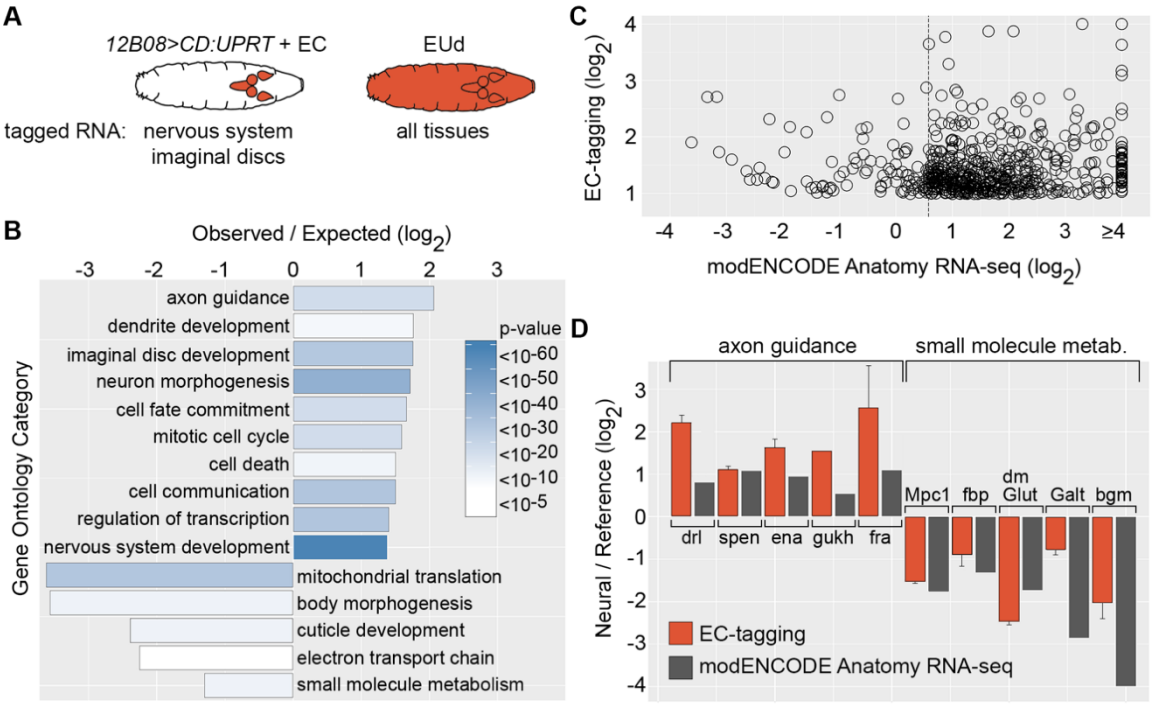

Figure 2.4: Comparison of EC-tagging and dissection-based transcriptome profiling. (A) Expected specificity of RNA tagging in *12B08>CD:UPRT* larvae fed 5EC versus larvae fed 5EUd. (B) GO categories overrepresented among 12B08 EU-RNA enriched and depleted genes. Observed / expected value = frequency of category genes in the 12B08 EU-RNA dataset / frequency in the *Drosophila* genome for the 1,279 genes enriched in 12B08 EU-RNA (plotted as positive values) and the 405 genes depleted in 12B08 EU-RNA (plotted as negative values). Heatmap = Bonferroni-corrected p-values. (C) Relative expression levels for 609 genes enriched ≥2-fold in 12B08 EU-RNA with corresponding modENCODE Anatomy RNA-seq data. 12B08 / whole larvae EU-RNA ratios are plotted on the y-axis and modENCODE CNS / carcass ratio or imaginal disc / carcass ratio is plotted on the x-axis. (D) 12B08 / whole larvae EU-RNA values (EC-tagging) and modENCODE Anatomy RNA-seq CNS / carcass (axon guidance category) or CNS / digestive system (small molecule metabolism category) ratios are shown as “Neural / Reference” values (y-axis). EC-tagging data are the average and standard error of the mean for multiple measurements across biological replicate microarrays.

To test our prediction that EC-tagging provides greater sensitivity and specificity than TU-tagging, we compared the ability of these methods to purify mRNA from mushroom body neurons of the larval brain. Mushroom body neurons comprise an

important learning and memory center [306] and while gene expression in the adult mushroom body has previously been investigated [307], [308], the transcriptional program of larval mushroom body neurons is less well-defined. We used *MB247-Gal4* to express CD:UPRT in mushroom body neurons and fed L3 larvae 1.0 mM 5EC or 1.0 mM 4-thiouracil (4TU) prior to purification of tagged RNAs. CD:UPRT-transgenic larvae work for EC-tagging and TU-tagging since the CD:UPRT enzyme converts 4-thiouracil as efficiently as the UPRT enzyme alone (Figure A.8). We refer to potential mushroom body-specific RNA samples as MB EU-RNA (EC-tagging) and MB TU-RNA (TU-RNA). MB EU-RNA was compared to whole larvae EU-RNA purified from EUd fed larvae and MB TU-RNA was compared to whole larvae TU-RNA purified from 4-thiouridine (4sUd) fed larvae. Biological replicate microarrays were analyzed for all samples and there was little variation between replicates but considerable variation between EC-tagging and TU-tagging samples (Figure A.9).

EC-tagging identified 1,011 mRNAs enriched two-fold or more in MB EU-RNA and TU-tagging identified 639 mRNAs enriched two-fold or more in MB TU-RNA. There was very little overlap in the set of enriched genes identified by EC-tagging and TU-tagging: only 51 genes were enriched in both MB EU-RNA and MB TU-RNA and we did not identify any functional relationship or cell type-specificity shared by these genes (according to GO analysis and Flybase annotations). To test for mushroom body mRNA enrichment, we analyzed 25 signaling pathway genes expressed in the adult mushroom body [307] (positive control genes, the selection criteria of which are described below in section 2.5.12) and 49 predicted muscle-specific genes [309] (negative control genes, the selection criteria of which are described below in section 2.5.12). As shown in Figure 2.5A, 23 positive control genes were enriched greater than 1.8-fold by EC-tagging and only one negative control gene was enriched by EC-tagging. In contrast, TU-tagging did not yield any enrichment of positive control mRNAs (signals were similar to those obtained for negative control genes) and 8 of the 25 mushroom body mRNAs were below the limit of detection in the MB TU-RNA sample (Figure 2.5A). Since *MB247* expresses Gal4 in a small group of brain neurons and *GMR12B08* expresses Gal4 broadly in the nervous system, we predicted that MB EU-RNA would have greater enrichment of mushroom body mRNAs and 12B08 EU-RNA would have greater enrichment of widely-expressed neuronal mRNAs. This was indeed the case: mRNAs expressed primarily in the mushroom body (based on published larval expression data ([310][311][312][313][314][315]) were strongly enriched in MB EU-RNA but absent or non-enriched in 12B08 EU-RNA (Figure 2.5B).

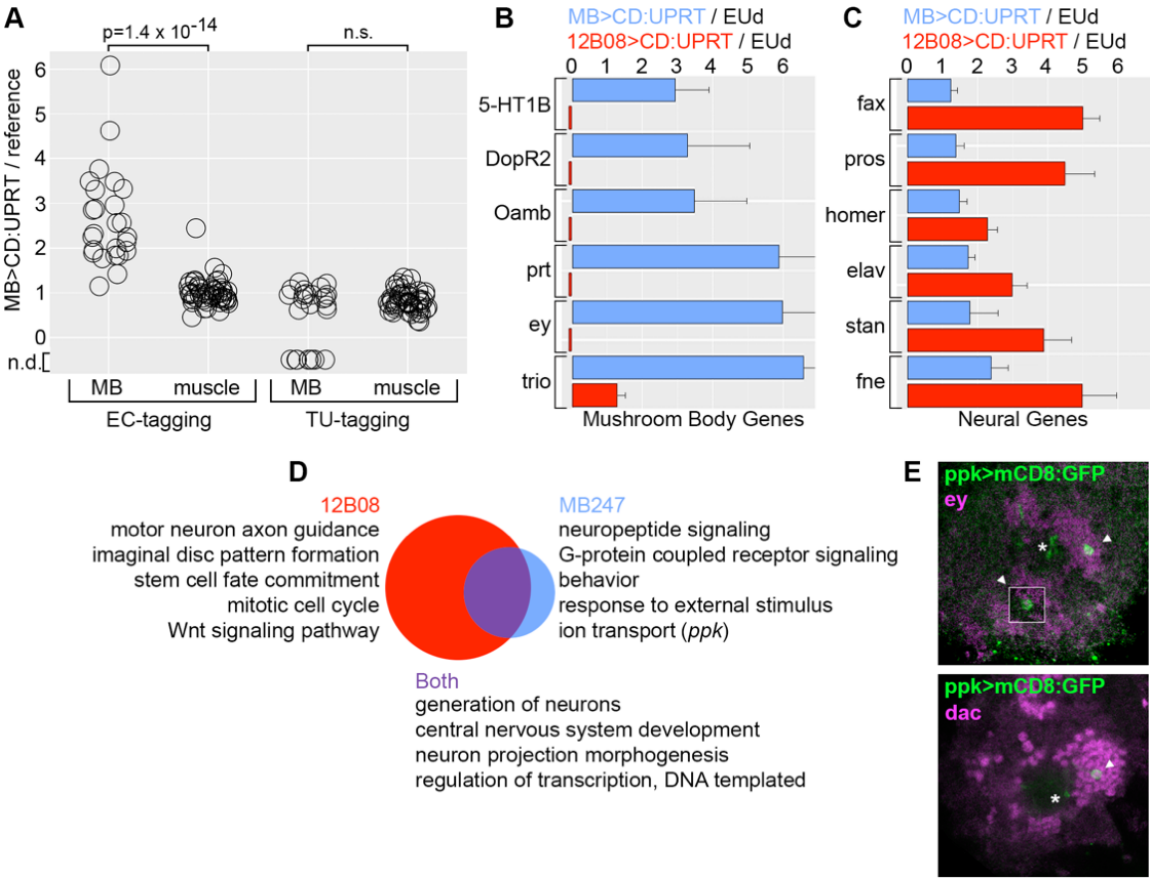

Figure 2.5: EC-tagging in larval mushroom body neurons. (A) MB / whole larvae EU-RNA ratios and MB / whole larvae TU-RNA ratios for 25 positive control mushroom body genes and 49 negative control muscle genes. Wilcoxon rank sum test p-value is shown (n.s. = not significant). Values below zero represent genes that were not detected (n.d.) in MB EU-RNA. (B and C) Enrichment of mushroom body transcripts versus broadly expressed neuronal transcripts in MB EU-RNA, 12B08 EU-RNA. Data are the average and standard error of the mean for multiple measurements across replicate microarrays. Values for error bars that don't fit on the graph are: prt (±2.3), ey (±2.4), trio (±3.5). Small red bars below zero indicate the gene was not detected in 12B08 EU-RNA. (D) GO categories enriched in the 12B08 versus MB datasets. Venn diagram represents the 210 GO categories enriched in the 12B08 dataset (red, 151 unique), the 75 GO categories enriched in the MB dataset (blue, 16 unique), and the 59 overlapping categories (purple). *Ppk* is listed as a gene of interest in the MB-specific "ion transport" category. (E) Confirmation of *ppk* expression in a small number of mushroom body neurons. Cell bodies (arrowhead) and partial dendrite projections (asterisk) are shown for GFP+ neurons in *ppk>UAS-mCD8:GFP* larval brains. Antibody staining for the mushroom body transcription factors (Ey) and (Dac) is shown in magenta. The dorsal region of a single brain hemisphere is shown (anterior down, medial left).

In contrast, mRNAs expressed broadly in the nervous system were strongly enriched in 12B08 EU-RNA and weakly enriched in MB EU-RNA (Figure 2.5C). Neither mushroom body genes nor broadly expressed nervous system genes were enriched in MB TU-RNA.

We next compared GO categories enriched in the 12B08 EU-RNA, MB EU-RNA, and MB TU-RNA datasets. Surprisingly, the only non-redundant GO category enriched by MB TU-tagging was “chitin-based cuticle development”, suggesting that non-specific incorporation of 4-thiouracil may be particularly strong in the epidermis (data not shown). In contrast, the MB EU-RNA data showed significant enrichment of categories associated with neural function (Figure 2.5D). Aligning the MB EU-RNA and 12B08 EU-RNA data revealed distinct gene expression categories. Of 210 non-redundant GO categories enriched in the 12B08 dataset, 151 were unique to this dataset and 59 were shared between the 12B08 and MB datasets. 12B08-specific GO categories include “motor neuron axon guidance”, “mitotic cell cycle”, and “imaginal disc pattern formation”. The absence of these categories from the MB dataset is expected since *MB247-Gal4* is not expressed in motor neurons, mitotic progenitors or imaginal discs [316]. Of 75 non-redundant GO categories enriched in the MB dataset, 16 were unique to the MB dataset. MB-specific GO categories are associated with mushroom body properties such as neuropeptide signaling, G protein-coupled receptor signaling, and behavior. Neuropeptide and G protein-mediated signaling pathways regulate activity in the adult mushroom body [317] and our data suggest these signaling systems also function in larval learning and memory. In contrast, Wnt and Notch signaling categories were only enriched in the 12B08 dataset. This likely reflects the fact that Wnt and Notch signaling is widespread in the nervous system [318], [319] and imaginal discs [320] and not restricted to or elevated in the mushroom body like the neuropeptide and G protein-mediated pathways.

“Ion transport” is another GO category unique to the MB dataset. Within this category, we were surprised to find the *pickpocket* gene identified as a MB-enriched transcript. Pickpocket is a voltage-insensitive ion channel involved in larval locomotion [303] and mechanical nociception [321]. Pickpocket is best known for its expression and function in the peripheral nervous system and so we sought to confirm *ppk* expression in mushroom body neurons. *Ppk-Gal4* matches endogenous *ppk* expression and is expressed in a small number of brain cells [303], but the identity of these *ppk-Gal4+* brain cells was not previously determined. We used *ppk-Gal4* to express *UAS-mCD8:GFP* (membrane-anchored GFP) and identified between two and four GFP+ mushroom body neurons per brain hemisphere.

Mushroom body identity was determined by co-localization with Eyeless and Dachshund (transcription factors expressed in the mushroom body [314]) (Figure 2.5E), and neuron projections into the mushroom body calyx, peduncle and lobes (Figure A.10). Our discovery of a small population of *ppk*-expressing mushroom body neurons confirms the sensitivity and specificity of EC-tagging.

2.4 Discussion

Here, we show that combinatorial control of CD expression, UPRT expression, and 5EC delivery allows purification of cell type-specific RNAs without the need to physically isolate cells of interest. While dissection-based transcriptome profiling experiments yield valuable information, such approaches are often labor intensive, may alter gene expression as a result of tissue manipulations, and may be limited in the degree of cell type-specificity that can be achieved. Here we show that EC-tagging yields tissue-specific gene expression data similar to those obtained by the dissection-based modENCODE Anatomy RNA-seq project.

Additionally, we show that EC-tagging provides a significant improvement over its methodological precursor TU-tagging. EC-tagging was sensitive and specific enough to enrich for rare mushroom body mRNAs from a mixture of all larval mRNAs, while TU-tagging failed to identify mushroom body mRNAs in parallel experiments. The failure of TU-tagging to enrich for mushroom body-specific mRNAs was likely due to widespread RNA-tagging via endogenous *Drosophila* UPRT [272]. Background RNA labeling is a known limitation of TU-tagging and may be partially avoided by dissection of relevant tissues, as previously described [266], [285], [322], [323]. In *Drosophila* larvae, non-specific TU-tagging appears strongest in tissues outside the CNS and CNS dissection has been used to improve the signal to noise [285], [323]. There are approximately 700 *MB247-Gal4*-positive mushroom body neurons in L3 larvae [316] and L3 larvae are composed of at least one million cells. We therefore estimate that in our mushroom body RNA tagging experiments, the target cells constitute as little as 0.07% of the population. Given this low percentage, it is not surprising that TU-tagging applied to whole larvae failed to enrich mushroom body mRNAs. In contrast, EC-tagging effectively identified known or predicted larval mushroom body transcripts and led to the discovery of a novel mushroom body-expressed gene, *ppk*. While target mRNA enrichment by EC-tagging in the *MB247-Gal4* and *12B08-Gal4* populations was robust, depletion of transcripts from non-target tissues was variable. As shown for MB EC-tagging, several muscle-specific genes had MB / whole larvae EU-RNA ratios close

to 1.0. These mRNAs are highly abundant in larvae (based on modENCODE RNA-seq data) and we expect such transcripts to be difficult to completely remove during EU-RNA purification. EC-tagging is more effective at depleting less abundant off-target transcripts, as demonstrated by the depletion of “cuticle development” and “small molecule metabolism” mRNAs in the 12B08 EC-tagging experiments. Our comparison of 12B08 EC-tagging and modENCODE data for small molecular metabolism mRNAs shows that the dissection-based method gives higher levels of depletion, but this is expected when analyzing relatively pure dissected samples (as in the modENCODE approach) versus analyzing mRNA purified from a mixture of all larval RNAs (as in EC-tagging). Another source of off-target transcripts may be RNA tagged via 5EU excreted from CD:UPRT+ cells, as observed in SH-SY5Y cells. However, depletion of muscle transcripts in our *ppk-Gal4 > CD:UPRT* experiments (where 5EU could be excreted from the CD:UPRT(+) neurons and taken up by the surrounding muscle fibers) and rare off-target transcript enrichment in our transcriptome profiling experiments (the 12B08 EC-tagging and MB EC-tagging experiments) argues against significant 5EU excretion during EC-tagging in *Drosophila*. We conclude that while enrichment of cell type-specific transcripts by EC-tagging is sensitive and robust, depletion of off-target transcripts may be variable and is likely due to non-specific capture of untagged RNAs during the purification step.

There are multiple parameters to consider when designing an EC-tagging experiment. One parameter is the duration of 5EC exposure. Long 5EC exposure increases the abundance of tagged RNAs in target cells and allows cell type-specific mRNA discovery starting from a small amount of input material. In our 24-hour EC-tagging experiments, EU-RNA for microarray analysis was obtained from 20 µg of biotinylated input RNA (starting from 20-30 L3 larvae). While we did not detect any morbidity, mortality, or major changes in gene expression after 24 hours of ubiquitous EC-tagging, future users of EC-tagging may want to investigate potential side effects in the context of their experimental system (particularly if feeding 5EC for more than 24 hours). It is important to note that long periods of 5EC exposure are not a requirement for effective EC-tagging. In addition to the fact that we detected robust dose-dependent EC-tagging in a small population of dopaminergic neurons after 6 hours of 5EC feeding (Figure 2.3B), we also managed to detect tagged RNA from CD:UPRT(+) mushroom body neurons after 3 hours of 5EC feeding and tagged RNA from all cells after 30 minutes of 5EUd feeding (Figure A.4). The rapid incorporation of 5EUd suggests that short exposure times will work for EC-tagging but will require increased amounts of input RNA (compared to what we used following a 24-hour exposure) for detection and purification of EU-RNA.

The type of RNA populations to be compared for expression profiling is another important consideration for EC-tagging. Here we compared purified EU-RNA from CD:UPRT(+) cells to purified EU-RNA from all cells (via 5EUd feeding). This design allowed comparison of equivalent biosynthetically tagged transcripts and ensured that each sample underwent identical processing steps. An alternative is to compare purified EU-RNA to input (pre-purification) RNA, but this approach may introduce biases. One potential problem is that EU is only incorporated into RNAs made during 5EC exposure while the input RNA contains all RNAs, including those transcribed prior to 5EC exposure. Therefore, weakly transcribed mRNAs that are degraded slowly will be more abundant in the input RNA, even if transcription and decay rates are equal in target and non-target cells. Conversely, rapidly degraded mRNAs will be more abundant in the purified EU-RNA pool, particularly when using short labeling times and enriching for nascent mRNAs. Another potential problem when comparing purified EU-RNA and input RNA is that the samples are processed differently prior to transcriptome profiling: the biotinylation and purification steps may alter EU-RNA relative to input RNA. These potential problems are avoided when comparing purified EU-RNA from CD:UPRT(+) cells to purified EU-RNA from all cells. Another design consideration for EC-tagging is the potential use of intersectional approaches to express CD and UPRT, or the split-CD halves plus UPRT, from different enhancers. This could refine cell type targeting in mixed cell cultures and *in vivo*. In *Drosophila* and other organisms with endogenous uracil incorporation pathways, we predict that combinatorial control of split-CD expression combined with enhanced 5EU incorporation via targeted UPRT expression will give the greatest intersectional expression specificity. As a final experimental design option, we found it useful to compare EC-tagging results from related cell populations with well-defined distinctions. *12B08-Gal4* EC-tagging and *MB247-Gal4* EC-tagging both enriched for neural transcripts but comparing transcriptome data from each Gal4 line allowed us to distinguish broadly expressed neural genes from mushroom body-specific neural genes. These data should prove useful for identifying novel mushroom body properties, as demonstrated by our discovery of *pickpocket*-expressing mushroom body neurons. The discovery of these neurons reveals previously unknown cellular heterogeneity in the larval mushroom body and suggests that the *pickpocket*-expressing neurons respond to modalities that are distinct from those previously described in the mushroom body [324].

2.5 Approach

2.5.1 5-ethynylcytosine (5EC) synthesis

As described in Figure 2.6, 5-ethynylcytosine (5EC) was prepared by coupling 5-iodocytosine (1) with trimethylsilylacetylene under Sonogashira conditions to afford the intermediate 2 in 87% yield [325]. The trimethylsilyl protecting group was removed with concentrated aqueous NH3 to give 5EC. The intermediate (2) and final product were spectroscopically characterized and the data for 5EC matched that reported.

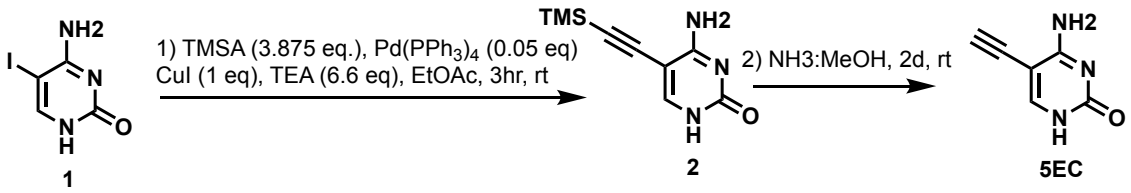

Figure 2.6: Scheme detailing the synthesis of 5-ethynylcytosine (5EC). Compound (1) is 5-iodocytosine. TMSA = Trimethylsilylacetylene. TEA = triethylamine.

Preparation of intermediate compound (2): A mixture of 5-iodocytosine (compound (1) in Figure 2.6, 105 mg, 0.44 mmol), $Pd(PPh_3)_2Cl_2$ (15 mg, 0.021 mmol), CuI (8 mg, 0.042 mmol), anhydrous triethylamine (268 mg, 2.65 mmol) and 0.8 mL of dry DMF was degassed by bubbling argon at 25 °C for 1 h. Trimethylsilyl acetylene (152 mg, 1.55 mmol) was added and the mixture was stirred at 25 °C for 45 min. The reaction mixture was diluted with MeOH and filtered (5 mL). The precipitate was washed with H_2O (3 × 10 mL), acetone (2 × 5 mL), and dried to give compound (2) (Figure 2.6) as an off-white solid: yield 80 mg (87%). ^{1}H NMR (DMSO-d_6) δ 11.11 – 10.67 (m, 1H), 7.73 (s, 2H), 6.61 – 6.30 (m, 1H), 0.20 (s, 9H).

Preparation of 5EC. A suspension of 70 mg (0.34 mmol) of compound (2) (Figure 2.6) in concentrated aqueous NH_3 (2 mL) and MeOH (0.5 mL) was stirred in a sealed reaction vessel for 2 days. The reaction mixture was concentrated under reduced pressure to obtain 3 as a brown solid: yield 40 mg (87%). ^{1}H NMR (DMSO-d6) δ 11.10 – 10.46 (m, 1H), 7.74 (s, 1H), 7.71 – 7.41 (m, 1H), 6.81 – 6.52 (m, 1H), 4.30 (s, 1H).

2.5.2 5-ethynyluracil (5EU) synthesis

5-Iodouracil (compound (1) in Figure 2.7, 2000 mg, 8.4 mmol, 1 eq), TMS-acetylene (2.4 mL, 16.8 mmol, 2 eq), Et3N (4.7 mL, 33.6 mmol, 4 eq), $Pd(PPh_3)_4$ (196mg, 0.17 mmol, 0.02 eq), and CuI (65 mg, 0.34 mmol, 0.04 eq) were dissolved in 25 mL of degassed EtOAc. The suspension was stirred at room temperature for 3 hrs under Ar. The suspension was then filtered and washed with EtOAc. The extract was collected and dissolved in 10 mL of 1 M NaOH and stirred at room temperature for 2 hrs. The solution was then diluted with 10 mL of H_2O and concentrated in vacuo. The residue was then redissolved in 10 mL of H_2O and AcOH was added until a pH of 5 was reached. The suspension was then set on ice for 30 mins and filtered. The extract was washed with H_2O, acetone, and Et2O. The extract was then dried in vacuo to give 5EU (823 mg, 72%) as an off white solid. Spectra are in agreement with those reported in the literature previously [326]. HRMS Calcd for $C_6H_4N_2O_2$ [M-H-] 135.0195, found 135.0195; 1H NMR (400 MHz, DMSO) δ 11.29 (s, 2H), 7.78 (s, 1H), 3.99 (s, 1H).

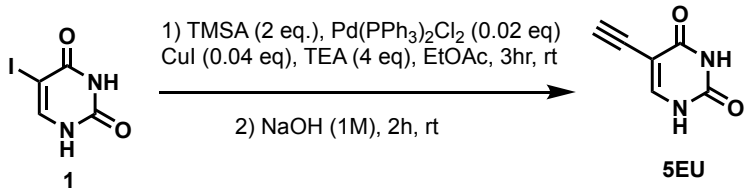

Figure 2.7: Scheme detailing the synthesis of 5-ethynyluracil (5EU). Compound (1) is 5-iodouracil. TMSA = Trimethylsilylacetylene. TEA = triethylamine.

2.5.3 Cell culture and expression constructs

HeLa cells (American Type Culture Collection (ATCC)) and SH-SY5Y human neuroblastoma cells (provided by Prof. Kitazawa) were cultured using standard methods and transfected using Lipofectamine (ThermoFisher). A *Saccharomyces cerevisiae* (*S.c.*) *CD:UPRT* fusion construct, *pSELECT-zeo-FcyFur* (InvivoGen), was used to PCR amplify *S.c.CD*, *S.c.UPRT* and *S.c.CD:UPRT* for the following constructs: *pcDNA3.3_HA-CD:UPRT*, *pcDNA3.3_GFP-S.c.CD*, *pcDNA3.3_GFP-S.c.CD:UPRT* and *pcDNA3.1(zeo)_mCherry-S.c.UPRT*.

Split CD constructs were made by chemical synthesis (IDT) of the N-terminal CD(A23L)1-77 and C-terminal CD(V108I, I140L, T95S, K177E)57-158 fragments. The N-terminal CD was fused to C-terminal leucine zipper sequence:

ALKKELQANKKELAQLKWELQALKKELAQ and the C-terminal CD was fused to N-terminal leucine zipper sequence: EQLEKKLQALEKKLAQLEWKNQAL-EKKLAQ [327]. The leucine zipper-fused split CD fragments were sub-cloned into *pcDNA3.3*.

2.5.4 *Drosophila* genetics

pUAS-HA-CD:UPRT-attB constructs (containing either a N-terminal HA-tagged *Saccharomyces cerevisiae S.c. CD:UPRT* fusion gene or a *Drosophila* codon-optimized *CD:UPRT* fusion gene) were used to generate second and third chromosome *UAS-CD:UPRT* lines for both the *S.c.CD:UPRT* and optimized *CD:UPRT*.

The following Gal4 lines were obtained from the Bloomington Drosophila Stock Center: *Act5C-Gal4* (#25374), *GMR12B08-Gal4* (#48489), *ppk-Gal4* (#32078 and #32079), *MB247-Gal4* (#50742), *Canton-S-iso2B* (#9514), *da-Gal4; da-Gal4* (#55849) and *10XUAS-IVS-mCD8-GFP* (#32185). *TH-Gal4* was provided by Prof. F. Wolf.

2.5.5 RNA-sequencing human cell lines

Library preparation (using oligo-dT priming), RNA-sequencing and data analysis were performed using the Beijing Genome Institute's RNA-Seq. service. Gene ontology analysis of differentially expressed genes was performed using DAVID [328] and only categories with an enrichment ≥ 2.0 and Bonferonni-corrected p-values of less than 0.001 were considered significant.

2.5.6 5EC toxicity assays

Toxicity assays in cell lines: 5,000 control HeLa cells or CD:UPRT(+) HeLa cells were added per well in a 96-well plate. Cells were pre-incubated for 24 hours prior to addition of the indicated concentration of 5EC or 5FC (InvivoGen). At the indicated timepoints, 10 µl of Cell Counting Kit-8 (CCK-8) solution (Sigma) was added to each well and 450 nm absorbance was measured one hour later. Percent cell viability was calculated as A_{450} nm treated cells / A_{450} nm untreated control x100.

Toxicity assays in Drosophila: *Act5C-Gal4 / CyO ; UAS-CD:UPRT* larvae and *Canton-S* controls were hatched onto standard fly media with or without 500 µM 5EC. Larval mortality was counted every 24 hours.

2.5.7 5EC / 5EUd treatment, RNA biotinylation, and EU-RNA detection

5EC and 5EUd (ThermoFisher) were suspended in DMSO and added to cell culture media or yeast-free *Drosophila* media at the indicated concentrations. *Drosophila* media must be yeast-free to avoid yeast converting 5EC to 5EUd and transfer of 5EUd to *Drosophila* that ingest the yeast. Total RNA extraction was performed using the standard Trizol method. RNA to be biotinylated (10 – 30 µg) was first treated with RNAse-free DNAse (Qiagen) followed by RNeasy Mini column (Qiagen) clean-up. RNA biotinylation was performed using PEG4-carboxamide-6-azidohexanyl-biotin and Click-iT reagents according the manufacturer's protocol (ThermoFisher) or biotin-dPEG7-azide (Sigma-Aldrich) and custom reagents as previously described [289].

For Click-iT-based biotinylation, 10- 30 µg of input RNA was mixed with 25 µl Click-iT EU buffer (buffer B), 4 µl CuSO4, and PEG4-carboxamide-6-azidohexanyl-biotin at a concentration of 1mM (final volume adjusted to 47.25 µl with RNAse free water) then mixed by pipetting before adding 1.25 µl Click-iT EU reaction buffer additive 1 (buffer E). The reaction was immediately mixed by pipetting and incubated 3 minutes at room temperature before adding 1.5 µl Click-iT EU reaction buffer additive 2 (buffer F) followed by a final round of mixing by pipetting. For the custom biotinylation reaction, 10 - 30 µg of input RNA (up to 34 µl) was mixed with 5 µl of 20 mg/ml tris-(3-hydroxypropyltriazolylmethyl) amine (THPTA), 1 µl of 100 mM CuSO4, 5 µl of 200 mM sodium ascorbate, 5 µl of 10 mM biotin-dPEG7-azide and RNAse-free water to adjust the final volume to 50 µl. In both cases, the biotinylation reaction was incubated in a thermomixer at 700 rpm, 25^{o}C for 30-45 minutes. The biotinylation reaction was stopped with addition of 450 µl HEPES buffer (10 mM HEPES pH7.5, 1 mM ethylenediaminetetraacetic acid (EDTA)) and 500 µl of chloroform followed by vigorous mixing, transfer to Phase Lock Gel Heavy tubes (ThermoFisher), and centrifugation at 16,000 x *g* for 10 minutes at 4^{o}C. The aqueous phase was subjected to a second round of chloroform extraction using Phase Lock Gel Heavy tubes and centrifugation at 16,000 x *g* for 10 minutes at 4^{o}C. RNA was precipitated from the final aqueous phase by adding 50 µl 5M NaCl and 450 µl isopropanol, mixing well, incubating at room temperature for a minimum of 10 minutes, then centrifuging at 12,000 x *g* for 15 minutes at 4 ^{o}C (longer incubation and centrifugation times may increase yields if a pellet is not visible after the first spin). Pelleted RNA was washed with 1.0 ml 75% ethanol twice then resuspended in 20 – 30 µl RNAse-free water. RNA blot detection of biotinylated RNA with streptavidin-HRP was performed as previously described [285]. Dot blots and

slot blots were loaded with either 1 µg or 5 µg of total RNA (equal loading for samples being compared on a single blot) following the biotinylation reaction and clean-up. RNA-transfer blots were loaded with 10 µg of total RNA treated with an equal volume of NorthernMax-Gly Sample Loading Dye (Ambion) following standard northern blot protocol.

2.5.8 EU-RNA capture on streptavidin beads

Biotinylated EU-RNA was captured using Dynabeads MyOne Strepatvidin T1 (Invitrogen) with 50 µl of beads for 20 µg of biotinylated RNA (roughly equivalent to the biotin-reacted RNA obtained from 20-30 third instar larvae). The following buffers were used, based on a previous protocol [329]: Solution A (0.1 M NaOH, and 0.05 M NaCl); Solution B (0.1 M NaCl); Tris.HCl-NaCl-EDTA (TNE) 2.0 buffer (10 mM Tris.HCl pH 7.5, 1 mM EDTA, and 2 M NaCl); Blocking & Washing (B&W) Buffer (5 mM Tris.HCl pH 7.5, 0.5 mM EDTA, and 1 M NaCl); TNE 0.2 Buffer (10 mM Tris.HCl pH 7.5, 1 mM EDTA, and 200 mM NaCl); and Wash Buffer 65 (100 mM Tris.HCl pH 7.5, 10 mM EDTA, 1 M NaCl and 0.1% Tween 20). Prior to adding RNA, beads were washed twice with B&W buffer at room temperature; twice with Solution A at room temperature; twice with Solution B at room temperature; twice with TNE 2.0 buffer at room temperature; once with Wash 65 Buffer at 65^{o}C with vigorous mixing; and twice with TNE 0.2 at room temperature. Beads were subsequently incubated in a blocking solution (10 mM Tris.HCl, pH 7.5; 1 mM EDTA; 0.2 M NaCl; 2 mg/ml nuclease-free bovine serum albumin (BSA); and 1 µg/ml poly(deoxyinosinic-deoxycytidylic) acid) for 24 hours at 4^{o}C. Following the blocking steps, beads were washed three times with B&W buffer. RNA samples were denatured at 70^{o}C for 5 minutes followed by an incubation period of 3 minutes on ice. Denatured RNA was incubated with the blocked beads in a mixture of B&W buffer, 2 µl of RNAseOUT Recombinant Ribonuclease Inhibitor (Invitrogen) and nuclease-free water for a final volume of 2.5 ml (for 10 µg of RNA) or 5 ml (for 20 µg of RNA). The RNA and beads mixture were incubated in the dark at room temperature for 30-45 minutes with gentle rotation to prevent the beads from settling. Beads were then subjected to a number of high stringency washes (1.0 ml each) to remove non-biotinylated RNA: four washes with TNE 2.0 at room temperature; four washes with B&W buffer at room temperature; four washes with Wash 65 Buffer at 65^{o}C with vigorous mixing; and four washes with TNE 0.2 buffer at 65^{o}C with vigorous mixing. After the last wash, the beads were directly used for RT-qPCR (detailed below in section 2.5.10) or cRNA synthesis (detailed below in section 2.5.11).

2.5.9 TU-tagging

Larvae were fed 1.0 mM 4-thiouracil (4TU) (Sigma-Aldrich) or 1.0 mM 4-thiouridine (4sUd) (Sigma-Aldrich) as previously described [285]. Whole larvae were used for total RNA extraction using Trizol reagent. Total RNA was reacted with MTSEA-biotin (Biotium) followed by streptavidin-bead purification and elution according to published protocols [287]. A total of 20 µg of input RNA was used for all purifications (matching input amounts used for EC-tagging experiments) and 100 ng of eluted TU-RNA was used for cRNA probe generation (as described below in section 2.5.11).

2.5.10 RT-qPCR

Real-time PCR quantitation was performed on a Rotor-Gene Q (Qiagen) in 20 µL reactions using QuantiTect Primer Assays (Qiagen) and SYBR green detection. *Ct* values were normalized to an *RpL32* internal reference and relative abundance calculated by the equation, fold-change = $2^{-\Delta(\Delta Ct)}$. RT-qPCR analysis was performed on biological replicate samples with cDNA synthesis performed using EU-RNA on beads for one sample and cDNA synthesis performed on eluted EU-RNA for the other sample. Dynabeads with bound EU-RNA or eluted EU-RNA were used to make cDNA using the SuperScript VILO cDNA Synthesis Kit (Invitrogen). For EU-RNA on beads, cDNA synthesis was performed with the recommended reaction volume scaled to 50 µl: After the final EU-RNA purification wash, the beads were re-suspended in 25 µl of TNE 0.2 buffer (10 mM Tris.HCl pH 7.5, 1 mM EDTA, and 200 mM NaCl). A total of 10 µl 5X VILO reaction mix was then added to the bead solution, mixed by pipetting, and incubated at 25°C for 10 minutes with continuous mixing on a thermomixer to prevent the beads from settling. Afterwards, 10 µl RNAse-free water and 5 µl Superscript enzyme mix were added to the reaction then mixed by pipetting. The reaction was incubated at 42°C for 1 hour with continuous mixing on a thermomixer. The reaction was then heated to 85°C for five minutes to terminate cDNA synthesis and to release cDNA from the beads. This cDNA was directly used in qPCR reactions. An alternative approach (used for one of the replicate RT-qPCR experiments) is to elute EU-RNA from the beads using an elution buffer (20 mM Tris.HCl, 1 mM EDTA, 0.5% SDS, 1 mM d-Biotin (Sigma-Aldrich), and 20 U Proteinase K (Life Technologies)), based on a previously described protocol [330]. For elution, beads with bound EU-RNA were incubated in 300 µl of elution buffer for 30 minutes with vigorous mixing on a thermomixer at 65°C. Beads were then collected by magnet and the supernatant was aliquoted to a new tube. EU-RNA was extracted from the supernatant once

with a mixture of 3M sodium acetate and acid phenol/chloroform, and twice with chloroform. EU-RNA was then precipitated with isopropanol and 2 µl of linear polyacrylamide (20 mg/ml). Pellets were washed twice with 75% ethanol and resuspended in nuclease-free water.

2.5.11 Microarrays

The Low Input Quick Amp Labeling Kit (Agilent) was used to make Cy3-labelled cRNA from EU-RNA bound to beads or 100 ng of eluted TU-RNA. cRNA synthesis from eluted TU-RNA followed the manufacturer's protocol. The protocol was slightly modified for cRNA synthesis from EU-RNA on beads. Following the final EU-RNA purification step (described above in section 2.5.8), approximately 6 µl of EU-RNA+beads remain. The EU-RNA plus beads mixture was combined with 3 µl of diluted One-Color Spike-In Control RNA (Agilent) and 5.4 µl of T7 primer mix. All subsequent cDNA synthesis steps were performed per the manufacturer's protocol, but all reagent volumes were increased 3-fold: 6 µl 5x first-strand buffer, 3 µl dithiothreitol (DTT), 1.5 µl dNTP mix, 3.6 µl Affinity Script RNAse block mix. The cDNA synthesis reaction was incubated at 40oC for two hours with continuous mixing on a thermomixer followed by incubation at 85oC for five minutes followed by immediate bead collection using a magnetic stand to remove the cDNA solution (approximately 22 - 25 µl cDNA). This cDNA was then used for cRNA synthesis according to the manufacturer's protocol, with transcription mix reagent volumes increased 3-fold: 9.6 µl 5X transcription buffer, 1.8 µl DTT, 3 µl NTP mix, 0.63 µl T7 RNA polymerase blend, 0.72 µl Cy3-CTP, and RNAse-free water to bring final volume to 48 µl. cRNA purification for TU-RNA and EU-RNA samples was performed using RNeasy Mini Kit columns (Qiagen).

Microarray analysis was performed using Agilent 4 x 44k Gene Expression Microarrays. All microarray data are based on pooled biological replicate RNA samples that were subsequently used for independent processing in duplicate microarrays (independent RNA extraction, biotinylation, EU-RNA / TU-RNA purification, and cRNA synthesis). A total of 1.65 µg of cRNA was hybridized to microarrays at 65^{o}C for 17 hours followed by washing according to standard Agilent protocols. Microarrays were scanned with a GenePix 4000B scanner. Post-processing of microarray data was performed using the computing environment R. Spots with fluorescence intensity < 66% above background were excluded. Spot fluorescence minus background fluorescence signal was normalized by first excluding the bottom 10% lowest fluorescence spots and the top 10% highest fluorescence spots, calculating the mean fluorescence for the remaining spots, then applying a

normalization factor to all spots so that the mean signal is equivalent across all microarrays directly compared to each other. Average signal intensity per spot was calculated from biological replicate microarrays and then used to calculate target EU-RNA / whole larvae EU-RNA (5EUd-fed) ratios and target TU-RNA / whole larvae TU-RNA (4sUd-fed) ratios. Ratios per spot were then used to calculate the average ratio and standard deviation per gene (most genes are represented by multiple spots on the microarray). For determination of enrichment in Gal4-driver targeted populations, spots with 12B08 EU-RNA, MB EU-RNA or MB TU-RNA normalized signal intensity less than 300 (cutoff determined by analysis of signal intensity for negative control genes that are not transcribed in larvae) were excluded from the per gene ratio calculations. For determining depletion, spots with whole larvae EU-RNA or whole larvae TU-RNA normalized signal intensity less than 300 were excluded from the per gene ratio calculations. All raw and normalized microarray data are available through the NCBI GEO series record GSE94346.

2.5.12 Transcriptome data analysis

Gene ontology analysis of all *Drosophila* data (Figures 2.4 and 2.5) was performed using GO-Term Finder [331] and only included named genes (i.e. genes known only by an annotation symbol or “CG number” were excluded as they tend to lack ontology information). Only categories with an enrichment ≥ 2.0 and Bonferonni-corrected *P*-values of less than 0.001 were considered significant. Redundant GO categories were identified based on nearly identical gene lists and similar category names. Alignment of all non-redundant significantly enriched GO categories from the MB247 and 12B08 datasets allowed identification of the overlapping and non-overlapping GO categories summarized in Figure 2.5D.

Positive control mushroom body genes shown in Figure 2.5A were selected from the Crocker et al. [307] list of neurotransmitter, neurotransmitter receptor, peptide and peptide receptor genes enriched in adult gamma mushroom body neurons with a z-score ≥ 0 (44 genes, as reported in Figure 4 of Crocker et al. [307]). From this set of 44, genes with microarray signal below background (no spots with normalized fluorescence intensity minus background > 300) for the 12B08 EU-RNA dataset were excluded (as these may represent adult mushroom body-specific genes), yielding 25 genes for analysis. Negative control muscle genes shown in Figure 2.5A were selected from the Schnorrer et al. [309] list of embryonic RNAi targets (77 genes, as reported in supplementary table 3 of Schnorrer et al. [309]). From this set of 77, genes with microarray signal below background (no spots with normalized fluorescence intensity minus background > 300) in the whole larvae

EU-RNA dataset were excluded (as these may not be expressed or only weakly expressed in larvae) yielding 56 genes. An additional 7 genes were removed from the muscle negative control set since they were also detected in adult mushroom body gamma neurons by RNA-seq [307], yielding 49 genes for analysis.

Chapter 3

Identification of novel regulators of dendrite arborization using cell type-specific RNA metabolic labeling

** The following has been reproduced from the following publication in PLOS ONE: **Aboukilila, M. Y.**, Sami, J. D., Wang, J., England, W., Spitale, R. C., and Cleary M. D. (2020). Identification of novel regulators of dendrite arborization using cell type-specific RNA metabolic labeling. ***PLOS ONE***. Dec 2; 15(12), e0240386. doi: 10.1371/journal.pone.0240386 [332]

3.1 Abstract

Obtaining neuron transcriptomes is challenging; their complex morphology and interconnected microenvironments make it difficult to isolate neurons without potentially altering gene expression. Multidendritic sensory neurons (md neurons) of *Drosophila* larvae are commonly used to study peripheral nervous system biology, particularly dendrite arborization. I sought to test if EC-tagging, a biosynthetic RNA tagging and purification method that avoids the caveats of physical isolation, would enable discovery of novel regulators of md neuron dendrite arborization. Our aims were twofold: discover novel md neuron transcripts and test the sensitivity of EC-tagging. RNAs were biosynthetically tagged by expressing CD:UPRT (a nucleobase-converting fusion enzyme) in md neurons and feeding 5-ethynylcytosine (EC) to larvae. Only CD:UPRT-expressing cells are competent to convert EC into 5-ethynyluridine-monophosphate which is subsequently incorporated into nascent RNA transcripts. Tagged RNAs were purified and used for RNA-sequencing. Reference RNA was prepared in a similar manner using 5-ethynyluridine (EUd) to tag RNA in all cells and negative control RNA-seq was performed on “mock tagged” samples to identify non-specifically purified transcripts. Differential expression analysis identified md neuron enriched and depleted transcripts. Three candidate genes encoding RNA-binding proteins (RBPs) were tested for a role in md neuron dendrite arborization. Loss-of-function for the m6A-binding factor Ythdc1 did not cause any dendrite arborization defects while RNAi of the other two candidates, the poly(A) polymerase Hiiragi and the translation regulator Hephaestus, caused significant defects in dendrite arborization.

3.2 Introduction

Neuron development requires regulation of gene expression at the transcriptional and post-transcriptional levels. *Drosophila* peripheral nervous system (PNS) neurons provide a useful model for investigating these mechanisms. Sensory neurons of the larval PNS are classified according to dendrite morphology: external sensory and chordotonal neurons have a single dendrite, bipolar dendrite neurons have two unbranched dendrite projections, and multidendritic (md) neurons have more complex dendritic arborization. Md neurons innervate the larval body wall and function as touch receptors, proprioceptors, thermoreceptors, or nociceptors. Md neurons have proven useful for investigating the molecular mechanisms that control dendrite arborization . Foundational work used a mutagenesis screen to identify genes that regulate dendrite arborization [333]. Others have taken a reverse genetics approach and tested candidates through RNA-interference (RNAi) based on the functional properties of candidates [65], [276]. The ability to induce neuron-specific RNAi in *Drosophila* makes reverse genetics an attractive approach and the efficacy of candidate choice can be improved by selecting genes from neuron-specific transcriptome data.

Transcriptome profiling of dendritic arborization (da) neurons, a subclass of md neurons, has been performed using fluorescence-activated cell sorting (FACS) [334] or magnetic bead-based purification [64]. These studies used differential expression data to select candidates and demonstrated roles for those genes in da neuron dendrite arborization. One caveat of physical isolation is that neurons are removed from their natural environment and undergo processing prior to RNA extraction, possibly inducing transcriptional and post-transcriptional responses that do not reflect *in vivo* gene expression. An alternative approach is to use biosynthetic RNA tagging methods that do not require physical isolation and enrich for nascent and recently-transcribed mRNAs [223]. These methods use metabolic labeling, under *in vivo* conditions, to generate tagged RNAs in the cells of interest. Tagged RNAs are subsequently purified from total RNA of animals or tissues. We recently described a cell type-specific biosynthetic RNA tagging method called EC-tagging [280]. EC-tagging works via targeted expression of a nucleobase-converting fusion enzyme composed of cytosine deaminase and uracil phosphoribosyltransferase (CD:UPRT). Metazoans lack cytosine deaminase activity and have varying endogenous uracil phosphoribosyltransferase activity, depending on organism or cell type [272], [335]. Only cells expressing CD:UPRT are competent to convert the bio-orthogonal base 5-ethynylcytosine (5-EC) into 5-ethynyluracil (via CD activity) and subsequently into 5-ethynyluridine monophosphate (via

transgenic UPRT and endogenous pathways) which is ultimately incorporated into nascent RNAs. The 5-ethynyl group allows click-chemistry-based biotinylation of tagged RNAs and subsequent purification on streptavidin beads. We previously demonstrated the utility of EC-tagging in the *Drosophila* central nervous system (CNS) [280]. This initial work used a microarray platform to analyze transcriptomes of relatively large populations of neurons (the entire larval CNS and the mushroom body neurons). To further test the specificity and sensitivity of this technique and to discover novel regulators of dendrite arborization, here we combine EC-tagging with RNA-sequencing to generate md neuron transcriptome profiles.

3.3 Results

3.3.1 EC-tagging enriches for larval md neuron-specific transcripts

To identify genes transcribed in all md neurons, we used *Gal4*$^{109(2)80}$ [333] to drive *UAS-CD:UPRT* and fed 5EC for 12 hours to L3 larvae staged between 72 – 84 hours after hatching. Though formed in embryos, md neuron dendrites continue growth, elongation and/or arborization throughout the L3 stage [334], thus we predicted relevant genes of interest would be transcribed during this timeframe. Based on a previously described neural EC-tagging time-course [280], we estimate it takes six hours before ingested 5EC is metabolized to the point that widespread RNA tagging occurs in target neurons. The twelve-hour 5EC feeding is therefore expected to generate a population of tagged RNAs synthesized over approximately six hours. At the end of 5EC feeding, larval carcass (containing primarily muscle, epidermis, and the peripheral neurons of interest) was dissected to remove CNS neurons that express *Gal4*$^{109(2)80}$. A reference sample was prepared by feeding 5-ethynyluridine (5EUd) to stage-matched *UAS-CD:UPRT* larvae, in the absence of any Gal4. 5EUd is incorporated into RNA independent of CD:UPRT and thus provides a reference containing mRNAs transcribed in all cells over the same labeling period. As a negative control, we prepared “mock-tagged” samples in which larvae were not fed 5EC or 5EUd but were subjected to the same carcass dissection and RNA processing. The mock sample serves as a control for the stringency of the purification and allows identification of transcripts that may be purified independent of EC-tagging. This type of mock reference has proven useful in other biosynthetic RNA labeling experiments [268], [336].

For all three sample types (5EC-tagged, 5EUd-tagged and mock-tagged), equal amounts of total RNA were biotinylated and applied to streptavidin beads. RNA captured on the beads was directly used to prepare sequencing libraries. The number of mapped reads per sample agreed with the expected yield of tagged RNA: 5EUd-tagging (expected high yield, RNA tagging in all cells) gave 48 – 56.6 million reads, 5EC-tagging (expected low yield, RNA tagging only in rare md neurons) gave 2.7 – 7.7 million reads, and mock-tagging (background) gave 0.11 – 0.13 million reads. 5EC-tagged biological replicates and 5EUd-tagged biological replicates had a high degree of RNA-seq correlation, while the correlation for mock-tagged replicates was much lower (Figure 3.1).

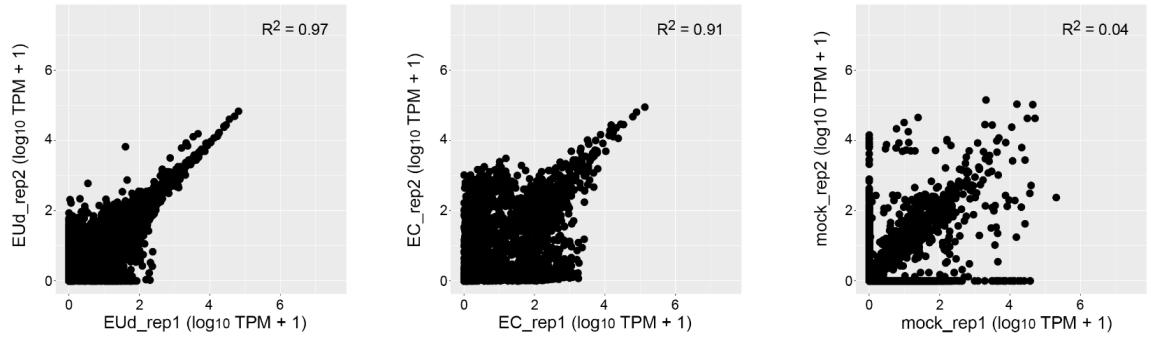

Figure 3.1: Transcript level correlations for biological replicates. 5EC-tagged biological replicates and 5EUd-tagged biological replicates had a high degree of RNA-seq correlation, while the correlation for mock-tagged replicates was much lower. TPM = transcripts per million

To identify transcripts enriched in md neurons, we performed differential expression (DE) analysis to compare 5EC-tagged RNA (EC-RNA) and 5EUd-tagged RNA (ref-RNA). This differential expression analysis was performed using two versions of the ref-RNA: 1) the complete RNA-seq dataset and 2) a randomly generated subset of 2.7 million reads (see “Approach” section below). The random subset matches the read depth of the lowest yield EC-RNA library, thus controlling for possible sample size effects.

DE analysis identified 937 enriched transcripts and 236 depleted transcripts (minimum two-fold difference and adjusted p-value < 0.05). To address potential non-specific purification among the enriched transcripts, we compared transcript levels between EC-RNA and mock-RNA. This comparison identified 85 transcripts with no significant enrichment compared to mock-RNA, thus reducing the list of md

neuron transcripts to 852. Similar background correction for depleted transcripts is not possible since transcripts that are rare or absent in md neurons are expected to be low in EC-RNA and mock-RNA. In the background-corrected dataset, known md neuron transcripts are among the most significantly enriched and known muscle-specific transcripts are among the most significantly depleted (Figure 3.2). The top 60 enriched or depleted genes are listed in (Figure 3.3).

EC-RNA compared to the subset ref-RNA yielded 571 enriched transcripts and 130 depleted transcripts (minimum two-fold difference and adjusted p-value < 0.05) and the background correction procedure removed 39 transcripts from the enriched list. Enriched and depleted transcripts were similar regardless of the type of ref-RNA used (data not shown). We also performed gene ontology (GO) analysis (Tables 3.1A & 3.1B) on the complete ref-RNA DE results (Figure 3.4A) and the subset ref-RNA DE results (Figure 3.4B). Both approaches yielded multiple neuron-specific GO categories including “peripheral nervous system development” and “dendrite morphogenesis”. The “synaptic growth at neuromuscular junction” GO category reflects the fact that enriched genes in this category function in the synapses of motor neurons and md sensory neurons. Non-neural GO categories, “dorsal closure” and “border follicle cell migration”, reflect the fact that many neurite growth or morphogenesis genes (e.g., *stathmin*, *shot*, *kay*, *shn*, *aop*) are also involved in these processes. In addition to the EC-tagged data, we performed GO analysis on DE results comparing mock-RNA to the complete or subset ref-RNA. Importantly, the mock-tagged DE data did not result in any significant GO category enrichment.

Given the agreement between EC-RNA compared to the full or subset ref-RNA, we focused subsequent analyses on the background-corrected EC-RNA versus full ref-RNA. In addition to the genes listed in (Figure 3.3), this dataset contains many previously described md neuron genes (according to Flybase annotations and associated references), including transcription regulators (*ab*, *ttk*, *stan*, *cnc*, *jim*, *kay*, *gro*), RNA-binding factors (*bel*, *Caper*, *Fmrp*, *sqd*, *stau*, *rump*), ion channels (*Piezo*, *SK*), signal receptors and transducers (*EcR*, *Egfr*, *Rac1*, *spin*, *puc*), and cytoskeletal factors (*spas*, *shot*). We also identified multiple transcripts encoding general regulators of neurotransmission, including *Frq1*, *brp*, *Csp*, and *Rim*.

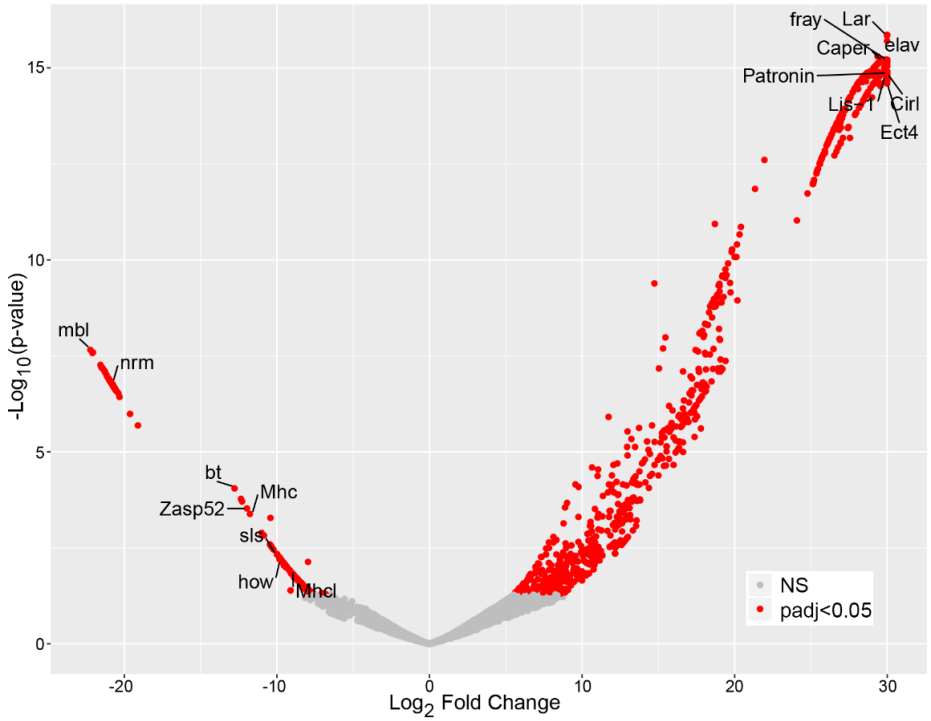

Figure 3.2: Identification of md neuron enriched and depleted transcripts.
Volcano plot of differential expression results showing the log2 fold change for EC-tagged TPM / EUd-tagged TPM (x-axis) and the adjusted p-value for each transcript (y-axis). NS = not significant. Select genes with known md neuron expression (enriched side of plot) and known muscle expression (depleted side of plot) are labeled.

While differences in experimental design and target cell populations limit the validity of broad comparisons between our data and prior transcriptome studies, we selected two gene lists from prior studies to compare with our enriched gene set. Iyer et al. identified 40 transcription factor genes enriched in class I and/or class IV da neurons compared to whole larvae [64]. Our enriched gene set contains 6 of these 40 genes, a moderate but significant over-representation (Fisher's exact test comparing representation in the EC-RNA dataset to representation in the Drosophila genome, p-value = 0.03). Hattori et al. identified 24 genes expressed in class I and/or class IV da neurons for which RNAi caused dendritic arborization phenotypes [334]. Our md neuron enriched gene set contains 10 of these 24 genes, a significant over-representation (Fisher's exact test, p-value = 5×10^{-6}).

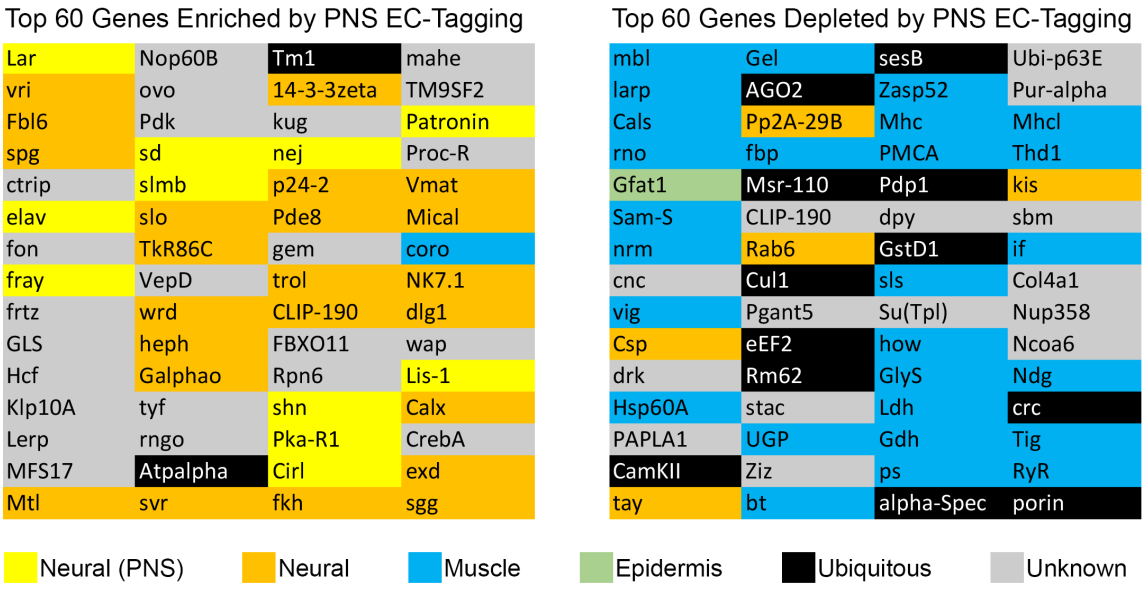

Figure 3.3: Top md neuron enriched and depleted transcripts.
Only named genes are included, genes known only by "CG number" were excluded. The primary tissue expression pattern is color coded. Tissue expression was determined by searching Flybase annotations and published literature. "Neural (PNS)" indicates known expression in larval md neurons. "Neural" indicates expression in the central nervous system at any stage. "Muscle" indicates expression in any type of muscle at any stage. "Epidermis" indicates expression in epidermis at any stage. "Ubiquitous" indicates either widespread expression or evidence of expression in both neurons and muscle. "Unknown" indicates the literature do not support assignment to any of the other categories

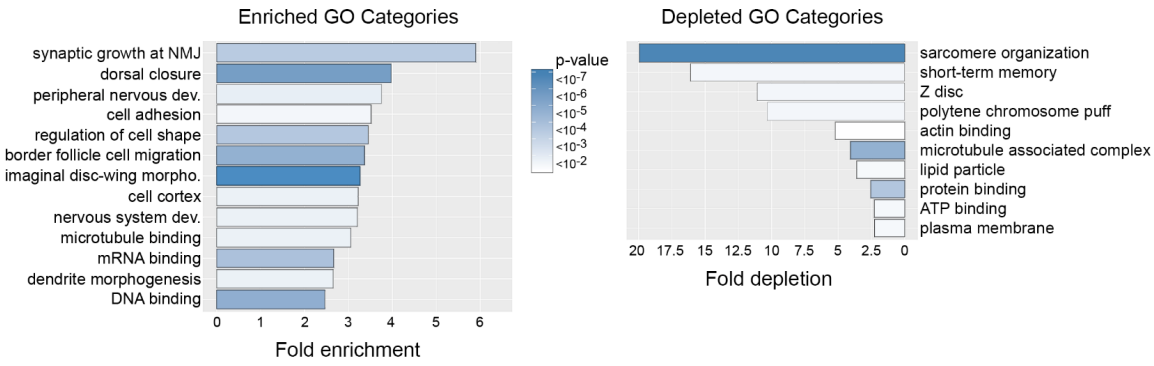

Figure 3.4A: Gene ontology of enriched and depleted transcripts using complete ref-RNA DE results. Observed / expected value = frequency of category genes in EC-RNA / frequency in the Drosophila genome. Heatmap = Bonferroni-corrected *P*-values. NMJ = neuromuscular junction.

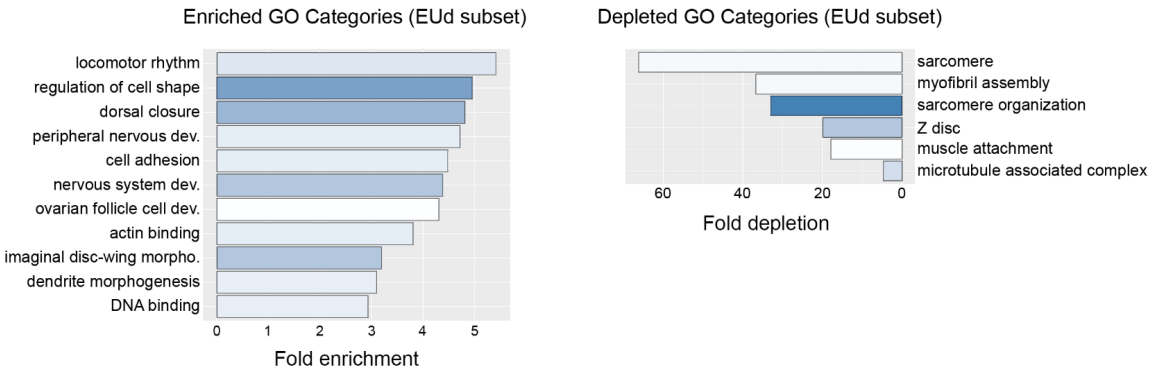

Figure 3.4B: Gene ontology of enriched and depleted transcripts using subset ref-RNA DE results (derived from the randomly generated subset of 2.7 million reads). Observed / expected value = frequency of category genes in EC-RNA / frequency in the Drosophila genome. Heatmap = Bonferroni-corrected *P*-values.

GO Term	Definition	*P*-Value	FDR	Count	Fold Change
0051124	Synaptic growth at NMJ	$1.4x10^{-4}$	$1.3x10^{-4}$	15	5.9
0007391	Dorsal closure	$6.9x10^{-6}$	$6.5x10^{-6}$	26	4.0
0007422	PNS development	$1.7x10^{-3}$	$1.6x10^{-3}$	20	3.8
0007155	Cell adhesion	$2.4x10^{-3}$	$2.3x10^{-3}$	21	3.5
0008360	Regulation of cell shape	$9.6x10^{-4}$	$9x10^{-4}$	23	3.5
0007298	Border follicle cell migration	$7.2x10^{-5}$	$6.7x10^{-5}$	28	3.4
0007476	Imaginal disc wing morphogenesis	$6.5x10^{-9}$	$6.1x10^{-9}$	45	3.4
0005938	Cell cortex	$2.2x10^{-3}$	$7.3x10^{-3}$	21	3.2
0007399	Nervous system development	$3.6x10^{-3}$	$3.4x10^{-3}$	23	3.2
0008017	Microtubule binding	$4.1x10^{-3}$	$1.1x10^{-2}$	22	3.1
0003729	mRNA binding	$7.2x10^{-4}$	$1.8x10^{-3}$	31	2.7
0048813	Dendrite morphogenesis	$2.8x10^{-3}$	$2.6x10^{-3}$	31	2.7
0043565	Sequence-specific DNA binding	$3x10^{-5}$	$7.7x10^{-5}$	44	2.5

Table 3.1A: Enriched Gene Ontology (GO) categories in md neurons.
Gene Ontology (GO) analysis using DAVID. *P*-values are Bonferroni-corrected values. NMJ = Neuromuscular junction. PNS = peripheral nervous system.

GO Term	Definition	*P*-Value	FDR	Count	Fold Change
0045214	Sarcomere organization	$7.1x10^{-7}$	$1.3x10^{-6}$	10	19.9
0007614	Short-term memory	$2.8x10^{-3}$	$5.3x10^{-3}$	7	16.1
0030018	Z disc	$7.8x10^{-3}$	$4.2x10^{-2}$	7	11.1
0005703	Polytene chromosome puff	$2.4x10^{-3}$	$1.3x10^{-2}$	8	10.3
0003779	Actin binding	$1.1x10^{-2}$	$5.8x10^{-2}$	11	5.2
0005875	Microtubule associated complex	$2.2x10^{-5}$	$1.2x10^{-4}$	22	4.1
0005811	Lipid particle	$2.3x10^{-3}$	$1.2x10^{-2}$	18	3.6
0005515	Protein binding	$7.6x10^{-4}$	$4x10^{-3}$	31	2.5
0005524	ATP binding	$5.4x10^{-3}$	$2.8x10^{-2}$	32	2.3
0005886	Plasma membrane	$5.7x10^{-3}$	$3.1x10^{-2}$	32	2.3

Table 3.1B: Depleted Gene Ontology (GO) categories in md neurons.
Gene Ontology (GO) analysis of genes enriched in md neurons using DAVID functional annotation clustering. *P*-values are Bonferroni-corrected values.

3.3.2 Candidate testing identifies novel regulators of md neuron dendrite arborization

We next sought to test the function of novel candidate genes in md neuron dendrite arborization. We focused on genes encoding mRNA-binding proteins (a significantly enriched GO category, (Figure 3.4A)) based on our interest in post-transcriptional control of mRNA processing [126]. Out of 20 enriched RNA-binding proteins (RBPs), 10 (*rump*, *fus*, *bru1*, *sqd*, *stau*, *shep*, *elav*, *Fmr1*, *BicD*, and *Caper*) have previously-described functions in md neuron dendrite arborization (based on Flybase annotations or an RNAi screen of RBPs [276]. The RNAi screen of Olesnicky et al. [276] tested 7 additional RBPs that we identified as md neuron-enriched but did not detect any dendrite arborization defects, suggesting these RBPs have functions irrelevant to dendrite morphogenesis. We focused on the remaining 3 RBPs with no available md neuron information: *ythdc1* (also known as *YT521-B*), *hiiragi* (*hrg*), and *hephaestus* (*heph*). Ythdc1 is a nuclear-localized m6A binding protein that regulates alternative splicing [337]. Hiiragi is a poly(A) polymerase that acts on nascent mRNAs and regulates poly(A) tail length of cytoplasmic mRNAs in oocytes [338]. Hephaestus is a polypyrimidine tract binding protein that represses translation of *oskar* in oocytes [339].

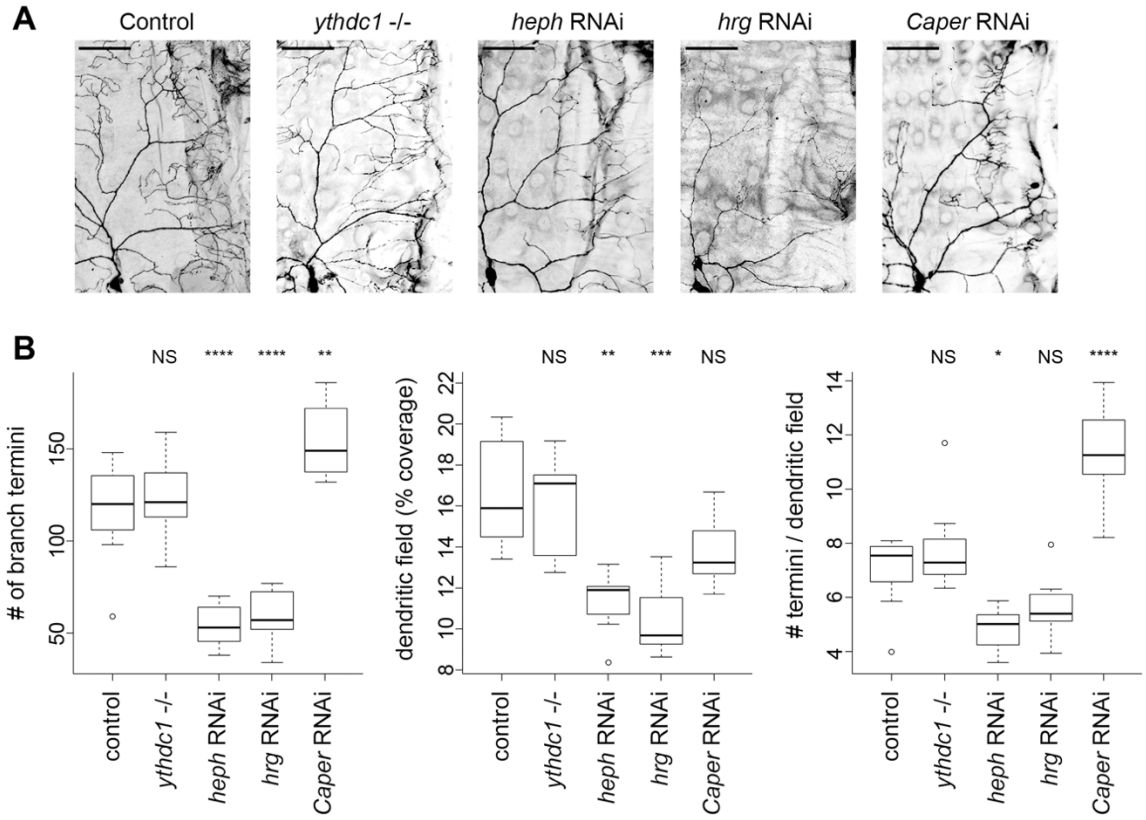

Figure 3.5. Identification of novel regulators of md neuron dendrite arborization. (A) Dendrite arborization in control and mutant class IV ddaC neurons. A representative image is shown for each genotype. The same region was analyzed in all cases, with the cell body positioned at lower left. Larva anterior is to the left and dorsal is at the top. Scale bar = 50 mm. (B) Quantification of dendrite arborization. Within the window applied to all neurons (as shown in panel A), the number of branch termini were counted, and the total dendrite length was traced & quantified (pixels) then divided by the total pixels of the window to calculate the dendritic field (% coverage). The number of termini per neuron was divided by the dendritic field % coverage to calculate # termini / dendritic field. Sample sizes: control n = 9, *ythdc1-/-* n = 9, *heph* RNAi n = 8, *hrg* RNAi n = 8, *Caper* RNAi n = 8. Data were analyzed using ANOVA with Tukey HSD post-test. *P*-value code: NS=non-significant, **** ≤ 0.0001, *** ≤ 0.001, ** ≤ 0.01, * ≤ 0.05.

As shown in (Figure 3.5) above, we crossed a single *UAS-RNAi* line for each gene of interest to $Gal4^{477}$, *UAS-mCD8::GFP* [276]. The membrane-tethered GFP

allowed us to measure the number of dendrite branch termini and dendritic field size in ddaC neurons of late L3 larvae. *Gal4^{477}* expression begins in newly differentiated class IV da neurons of embryos and continues throughout larval development [340]. *Gal4^{477}*, *UAS-mCD8::GFP* crossed to wildtype served as a negative control. As a positive control, we selected a known md neuron RBP enriched in our dataset, *Caper*. Caper regulates alternative splicing and is required for proper dendrite arborization of the ddaC class IV da neuron [187]. *Caper* RNAi caused a significant increase in dendrite branch termini but no increase in dendritic field size since the terminal branches tended to be short and tightly clustered (Figure 3.5). These *Caper* RNAi results are very similar to the previously-described *Caper* loss-of-function phenotype [187]. For the analysis of *ythdc1*, we used a previously described loss of function mutant [341] combined with *Gal4^{477}*, *UAS-mCD8::GFP* as well as a *ythdc1* RNAi line. Neither *Ythdc1* loss of function (Figure 3.5) nor *ythdc1* RNAi (data not shown) affected the number of dendrite branch termini or field coverage. In contrast, *Heph* RNAi caused a significant decrease in the number of branch termini and field size (Figure 3.5). *Hrg* RNAi also caused a significant decrease in branch termini and field size, but the termini / field size value was not significantly different from controls (Figure 3.5). While limited to the individual RNAi lines tested, these results suggest that *heph* knockdown primarily affects branching, resulting in fewer termini and reduced dendritic field size, while *hrg* knockdown primarily affects dendrite growth without directly affecting branching.

3.4 Discussion

We selected larval multidendritic (md) sensory neurons for transcription profiling for two reasons: 1) this cell population presents a good target for testing the specificity and sensitivity of EC-tagging and 2) md neurons have previously been used to identify post-transcriptional regulators of dendrite arborization and we reasoned that EC-tagging would enable identification of additional genes in this category. Our prior EC-tagging work (Chapter 2 above [280]) used a microarray platform and focused on relatively large populations of cells (all neurons of the central nervous system and mushroom body neurons). In contrast, this work demonstrates that EC-tagging can be combined with RNA-seq and is sensitive enough to identify transcripts in a rare neuronal population. We estimate there are 484 md neurons per larva (22 md neurons per hemi-segment [17]) compared to tens of thousands of cells in the larval carcass. Using EUd-tagged and mock-tagged references, we obtained significant enrichment of expected md sensory neuron transcripts and a list of potential novel regulators of md neuron development and function.

Neuronal metabolic RNA labeling experiments have revealed that profiling newly transcribed mRNAs can reveal gene expression dynamics that are missed by more traditional steady-state measurements [17], [271]. Analysis of mRNAs synthesized over a relatively short period likely aided our detection of transcripts that have a high rate of decay, such as transcription factors, signaling factors, and RNA binding proteins (classes of genes we have shown to encode low stability mRNAs [126]). For example, in the embryonic nervous system, mRNAs encoding the three RBPs we selected for analysis (*ythdc1*, *heph*, and *hrg*) all have below average half-lives [126]. As previously described [223], metabolic RNA tagging approaches are most effective when comparing purified target cell RNA to a reference generated by metabolic tagging in all cell types of the starting material (tissue or whole animal). For this reason, any genes transcribed in more abundant cells of the carcass are unlikely to be identified as md neuron-enriched in this study. For example, Iyer et al. identified the transcription factors *Poxm* and *Hand* as transcribed in da neurons [64], but these genes are also transcribed in larval muscle and are abundant in our EUd ref-RNA. EC-tagging may be best suited for the discovery of differentially transcribed genes while physical isolation methods such as FACS are better suited for defining complete transcriptomes. Depending on experiment goals, the potential for a less comprehensive transcriptome profile generated by EC-tagging should be weighed against the risks of perturbing gene expression through the use of physical isolation.

3.5 Approach

3.5.1 *Drosophila* genetics

The following lines were obtained from the Bloomington *Drosophila* Stock Center: Oregon-R-P2 (wildtype) (stock # 2376), $Gal4^{477}$, *UAS-mCD8::GFP* (stock # 8746), *UAS-ythdc1{RNAi}* (stock #34627), *UAS-hrg{RNAi}* (stock # 33378), *UAS-heph{RNAi}* (stock # 55655). For EC-tagging, $Gal4^{109(2)80}$ (stock # 8769) was combined with *UAS-CD:UPRT* on the 3rd chromosome (stock # 77120) to make the stable line $Gal4^{109(2)80}$*; UAS-CD:UPRT*. The ythdc1 loss of function mutant, *YT521-B[NP2]/ TM6C -1*, was provided by Dr. Eric Lai.

3.5.2 EC-tagging, RNA purification and library preparation

5-ethynylcytosine (5EC) was synthesized as previously described [280]. Biological replicates were prepared by carrying out 5EC, 5EUd, or mock feeding,

carcass dissections and RNA processing independently. Larvae were reared at 25°C and fed 1 mM 5EC or 5EUd from 72 – 84 hours after hatching. Total carcass RNA was extracted using Trizol. For each treatment, duplicate 20 µg RNA samples (obtained from 25 – 30 carcasses) were biotinylated using Click-iT Nascent RNA Capture reagents (ThermoFisher) and purified on Dynabeads MyOne Streptavidin T1 magnetic beads (ThermoFisher) as previously described [280].

After the final wash, beads were combined with NuGen Ovation Universal RNA-Seq reagents, following the manufacturer's protocol beginning at the step of first strand cDNA synthesis. Primer annealing and cDNA synthesis were performed in a heated lid thermomixer to ensure beads did not settle. After cDNA synthesis, beads were washed three times with 500 µl 1X PBS, discarding the supernatant each time. Beads were resuspended in 50 µl RNaseA/T1/H elution mix (1X RNAse H buffer, 12.5 mM D-biotin, RNase A/T1 cocktail (0.1 U/µl), RNase H (0.1 U/µl)) and incubated at 37°C for 30 minutes at 1,000 rpm in a thermomixer. The reaction was stopped by adding 1 µl of DMSO and heating at 95°C for 4 minutes. Beads were collected on a magnet and the supernatant was mixed with DNA binding buffer and applied to a Zymogen DNA Clean and Concentrator-5 column to purify first-strand cDNA. Following purification, the duplicate samples were combined into a single tube and the volume was reduced to 10 µl using a SpeedVac concentrator. The samples were then used to make second-strand cDNA according to the NuGen Ovation Universal RNA-Seq protocol, including adapter ligation and ribosomal RNA depletion using a *Drosophila*-specific AnyDeplete rRNA primer mixture. Libraries were amplified and purified according to the NuGen protocol and quality was assessed using an Agilent Bioanalyzer DNA high-sensitivity chip.

3.5.3 RNA-sequencing and bioinformatics

Sequencing was performed on a HiSeq 2500. Sequence data were trimmed using *Trimmomatic* prior to mapping to the *Drosophila melanogaster* cDNA transcriptome (BDGP6) using *kallisto*. Differential expression analysis was performed using *DESeq2* [344]. The EUd-RNA reference subset was obtained using the *shuf* command in UNIX to randomly select 2.7 million reads from the EUd-RNA BAM files. Gene ontology analysis was performed using DAVID functional annotation clustering [328], with the pre-loaded *Drosophila melanogaster* gene set as background, high classification stringency and default settings for all other parameters. Unnamed genes (those identified only by CG number) were excluded from GO analysis. Only categories with an enrichment of ≥ 2.0 and Bonferonni-corrected p-values of < 0.01 were considered significant.

3.5.4 Imaging and quantification of dendrite morphology

Dendrite morphology was analyzed in wandering larval stages. Larval fillet preparations were fixed using formaldehyde and stained with rat anti-mCD8 (ThermoFisher) at 1:100 followed by Alexa Fluor 488 anti-rat secondary antibody (ThermoFisher) at 1:200. Imaging was performed using a Zeiss LSM 880 confocal microscope. The number of branch termini and total dendrite length were quantified in Z-series projections. Branch terminal counting and dendrite tracing were performed using Adobe Photoshop and dendrite length (pixels) were quantified using Zeiss Zen Blue software. Dendritic field (% coverage) values were calculated by dividing the number of pixels in the dendrite trace by the total number of pixels in the area analyzed (the fixed-size analysis window applied to all neurons). All statistical analyses were performed in R. Normal distribution of the data for each genotype was confirmed using the Wilk-Shapiro test. Statistical significance was determined using ANOVA with Tukey HSD post-test.

Chapter 4

Synthesis & Future Directions

The work presented in this study provides a novel framework of genome-wide analysis of RNA metabolism that can be utilized to study transcriptional & post-transcriptional regulation of gene expression with a high level of specificity & sensitivity. As the list of biological functions performed by RNA continues to expand, especially with genomic research moving away from isolated cultures of cells and into more complex environments like tissues and whole animals, developing new and highly stringent methods to achieve nascent & bulk RNA isolation & analysis under *in vivo* conditions with high spatiotemporal control becomes a crucial limiting step to fully understand RNA expression and function in complex environments. The results of this study show that EC-tagging overcomes nearly all the major hurdles of cell type-specific tagging of RNA. First, we show that a dual-enzyme system is highly robust and results in very specific RNA tagging. We also demonstrate that our method is amenable to split-enzyme designs, which will be valuable for fine-tuning cell targeting. Additionally, this work demonstrates that EC-tagging is sensitive enough to identify transcripts from a rare neuronal subpopulation of 484 neurons. Perhaps most importantly, we show that our approach allows *in vivo* analyses, even within complex tissue environments such as the nervous system.

Profiling of the transcriptome of the *Drosophila* multidendritic (md) sensory neurons using EC-tagging also helped shed some light into how post-transcriptional regulation of gene expression can regulate neurite development. RNA-binding proteins (RBPs) have previously been shown to play important roles in md neuron dendrite arborization [276]. Given the significance of this class of post-transcriptional regulators in dendrite arborization, we prioritized the analysis of RBPs from among all the candidate regulators of md neuron development identified in this study. Olesnicky et al. used a comprehensive RNAi-based screen to identify a large number of RBPs that affect class IV da neuron dendrite morphogenesis. We identified three additional md neuron-enriched RBPs of interest: *ythdc1*, *hrg* and *heph*. Knockdown of *hrg* and *heph* resulted in dendrite arborization defects while *ythdc1* loss-of-function and knockdown had no effect. The lack of a dendrite arborization phenotype in the *ythdc1* mutants may indicate this is a false positive (not expressed in multidendritic (md) sensory neurons). It is

difficult to test this possibility without a Ythdc1 antibody, but the widespread expression of Ythdc1 in CNS neurons [337] suggests a general neural function. An alternative explanation is that Ythdc1 controls splicing of transcripts that are irrelevant to dendrite arborization. *Drosophila* motor neurons that lack m^6A, the RNA modification recognized by Ythdc1, do not have growth or patterning defects but do have a moderate increase in the number of synaptic boutons and active zones per bouton [337]. Loss of Ythdc1 in multidendritic (md) sensory neurons may similarly affect synapses or synaptic activity, which are phenotypes that would not be detected in our analysis.

The *hrg* RNAi phenotype may be explained by Hrg's interaction with Orb, an ortholog of human cytoplasmic polyadenylation element binding protein 1. Hypomorphic alleles of *orb* cause dendrite arborization defects in class IV da neurons [343][344], with decreased branching and decreased field size similar to what we observed in *hrg* RNAi neurons. Hrg and Orb may regulate cytoplasmic polyadenylation in md neurons, likely targeting mRNAs encoding regulators of dendrite growth. On the other hand, Heph may affect dendrite arborization via its repression of *oskar* (*osk*) translation. Oskar is necessary for proper localization of *nanos* mRNA in class IV da neurons and *osk* loss-of-function decreases dendrite branching [344][168], similar to the phenotype we observe in *heph* RNAi neurons. *Osk* mRNA is transported along dendrites [191], [344] and Heph likely represses *osk* translation during transport, as it does in oocytes [339]. In this model, *heph* knockdown may cause a phenotype similar to *osk* loss-of-function due to altered Osk distribution in dendrites. Confirming these predicted interactions and further defining mechanisms by which Hrg and Heph control dendrite arborization will be important areas of future investigation.

It is worth noting that use of EC-tagging is not limited to studies of differential gene expression. Its usage could be expanded to address other aspects of RNA biology. For instance, subjecting the cell(s) of interest to brief pulses of 5-ethynylcytosine (5EC) can be used to directly measure transcription rates and to study the expression of rare transcripts, similar to what was done with TU-tagging [223]. An additional step of physical enrichment of the cell(s) of interest following EC-tagging pulse can overcome the very low yields of tagged RNA expected with such short pulses [345]. In addition to studying transcription rates, different aspects of post-transcriptional regulation of gene expression could be investigated by coupling EC-tagging with other tools that facilitate the analysis of particular RNA regulation processes. For example, since noncoding RNAs are expected to incorporate the 5-ethynyluridine tag, a genome-wide analysis of global noncoding

RNAs can be done or a focus on micro-RNAs can be achieved by combining EC-tagging and miRAP [259]. Cell type-specific RNA decay kinetics, on the other hand, can be measured by using the pulse-chase approach, in which the cells are exposed to untagged uridine following their exposure to 5-ethynylcytosine (5EC) for specific time intervals. By comparing the RNAs that continue to be enriched at different chase time intervals to those that are enriched after the initial pulse of 5-ethynylcytosine (5EC), we can infer the half-lives of different transcripts [126]. *In vivo* cell type-specific imaging of tagged RNA can be achieved by coupling fluorophores to the 5-ethynyluridine (5EUd) in the tagged RNAs following EC-tagging. This could help in studying trafficking kinetics & localization of RNA, as well as visualization of RNA transcription & turnover. Indeed, by coupling EC-tagging & RNA imaging, we recently found that ribosomal RNA (rRNA) is robust in neural progenitors but limited in post-mitotic neurons, supporting a model in which neuron-specific translation programs are established by rRNA inheritance [346]. Alternative splicing and the differential expression of different isoforms could also be addressed by coupling EC-tagging with one of the recently developed long-read RNA sequencing platforms (like those developed by Pacific Biosciences and Oxford Nanopore Technologies [347]). Indeed, combining metabolic RNA labeling with direct the long-read sequencing capability of Oxford Nanopore Technologies has already been demonstrated [348], [349]. Finally, combining of EC-tagging with miCLIP [350] and 5PSeq [351] has been proposed to identify neural-specific N^6-methyladenosine (m^6A) RNA profiles and the role N^6-methyladenosine (m^6A) plays in regulating mRNA translation.

With the evident advantages that novel metabolic RNA tagging techniques, like EC-tagging, provide to isolate cell type-specific RNA, big efforts have been dedicated to expanding the chemical toolkits that such techniques rely upon. For example, approaches that rely on “nucleoside recoding” and targeted “uncaging” of inert nucleoside analogue to achieve cell type-specific RNA enrichment have been developed [255]. With the continuously evolving field of metabolic RNA tagging, a comprehensive and detailed comparison of the available techniques is required to establish standards through which more optimal tools could be developed and benchmarked. This will yield an expanding set of creative applications to address important questions in developmental biology.

Appendix A

Appendix

A.1 Supplemental data

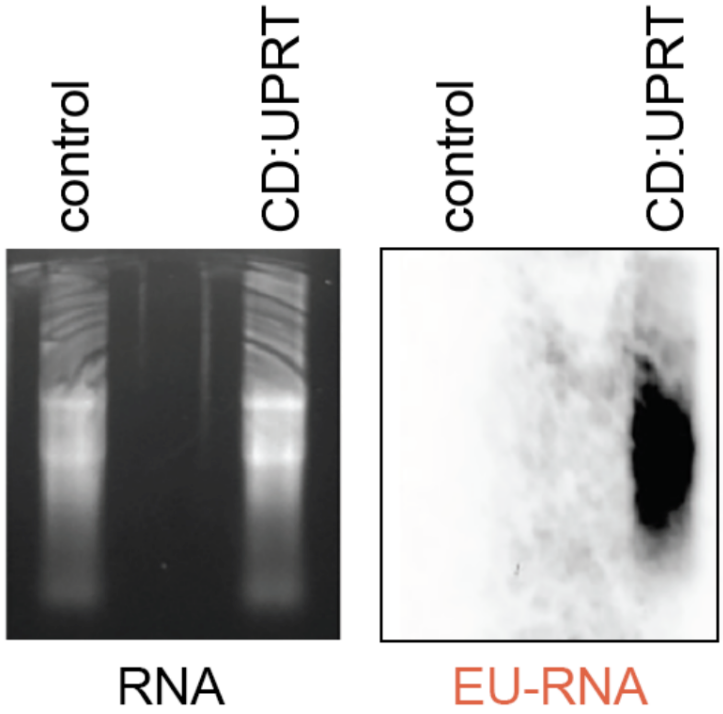

Figure A.1: EC-tagging of RNA confirmed by RNA-transfer blot. Control and CD:UPRT(+) SH-SY5Y cells were exposed to 500µM 5EC for six hours prior to total RNA extraction, biotinylation and separation on an agarose gel. Ethidium bromide-stained RNA is shown on the left. RNA was transferred to a nylon membrane and probed with streptavidin-HRP to detect EU-RNA.

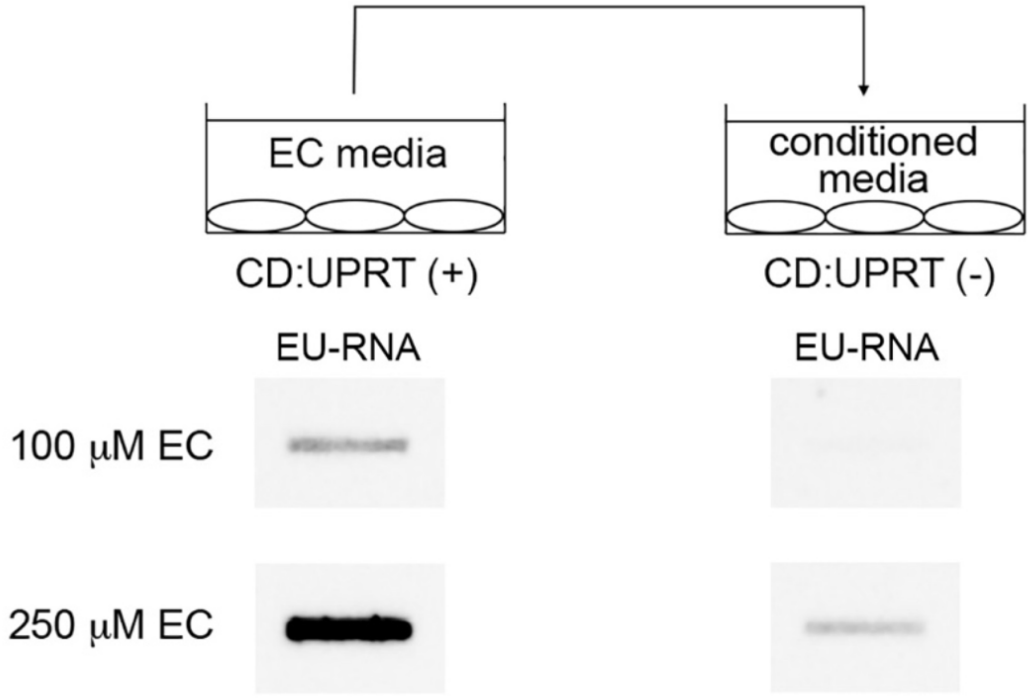

Figure A.2: CD:UPRT(+) cells exposed to 5EC excrete 5EU. The experiment design is summarized in the scheme at the top of the figure. The corresponding EU-RNA slot blot signal is shown below each cell type and condition: CD:UPRT(+) cells exposed to 5EC (left) and CD:UPRT(-) cells exposed to conditioned media (right). The concentration of 5EC added to the CD:UPRT(+) cells is listed at the left.

A

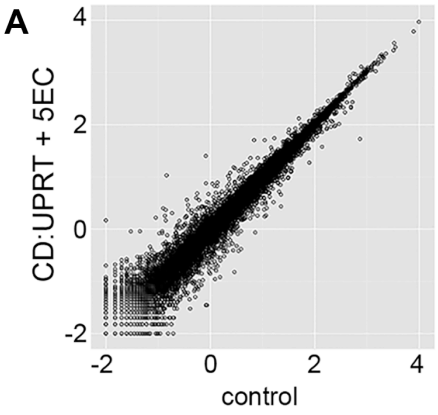

B

Sample	Reads	Bases	Mapped Reads (%)	Perfect Match (%)
CD:UPRT + 5EC 1	99,627,666	4,881,755,634	90.21	79.97
CD:UPRT + 5EC 2	98,977,612	4,849,902,988	90.22	80.07
control 1	81,134,932	3,975,611,668	82.81	73.54
control 2	83,898,655	4,111,034,095	82.44	73.13
Sample	**Mismatch (%)**	**Unique Match (%)**	**Multi-position Match (%)**	**Unmapped Reads (%)**
CD:UPRT + 5EC 1	10.24	77.11	13.1	9.79
CD:UPRT + 5EC 2	10.14	76.95	13.27	9.78
control 1	9.27	70.54	12.27	17.19
control 2	9.31	70.31	12.13	17.56

Figure A.3: RNA-seq comparison of EC-tagged vs. control HeLa cells. (A) RNA-seq counts ($\log_{10}$ of FPKM) for 19,503 genes expressed in CD:UPRT(+) cells exposed to 5EC for six hours and CD:UPRT(-) control cell that were not exposed to 5EC. (B) RNA-seq read and mapping information

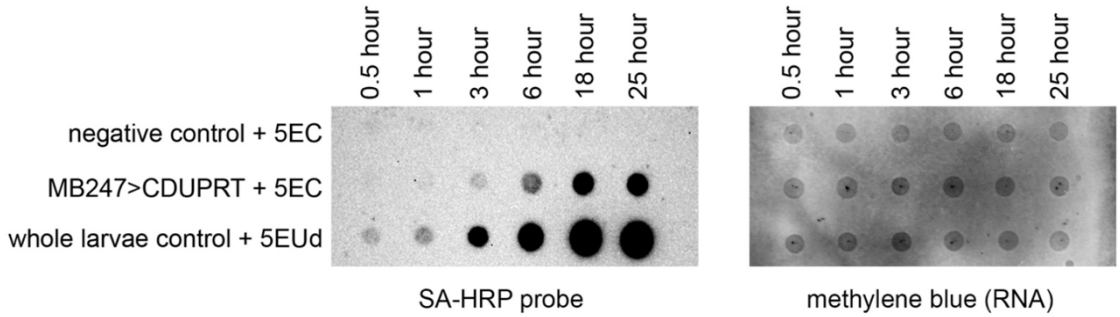

Figure A.4: Time-dependent EC-tagging. Dot blot detection of EU-RNA from L3 larvae fed 5EC for the indicated duration. Equal amounts of total RNA were loaded per sample (methylene blue stain)

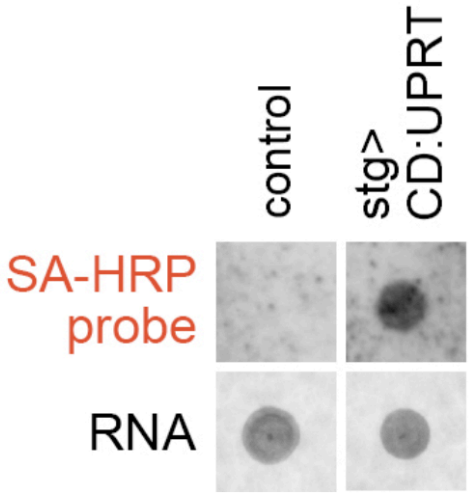

Figure A.5: *Drosophila* Embryo EC-tagging. Embryos (0 – 18 hours after egg laying) were permeabilized and treated with 1.0 mM 5EC for 3 hours using methods previously established for TU-tagging in *Drosophila* embryos [285]. Stg refers to the *GMR32C12* line that expresses Gal4 under the control of *string* regulatory elements (activating CD:UPRT expression primarily in the nervous system starting as early as the germ-band extension stage). The RNA panel shows methylene blue-stained RNA. The SA-HRP probe panel shows detection of biotinylated EU-RNA by streptavidin-HRP.

A

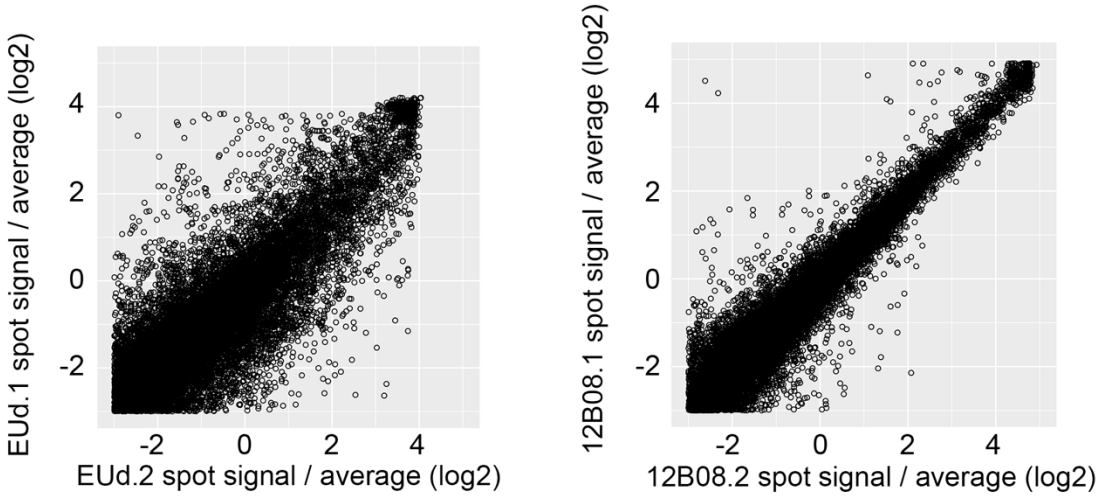

B

	EUd.1			
EUd.1	1	EUd.2		
EUd.2	**0.76**	1	12B08.1	
12B08.1	0.36	0.45	1	12B08.2
12B08.2	0.37	0.47	**0.8**	1

Figure A.6: Whole larvae EUd-tagging and 12B08 EC-tagging microarray reproducibility. (A) Individual spot signal intensity (F532 mean – background) divided by the average signal intensity of all spots, plotted for biological replicate microarrays. The EUd plot contains 28,136 spots with signal above background in both microarrays. (B) Correlation values (r-squared) for all pairwise comparisons. Biological replicate r-squared values are shown in bold type.

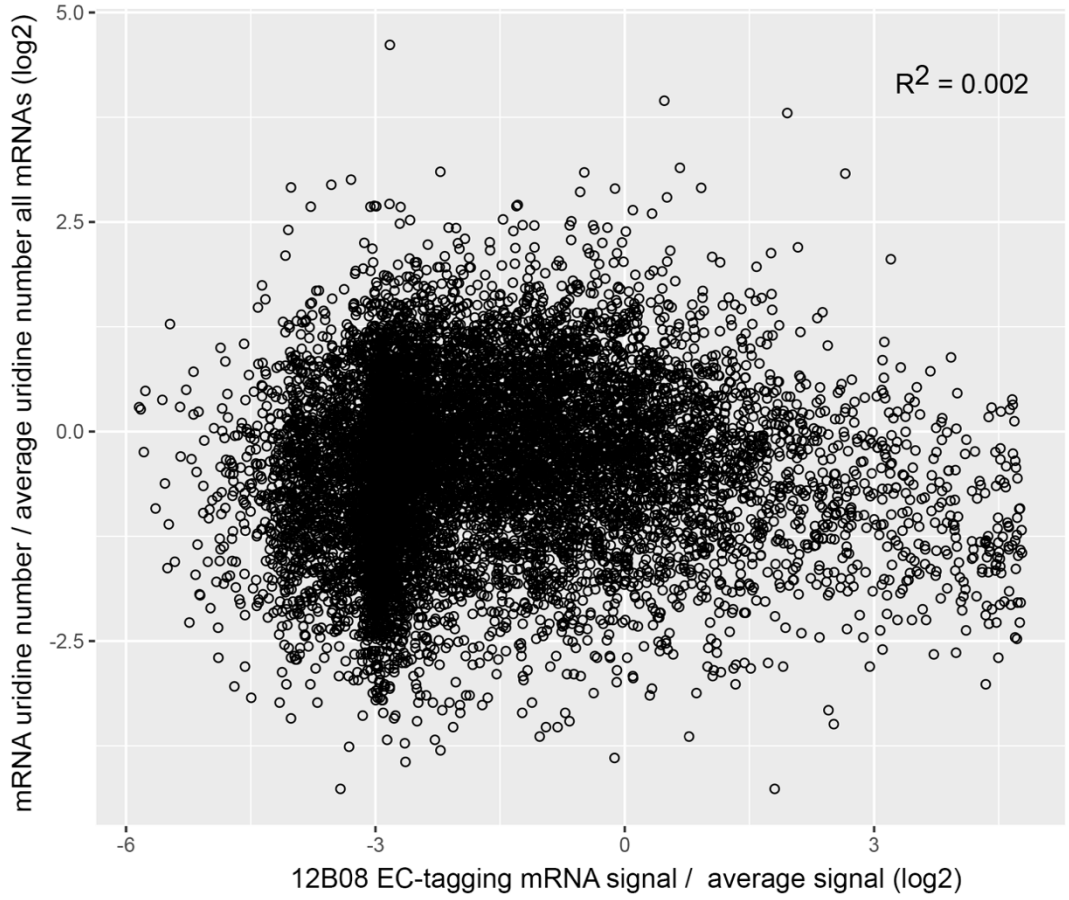

Figure A.7: No correlation between efficiency of mRNA purification and uridine number. Uridine number per transcripts was normalized to the mean for all *Drosophila* genes detected by microarray (y-axis). EC-tagging signal per gene was based on the average across 12B08 replicate microarrays divide by the average signal intensity for all genes (x-axis).

Figure A.8: Comparison of TU-tagging by CD:UPRT and UPRT. HeLa cells were transfected with vectors expressing the yeast CD:UPRT fusion or *Toxoplasma gondii* UPRT (*T.g.*UPRT), the enzyme traditionally used for TU-tagging. Control HeLa cells were transfected with empty vector. All cells were exposed to 50 μM 4-thiouracil for four hours followed by RNA extraction, biotinylation and slot blot probing with streptavidin-HRP. 5 μg of RNA was loaded for each sample.

A

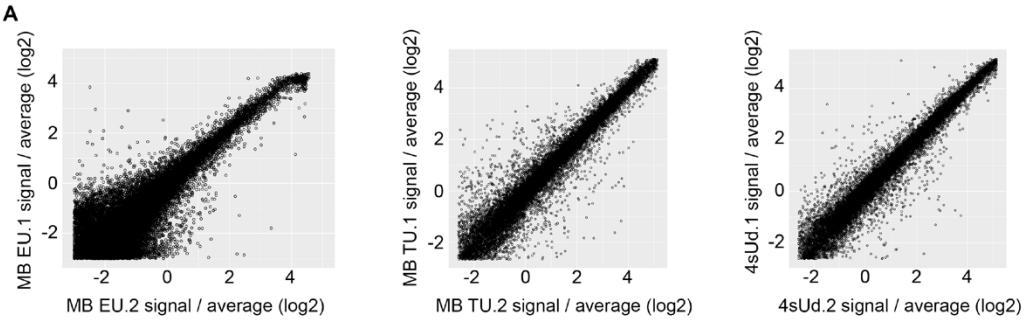

B

	MB EU.1	MB EU.2	MB TU.1	MB TU.2	EUd.1	EUd.2	4sUd.1	4sUd.2
MB EU.1	1							
MB EU.2	**0.72**	1						
MB TU.1	0.47	0.46	1					
MB TU.2	0.54	0.53	**0.95**	1				
EUd.1	0.36	0.45	0.64	0.63	1			
EUd.2	0.45	0.41	0.58	0.55	**0.76**	1		
4sUd.1	0.51	0.57	0.82	0.82	0.66	0.66	1	
4sUd.2	0.5	0.58	0.83	0.83	0.64	0.63	**0.93**	1

Figure A.9: Mushroom body EC-tagging and TU-tagging microarray reproducibility. (A) Individual spot signal intensity (F532 mean – background) divided by the average signal intensity for all spots, plotted for biological replicate microarrays. The MB EU plot contains 18,881 spots with signal above background in both microarrays. The MB TU plot contains 27,689 spots with signal above background in both microarrays. The 4sUd plot contains 28,243 spots with signal above background in both microarrays. (B) Correlation values (r-squared) for all pairwise comparisons. Biological replicate r-squared values are shown in bold type.

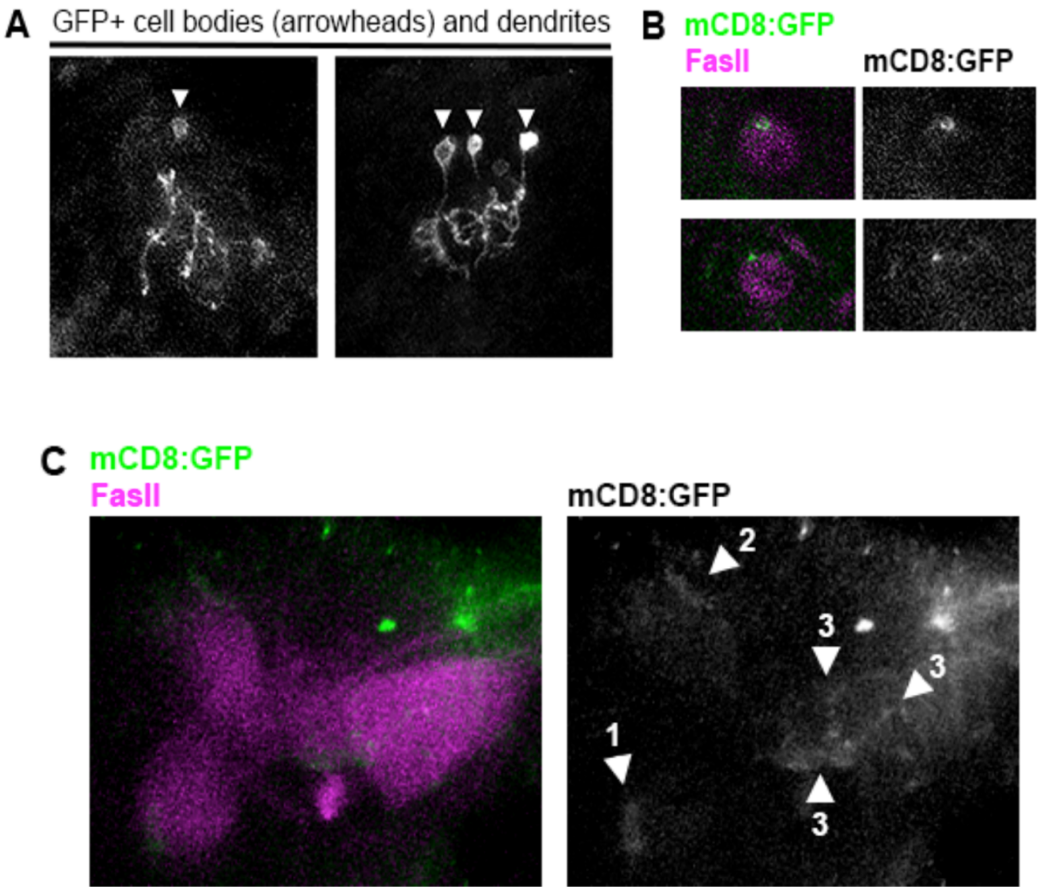

Figure A.10: *Ppk-Gal4* central brain neurons are mushroom body neurons. (A) Cell bodies and dendrite projections (with stereotypical mushroom body neuron morphology and location) identified by mCD8:GFP expression in *ppk>UAS-mCD8:GFP* larval brains. Dorsal regions from two different brains are shown, anterior is up, medial is right. (B) Axon projections of the mCD8:GFP(+) neurons in *ppk>UAS-mCD8:GFP* larval brains project through the outer edge of the mushroom body peduncle (identified by FasII stain). Examples from two different brains are shown. (C) Axons of mCD8:GFP(+) neurons in *ppk>UAS-mCD8:GFP* larval brains project through the mushroom body peduncle (arrowhead #1) and extend into the vertical lobe (arrowhead #2) and medial lobe (arrowheads labelled #3) of the mushroom body (identified by FasII stain). This minimal confocal projection only shows part of the axons within the peduncle and vertical lobe, while most of the axon pattern in the medial lobe is visible.

Bibliography

[1] A. A. Teleman, “Privileged Signaling for Brain Growth,” *Cell*, vol. 146, no. 3, pp. 346–347, Aug. 2011.

[2] H.-G. Bernstein, J. Steiner, P. C. Guest, H. Dobrowolny, and B. Bogerts, “Glial cells as key players in schizophrenia pathology: recent insights and concepts of therapy,” *Schizophrenia Research*, vol. 161, no. 1, pp. 4–18, Jan. 2015.

[3] E. M. Mohammed, “Environmental Influencers, MicroRNA, and Multiple Sclerosis,” *J Cent Nerv Syst Dis*, vol. 12, p. 1179573519894955, Jan. 2020.

[4] I. A. Droujinine and N. Perrimon, “Interorgan Communication Pathways in Physiology: Focus on *Drosophila*,” *Annual Review of Genetics*, vol. 50, no. 1, pp. 539–570, 2016.

[5] M. B. Gerstein et al., “Comparative analysis of the transcriptome across distant species,” *Nature*, vol. 512, no. 7515, pp. 445–448, Aug. 2014.

[6] S. H. Lye and S. Chtarbanova, “*Drosophila* as a Model to Study Brain Innate Immunity in Health and Disease,” *Int J Mol Sci*, vol. 19, no. 12, Dec. 2018.

[7] B. Ugur, K. Chen, and H. J. Bellen, “*Drosophila* tools and assays for the study of human diseases,” *Disease Models & Mechanisms*, vol. 9, no. 3, pp. 235–244, Mar. 2016.

[8] H. J. Bellen, C. Tong, and H. Tsuda, “100 years of *Drosophila* research and its impact on vertebrate neuroscience: a history lesson for the future,” *Nature Reviews Neuroscience*, vol. 11, no. 7, pp. 514–522, Jul. 2010.

[9] R. Urbach and G. M. Technau, “Neuroblast formation and patterning during early brain development in *Drosophila*,” *BioEssays,* vol. 26, no. 7, pp. 739–751, 2004.

[10] R. L. Miyares and T. Lee, “Temporal control of *Drosophila* central nervous system development,” *Current Opinion in Neurobiology*, vol. 56, pp. 24–32, Jun. 2019.

[11] K. H. Kang and H. Reichert, “Control of neural stem cell self-renewal and differentiation in *Drosophila*,” *Cell Tissue Res*, vol. 359, no. 1, pp. 33–45, Jan. 2015.

[12] B. J. Pearson and C. Q. Doe, “Specification of Temporal Identity in the Developing Nervous System,” *Annual Review of Cell and Developmental Biology*, vol. 20, no. 1, pp. 619–647, 2004.

[13] A. S. Bates, J. Janssens, G. S. Jefferis, and S. Aerts, “Neuronal cell types in the fly: single-cell anatomy meets single-cell genomics,” *Current Opinion in Neurobiology*, vol. 56, pp. 125–134, Jun. 2019.

[14] P. Ramon-Cañellas, H. P. Peterson, and J. Morante, “From Early to Late Neurogenesis: Neural Progenitors and the Glial Niche from a Fly’s Point of View,” *Neuroscience*, vol. 399, pp. 39–52, Feb. 2019.

[15] P. W. Johnson, C. Q. Doe, and S.-L. Lai, “*Drosophila* nucleostemin 3 is required to maintain larval neuroblast proliferation,” *Developmental Biology*, vol. 440, no. 1, pp. 1–12, Aug. 2018.

[16] K. Harding and K. White, “*Drosophila* as a Model for Developmental Biology: Stem Cell-Fate Decisions in the Developing Nervous System,” *Journal of Developmental Biology*, vol. 6, no. 4, p. 25, Dec. 2018.

[17] A. Singhania and W. B. Grueber, “Development of the embryonic and larval peripheral nervous system of *Drosophila*,” *Wiley Interdisciplinary Reviews: Developmental Biology*, vol. 3, no. 3, pp. 193–210, 2014.

[18] C. Q. Doe, “Molecular markers for identified neuroblasts and ganglion mother cells in the *Drosophila* central nervous system,” *Development*, vol. 116, no. 4, pp. 855–863, Dec. 1992.

[19] J. H. Byrne, The Oxford Handbook of Invertebrate Neurobiology. *Oxford University Press*, 2019.

[20] T. Isshiki, B. Pearson, S. Holbrook, and C. Q. Doe, “*Drosophila* Neuroblasts Sequentially Express Transcription Factors Which Specify the Temporal Identity of Their Neuronal Progeny,” *Cell*, vol. 106, no. 4, pp. 511–521, Aug. 2001.

[21] R. Grosskortenhaus, B. J. Pearson, A. Marusich, and C. Q. Doe, “Regulation of Temporal Identity Transitions in *Drosophila* Neuroblasts,” *Developmental Cell*, vol. 8, no. 2, pp. 193–202, Feb. 2005.

[22] C. Q. Doe, “Temporal Patterning in the *Drosophila* CNS,” *Annual Review of Cell and Developmental Biology*, vol. 33, no. 1, pp. 219–240, 2017.

[23] M. H. Syed, B. Mark, and C. Q. Doe, “Steroid hormone induction of temporal gene expression in *Drosophila* brain neuroblasts generates neuronal and glial diversity,” *eLife*, vol. 6.

[24] M. Baumgardt, I. Miguel-Aliaga, D. Karlsson, H. Ekman, and S. Thor, “Specification of Neuronal Identities by Feedforward Combinatorial Coding,” *PLOS Biology*, vol. 5, no. 2, p. e37, Feb. 2007.

[25] M. Landgraf and S. Thor, “Development of *Drosophila* motoneurons: Specification and morphology,” *Seminars in Cell & Developmental Biology*, vol. 17, no. 1, pp. 3–11, Feb. 2006.

[26] M. Baek and R. S. Mann, “Lineage and Birth Date Specify Motor Neuron Targeting and Dendritic Architecture in Adult *Drosophila*,” *J. Neurosci.*, vol. 29, no. 21, pp. 6904–6916, May 2009.

[27] M. D. Kim, Y. Wen, and Y.-N. Jan, “Patterning and organization of motor neuron dendrites in the *Drosophila* larva,” *Developmental Biology*, vol. 336, no. 2, pp. 213–221, Dec. 2009.

[28] M. Q. Clark, S. J. McCumsey, S. Lopez-Darwin, E. S. Heckscher, and C. Q. Doe, “Functional Genetic Screen to Identify Interneurons Governing Behaviorally Distinct Aspects of *Drosophila* Larval Motor Programs,” *G3: Genes, Genomes, Genetics*, vol. 6, no. 7, pp. 2023–2031, Jul. 2016.

[29] W. B. Grueber, L. Y. Jan, and Y. N. Jan, “Tiling of the *Drosophila* epidermis by multidendritic sensory neurons,” *Development*, vol. 129, no. 12, pp. 2867–2878, Jun. 2002.

[30] K. Yildirim, J. Petri, R. Kottmeier, and C. Klämbt, “*Drosophila* glia: Few cell types and many conserved functions,” *Glia*, vol. 67, no. 1, pp. 5–26, 2019.

[31] S. Yadav et al., “Glial ensheathment of the somatodendritic compartment regulates sensory neuron structure and activity,” *PNAS*, vol. 116, no. 11, pp. 5126–5134, Mar. 2019.

[32] N. Mora et al., “A Temporal Transcriptional Switch Governs Stem Cell Division, Neuronal Numbers, and Maintenance of Differentiation,” *Developmental Cell*, vol. 45, no. 1, pp. 53-66.e5, Apr. 2018.

[33] M. D. Abdusselamoglu, E. Eroglu, T. R. Burkard, and J. A. Knoblich, “The transcription factor Odd-paired regulates temporal identity in transit-amplifying neural progenitors via an incoherent feed-forward loop,” *BioRxiv*, p. 576736, Mar. 2019.

[34] L. F. Sullivan, T. L. Warren, and C. Q. Doe, “Temporal identity establishes columnar neuron morphology, connectivity, and function in a Drosophila navigation circuit” eLife, 8:e43482, p. 24, Feb. 2019.

[35] C. C. F. Homem, M. Repic, and J. A. Knoblich, “Proliferation control in neural stem and progenitor cells,” *Nature Reviews Neuroscience*, vol. 16, no. 11, pp. 647–659, Nov. 2015.

[36] M. Q. Clark, A. A. Zarin, A. Carreira-Rosario, and C. Q. Doe, “Neural circuits driving larval locomotion in *Drosophila*,” *Neural Development*, vol. 13, no. 1, p. 6, Apr. 2018.

[37] H. Li et al., “Fly Cell Atlas: a single-cell transcriptomic atlas of the adult fruit fly,” *BioRxiv*, p. 2021.07.04.451050, Jul. 2021.

[38] O. Birkholz, C. Rickert, J. Nowak, I. C. Coban, and G. M. Technau, “Bridging the gap between postembryonic cell lineages and identified embryonic neuroblasts in the ventral nerve cord of *Drosophila melanogaster*,” *Biology Open*, vol. 4, no. 4, pp. 420–434, Apr. 2015.

[39] H. L. and James W Truman, “Lineage mapping identifies molecular and architectural similarities between the larval and adult *Drosophila* central nervous system,” *Elife*, vol. 5, no. 13399, 2016.

[40] M. Losada-Pérez, N. García-Guillén, and S. Casas-Tintó, “A novel injury paradigm in the central nervous system of adult *Drosophila*: molecular, cellular and functional aspects,” *Disease Models & Mechanisms*, vol. 14, no. 5, Jun. 2021.

[41] W.-L. Charng, S. Yamamoto, and H. J. Bellen, “Shared mechanisms between *Drosophila* peripheral nervous system development and human neurodegenerative diseases,” *Current Opinion in Neurobiology*, vol. 27, pp. 158–164, Aug. 2014.

[42] E. Braems, P. Tziortzouda, and L. Van Den Bosch, “Exploring the alternative: Fish, flies and worms as preclinical models for ALS,” *Neuroscience Letters*, vol. 759, p. 136041, Aug. 2021.

[43] B. Lu and H. Vogel, “*Drosophila* Models of Neurodegenerative Diseases,” *Annual Review of Pathology: Mechanisms of Disease*, vol. 4, no. 1, pp. 315–342, 2009.

[44] Y. Fang and N. M. Bonini, “Axon Degeneration and Regeneration: Insights from *Drosophila* Models of Nerve Injury,” *Annual Review of Cell and Developmental Biology*, vol. 28, no. 1, pp. 575–597, 2012.

[45] K. Furusawa and K. Emoto, “Spatiotemporal regulation of developmental neurite pruning: Molecular and cellular insights from *Drosophila* models,” *Neuroscience Research*, vol. 167, pp. 54–63, Jun. 2021.

[46] C. A. Goldsmith, N. S. Szczecinski, and R. D. Quinn, “Neurodynamic modeling of the fruit fly *Drosophila melanogaster*,” *Bioinspir. Biomim.*, vol. 15, no. 6, p. 065003, Sep. 2020.

[47] H. Bolus, K. Crocker, G. Boekhoff-Falk, and S. Chtarbanova, “Modeling Neurodegenerative Disorders in *Drosophila melanogaster*,” *International Journal of Molecular Sciences*, vol. 21, no. 9, Art. no. 9, Jan. 2020.

[48] T. Kim, B. Song, and I.-S. Lee, “*Drosophila* Glia: Models for Human Neurodevelopmental and Neurodegenerative Disorders,” *International Journal of Molecular Sciences*, vol. 21, no. 14, Art. no. 14, Jan. 2020.

[49] M. M. Rolls, “Neuronal polarity in *Drosophila*: Sorting out axons and dendrites,” *Developmental Neurobiology*, vol. 71, no. 6, pp. 419–429, 2011.

[50] J. Malin and C. Desplan, “Neural specification, targeting, and circuit formation during visual system assembly,” *PNAS*, vol. 118, no. 28, Jul. 2021.

[51] J. M. Dorskind and A. L. Kolodkin, “Revisiting and refining roles of neural guidance cues in circuit assembly,” *Current Opinion in Neurobiology*, vol. 66, pp. 10–21, Feb. 2021.

[52] C. J. Weaver and F. E. Poulain, “From whole organism to ultrastructure: progress in axonal imaging for decoding circuit development,” *Development*, vol. 148, no. 18, Jul. 2021.

[53] A. Linskens and K. Lee, “Molecular Origins of the Pair1 and Moonwalker Descending Neuron’s Neural Circuitry in *Drosophila*” 2021, Available: https://scholarsbank.uoregon.edu/xmlui/handle/1794/26439

[54] R. Pinto-Costa and M. M. Sousa, “Microtubules, actin and cytolinkers: how to connect cytoskeletons in the neuronal growth cone,” *Neuroscience Letters*, vol. 747, p. 135693, Mar. 2021.

[55] E. C. Olesnicky and E. G. Wright, “*Drosophila* as a Model for Assessing the Function of RNA-Binding Proteins during Neurogenesis and Neurological Disease,” *J Dev Biol*, vol. 6, no. 3, Aug. 2018.

[56] M. R. C. Bhattacharya et al., “A Model of Toxic Neuropathy in *Drosophila* Reveals a Role for MORN4 in Promoting Axonal Degeneration,” *J. Neurosci.*, vol. 32, no. 15, pp. 5054–5061, Apr. 2012.

[57] Y.-N. Jan and L. Y. Jan, “Branching out: mechanisms of dendritic arborization,” *Nature Reviews Neuroscience*, vol. 11, no. 5, pp. 316–328, May 2010.

[58] V. A. Kulkarni and B. L. Firestein, “The dendritic tree and brain disorders,” *Molecular and Cellular Neuroscience*, vol. 50, no. 1, pp. 10–20, May 2012.

[59] T. Copf, “Impairments in dendrite morphogenesis as etiology for neurodevelopmental disorders and implications for therapeutic treatments,” *Neuroscience & Biobehavioral Reviews*, vol. 68, pp. 946–978, Sep. 2016.

[60] C. R. Tessier and K. Broadie, “*Drosophila* fragile X mental retardation protein developmentally regulates activity-dependent axon pruning,” *Development*, vol. 135, no. 8, pp. 1547–1557, Apr. 2008.

[61] R. Chakraborty et al., “Characterization of a *Drosophila* Alzheimer’s Disease Model: Pharmacological Rescue of Cognitive Defects,” *PLOS ONE*, vol. 6, no. 6, p. e20799, Jun. 2011.

[62] S. Herzmann, I. Götzelmann, L.-F. Reekers, and S. Rumpf, “Spatial regulation of microtubule disruption during dendrite pruning in *Drosophila*,” *Development*, vol. 145, no. 9, May 2018.

[63] V. HARTENSTEIN, “Development of *Drosophila* larval sensory organs: spatiotemporal pattern of sensory neurones, peripheral axonal pathways and sensilla differentiation,” *Development*, vol.102, no.4, pp.869–886, Apr. 1988.

[64] E. P. R. Iyer et al., “Functional Genomic Analyses of Two Morphologically Distinct Classes of *Drosophila* Sensory Neurons: Post-Mitotic Roles of Transcription Factors in Dendritic Patterning,” *PLOS ONE*, vol. 8, no. 8, p. e72434, Aug. 2013.

[65] J. Z. Parrish, M. D. Kim, L. Y. Jan, and Y. N. Jan, “Genome-wide analyses identify transcription factors required for proper morphogenesis of *Drosophila* sensory neuron dendrites,” Genes Dev., vol. 20, no. 7, pp. 820–835, Apr. 2006.

[66] Y. Ou, B. Chwalla, M. Landgraf, and D. J. van Meyel, “Identification of genes influencing dendrite morphogenesis in developing peripheral sensory and central motor neurons,” *Neural Development*, vol. 3, no. 1, p. 16, Jul. 2008.

[67] M. Schena, D. Shalon, R. W. Davis, and P. O. Brown, “Quantitative Monitoring of Gene Expression Patterns with a Complementary DNA Microarray,” *Science*, vol. 270, no. 5235, pp. 467–470, Oct. 1995.

[68] A. Mortazavi, B. A. Williams, K. McCue, L. Schaeffer, and B. Wold, “Mapping and quantifying mammalian transcriptomes by RNA-Seq,” *Nature Methods*, vol. 5, no. 7, pp. 621–628, Jul. 2008.

[69] V. Iyer, C. Horak, C. Scafe *et al*, “Genomic binding sites of the yeast cell-cycle transcription factors sbf and mbf” *Nature*, 409, no. 533–538, 2001.

[70] K. C. Martin and A. Ephrussi, “mRNA Localization: Gene Expression in the Spatial Dimension,” *Cell*, vol. 136, no. 4, pp. 719–730, Feb. 2009.

[71] J. D. Richter and P. Lasko, “Translational Control in Oocyte Development,” *Cold Spring Harb Perspect Biol*, vol. 3, no. 9, p. a002758, Sep. 2011.

[72] S. C. Hughes and A. J. Simmonds, “*Drosophila* mRNA Localization During Later Development: Past, Present, and Future,” *Front. Genet*., vol. 10, 2019.

[73] M. Stapleton, J. W. Carlson, and S. E. Celniker, “RNA editing in *Drosophila melanogaster*: New targets and functional consequences,” *RNA*, vol. 12, no. 11, pp. 1922–1932, Nov. 2006.

[74] S. Maas, “Posttranscriptional recoding by RNA editing,” *Advances in Protein Chemistry and Structural Biology*, vol. 86, pp. 193–224, 2012.

[75] J. C. Meier, S. Kankowski, H. Krestel, and F. Hetsch, “RNA Editing—Systemic Relevance and Clue to Disease Mechanisms?” *Front. Mol. Neurosci*., vol. 9, 2016.

[76] W. Wei, X. Ji, X. Guo, and S. Ji, “Regulatory Role of N*6*-methyladenosine (m*6*A) Methylation in RNA Processing and Human Diseases,” *Journal of Cellular Biochemistry*, vol. 118, no. 9, pp. 2534–2543, 2017.

[77] H. Krestel and J. C. Meier, “RNA Editing and Retrotransposons in Neurology,” *Front Mol Neurosci*, vol. 11, May 2018.

[78] M. Schmid and T. H. Jensen, “Controlling nuclear RNA levels,” *Nature Reviews Genetics*, p. 1, May 2018.

[79] P. H. Patel, S. A. Barbee, and J. T. Blankenship, “GW-Bodies and P-Bodies Constitute Two Separate Pools of Sequestered Non-Translating RNAs,” *PLOS ONE*, vol. 11, no. 3, p. e0150291, Mar. 2016.

[80] N. Standart and D. Weil, “P-Bodies: Cytosolic Droplets for Coordinated mRNA Storage,” *Trends in Genetics*, vol. 34, no. 8, pp. 612–626, Aug. 2018.

[81] S. Chandra, D. Vimal, D. Sharma, V. Rai, S. C. Gupta, and D. K. Chowdhuri, “Role of miRNAs in development and disease: Lessons learnt from small organisms,” *Life Sciences*, vol. 185, pp. 8–14, Sep. 2017.

[82] J. H. Noh, K. M. Kim, W. G. McClusky, K. Abdelmohsen, and M. Gorospe, “Cytoplasmic functions of long noncoding RNAs,” *Wiley Interdisciplinary Reviews: RNA*, vol. 9, no. 3, p. e1471, 2018.

[83] P. Hoch-Kraft, J. Trotter, and C. Gonsior, “Missing in Action: Dysfunctional RNA Metabolism in Oligodendroglial Cells as a Contributor to Neurodegenerative Diseases?” *Neurochem Res*, Mar. 2019.

[84] M. Wang, L. Ogé, M.-D. Perez-Garcia, L. Hamama, and S. Sakr, “The PUF Protein Family: Overview on PUF RNA Targets, Biological Functions, and Post Transcriptional Regulation,” *Int J Mol Sci*, vol. 19, no. 2, Jan. 2018.

[85] T. Glisovic, J. L. Bachorik, J. Yong, and G. Dreyfuss, “RNA-binding proteins and post-transcriptional gene regulation,” *FEBS Lett*, vol. 582, no. 14, pp. 1977–1986, Jun. 2008.

[86] A. Parchure, M. Munson, and V. Budnik, “Getting mRNA-Containing Ribonucleoprotein Granules Out of a Nuclear Back Door,” *Neuron*, vol. 96, no. 3, pp. 604–615, Nov. 2017.

[87] A. Castello et al., “Insights into RNA Biology from an Atlas of Mammalian mRNA-Binding Proteins,” *Cell*, vol. 149, no. 6, pp. 1393–1406, Jun. 2012.

[88] S. Gerstberger, M. Hafner, and T. Tuschl, “A census of human RNA-binding proteins,” *Nature Reviews Genetics*, vol. 15, no. 12, pp. 829–845, Dec. 2014

.

[89] K. E. Lukong, K. Chang, E. W. Khandjian, and S. Richard, “RNA-binding proteins in human genetic disease,” *Trends in Genetics*, vol. 24, no. 8, pp. 416–425, Aug. 2008.

[90] D. Gemmill, S. D’souza, V. Meier-Stephenson, and T. R. Patel, “Current approaches for RNA labelling to identify RNA-binding proteins,” *Biochem. Cell Biol.*, Mar. 2019.

[91] V. A. Gennarino et al., “Pumilio1 Haploinsufficiency Leads to SCA1-like Neurodegeneration by Increasing Wild-Type Ataxin1 Levels,” *Cell*, vol. 160, no. 6, pp. 1087–1098, Mar. 2015.

[92] B. M. Lunde, C. Moore, and G. Varani, “RNA-binding proteins: modular design for efficient function,” *Nature Reviews Molecular Cell Biology*, vol. 8, no. 6, pp. 479–490, Jun. 2007.

[93] P. Linder and E. Jankowsky, “From unwinding to clamping — the DEAD box RNA helicase family,” *Nature Reviews Molecular Cell Biology*, vol. 12, no. 8, pp. 505–516, Aug. 2011.

[94] A. Cléry, M. Blatter, and F. H.-T. Allain, “RNA recognition motifs: boring? Not quite,” *Current Opinion in Structural Biology*, vol. 18, no. 3, pp. 290–298, Jun. 2008.

[95] M. W. Hentze, A. Castello, T. Schwarzl, and T. Preiss, “A brave new world of RNA-binding proteins,” *Nature Reviews Molecular Cell Biology*, vol. 19, no. 5, pp. 327–341, May 2018.

[96] S. Dixit and J. Lukeš, “Combinatorial interplay of RNA-binding proteins tunes levels of mitochondrial mRNA in trypanosomes,” *RNA*, vol. 24, no. 11, pp. 1594–1606, Nov. 2018.

[97] K. S. Moore and M. von Lindern, “RNA Binding Proteins and Regulation of mRNA Translation in Erythropoiesis,” *Front. Physiol.*, vol. 9, 2018.

[98] F. A. Tedeschi, S. C. Cloutier, E. J. Tran, and E. Jankowsky, “The DEAD-box protein Dbp2p is linked to noncoding RNAs, the helicase Sen1p, and R-loops,” *RNA*, vol. 24, no. 12, pp. 1693–1705, Dec. 2018.

[99] W. Lei, Z.-L. Wang, H.-J. Feng, X.-D. Lin, C.-Z. Li, and D. Fan, “Long non-coding RNA SNHG12promotes the proliferation and migration of glioma cells by binding to HuR,” *International Journal of Oncology*, vol. 53, no. 3, pp. 1374–1384, Sep. 2018.

[100] P. Grzechnik et al., “Nuclear fate of yeast snoRNA is determined by co-transcriptional Rnt1 cleavage,” *Nature Communications*, vol. 9, no. 1, p. 1783, May 2018.

[101] M. Baou, J. D. Norton, and J. J. Murphy, “AU-rich RNA binding proteins in hematopoiesis and leukemogenesis,” *Blood*, vol. 118, no. 22, pp. 5732–5740, Nov. 2011.

[102] F. Zhou et al., “HIV-1 Nef-induced lncRNA *AK006025* regulates *CXCL9/10/11* cluster gene expression in astrocytes through interaction with CBP/P300,” *Journal of Neuroinflammation*, vol. 15, no. 1, p. 303, Oct. 2018.

[103] E. Qiao et al., “Long noncoding RNA *TALNEC2* plays an oncogenic role in breast cancer by binding to EZH2 to target p57KIP2 and involving in p-p38 MAPK and NF-κB pathways,” *Journal of Cellular Biochemistry*, vol. 120, no. 3, pp. 3978–3988, 2019.

[104] R. W. Zealy, S. P. Wrenn, S. Davila, K.-W. Min, and J.-H. Yoon, “microRNA-binding proteins: specificity and function,” *Wiley Interdisciplinary Reviews: RNA*, vol. 8, no. 5, p. e1414, 2017.

[105] M. Falaleeva et al., “Dual function of C/D box small nucleolar RNAs in rRNA modification and alternative pre-mRNA splicing,” *PNAS*, vol. 113, no. 12, pp. E1625–E1634, Mar. 2016.

[106] A. E. Brinegar and T. A. Cooper, “Roles for RNA-binding proteins in development and disease,” *Brain Research*, vol. 1647, pp. 1–8, Sep. 2016.

[107] C. Clayton and M. Shapira, “Post-transcriptional regulation of gene expression in *trypanosomes* and *leishmanias*,” *Molecular and Biochemical Parasitology*, vol. 156, no. 2, pp. 93–101, Dec. 2007.

[108] S. Kishore, S. Luber, and M. Zavolan, “Deciphering the role of RNA-binding proteins in the post-transcriptional control of gene expression,” *Brief Funct Genomics*, vol. 9, no. 5–6, pp. 391–404, Dec. 2010.

[109] N. Shiina, “Liquid- and solid-like RNA granules form through specific scaffold proteins and combine into biphasic granules,” *J. Biol. Chem.*, vol. 294, no. 10, pp. 3532–3548, Mar. 2019.

[110] J. R. Buchan and R. Parker, “Eukaryotic Stress Granules: The Ins and Outs of Translation,” *Molecular Cell*, vol. 36, no. 6, pp. 932–941, Dec. 2009.

[111] D. Trigo, A. Nadais, and O. A. B. da Cruz e Silva, “Unravelling protein aggregation as an ageing related process or a neuropathological response,” *Ageing Research Reviews*, vol. 51, pp. 67–77, May 2019.

[112] B. P. Towler and S. F. Newbury, “Regulation of cytoplasmic RNA stability: Lessons from *Drosophila*,” *Wiley Interdisciplinary Reviews: RNA*, vol. 9, no. 6, p. e1499, 2018.

[113] E. G. Conlon and J. L. Manley, “RNA-binding proteins in neurodegeneration: mechanisms in aggregate,” *Genes Dev.*, vol. 31, no. 15, pp. 1509–1528, Aug. 2017.

[114] Q. Zhou et al., “LUCAT1 promotes colorectal cancer tumorigenesis by targeting the ribosomal protein L40-MDM2-p53 pathway through binding with UBA52.,” *Cancer Sci*, vol. 110, no. 4, pp. 1194–1207, Apr. 2019.

[115] A. E. M. Newman, H. Hess, B. K. Woodworth, and D. R. Norris, “Time as tyrant: The minute, hour and day make a difference for corticosterone concentrations in wild nestlings,” *General and Comparative Endocrinology*, vol. 250, pp. 80–84, Sep. 2017.

[116] M. Esteller, “Non-coding RNAs in human disease,” *Nature Reviews Genetics*, vol. 12, no. 12, pp. 861–874, Dec. 2011.

[117] D. Dominguez et al., “Sequence, Structure, and Context Preferences of Human RNA Binding Proteins,” *Molecular Cell*, vol. 70, no. 5, pp. 854-867.e9, Jun. 2018.

[118] D. Ray et al., “A compendium of RNA-binding motifs for decoding gene regulation,” *Nature*, vol. 499, no. 7457, pp. 172–177, Jul. 2013.

[119] E. C. Wheeler, E. L. V. Nostrand, and G. W. Yeo, “Advances and challenges in the detection of transcriptome-wide protein–RNA interactions,” *Wiley Interdisciplinary Reviews: RNA*, vol. 9, no. 1, p. e1436, 2018.

[120] R. B. Darnell, “HITS-CLIP: panoramic views of protein–RNA regulation in living cells,” *Wiley Interdisciplinary Reviews: RNA*, vol. 1, no. 2, pp. 266–286, 2010.

[121] J. Ule, K. B. Jensen, M. Ruggiu, A. Mele, A. Ule, and R. B. Darnell, “CLIP Identifies Nova-Regulated RNA Networks in the Brain,” *Science*, vol. 302, no. 5648, pp. 1212–1215, Nov. 2003.

[122] Y. Xue et al., “Genome-wide Analysis of PTB-RNA Interactions Reveals a Strategy Used by the General Splicing Repressor to Modulate Exon Inclusion or Skipping,” *Molecular Cell*, vol. 36, no. 6, pp. 996–1006, Dec. 2009.

[123] E. Lara-Pezzi, M. Desco, A. Gatto, and M. V. Gómez-Gaviro, “Neurogenesis: Regulation by Alternative Splicing and Related Posttranscriptional Processes,” *Neuroscientist*, vol. 23, no. 5, pp. 466–477, Oct. 2017.

[124] B. Raj and B. J. Blencowe, “Alternative Splicing in the Mammalian Nervous System: Recent Insights into Mechanisms and Functional Roles,” *Neuron*, vol. 87, no. 1, pp. 14–27, Jul. 2015.

[125] R. S. Porter, F. Jaamour, and S. Iwase, “Neuron-specific alternative splicing of transcriptional machineries: Implications for neurodevelopmental disorders,” *Molecular and Cellular Neuroscience*, vol. 87, pp. 35–45, Mar. 2018.

[126] D. A. Burow, M. C. Umeh-Garcia, M. B. True, C. D. Bakhaj, D. H. Ardell, and M. D. Cleary, “Dynamic regulation of mRNA decay during neural development,” *Neural Development*, vol. 10, p. 11, Apr. 2015.

[127] K. Yap and E. V. Makeyev, “Regulation of gene expression in mammalian nervous system through alternative pre-mRNA splicing coupled with RNA quality control mechanisms,” *Mol Cell* Neurosci, vol. 56, pp. 420–428, Sep. 2013.

[128] T. Gte. Consortium, “The Genotype-Tissue Expression (GTEx) pilot analysis: Multitissue gene regulation in humans,” *Science*, vol. 348, no. 6235, pp. 648–660, May 2015.

[129] M. Irimia et al., “A Highly Conserved Program of Neuronal Microexons Is Misregulated in Autistic Brains,” *Cell*, vol. 159, no. 7, pp. 1511–1523, Dec. 2014.

[130] M. Liu et al., “Dual modality optical coherence and whole-body photoacoustic tomography imaging of chick embryos in multiple development stages,” *Biomed. Opt. Express, BOE*, vol. 5, no. 9, pp. 3150–3159, Sep. 2014.

[131] J. Merkin, C. Russell, P. Chen, and C. B. Burge, “Evolutionary Dynamics of Gene and Isoform Regulation in Mammalian Tissues,” *Science*, vol. 338, no. 6114, pp. 1593–1599, Dec. 2012.

[132] Y. Jin and H. Li, “Revisiting Dscam diversity: lessons from clustered protocadherins,” *Cell. Mol. Life Sci.*, vol. 76, no. 4, pp. 667–680, Feb. 2019.

[133] Y. Jin, H. Dong, Y. Shi, and L. Bian, “Mutually exclusive alternative splicing of pre-mRNAs,” *Wiley Interdisciplinary Reviews: RNA*, vol. 9, no. 3, p. e1468, 2018.

[134] B. Xu, Y. Shi, Y. Wu, Y. Meng, and Y. Jin, “Role of RNA secondary structures in regulating Dscam alternative splicing,” *Biochimica et Biophysica Acta (BBA) - Gene Regulatory Mechanisms*, Apr. 201.

[135] S. K. Miura, A. Martins, K. X. Zhang, B. R. Graveley, and S. L. Zipursky, “Probabilistic Splicing of Dscam1 Establishes Identity at the Level of Single Neurons,” *Cell*, vol. 155, no. 5, pp. 1166–1177, Nov. 2013.

[136] W. Wu, G. Ahlsen, D. Baker, L. Shapiro, and S. L. Zipursky, “Complementary Chimeric Isoforms Reveal Dscam1 Binding Specificity *In Vivo*,” *Neuron*, vol. 74, no. 2, pp. 261–268, Apr. 2012.

[137] G. J. Lah, J. S. S. Li, and S. S. Millard, “Cell-Specific Alternative Splicing of Drosophila Dscam2 Is Crucial for Proper Neuronal Wiring,” *Neuron*, vol. 83, no. 6, pp. 1376–1388, Sep. 2014.

[138] W. Tadros et al., “Dscam Proteins Direct Dendritic Targeting through Adhesion,” *Neuron*, vol. 89, no. 3, pp. 480–493, Feb. 2016.

[139] J. S. Malter, “Regulation of mRNA stability in the nervous system and beyond,” *Journal of Neuroscience Research*, vol. 66, no. 3, pp. 311–316, 2001.

[140] G. B. Gonsalvez & R. M. Long, “Spatial regulation of translation through RNA localization,” *F1000 biology reports*, vol. 4. 2012.

[141] C. Medioni, K. Mowry, and F. Besse, “Principles and roles of mRNA localization in animal development,” *Development*, vol. 18, no. 3263–3276, 2012.

[142] I. G. Bruno et al., “Identification of a MicroRNA that Activates Gene Expression by Repressing Nonsense-Mediated RNA Decay,” *Molecular Cell*, vol. 42, no. 4, pp. 500–510, May 2011.

[143] A. Ratti et al., “A role for the ELAV RNA-binding proteins in neural stem cells: stabilization of *Msi1* mRNA,” *Journal of Cell Science*, vol. 119, no. 7, pp. 1442–1452, Apr. 2006.

[144] H. Jung, C. G. Gkogkas, N. Sonenberg, and C. E. Holt, Eds., “Remote control of gene function by local translation,” *Cell*, vol. 1, no. 26–40, 2014.

[145] P. J. Lee, S. Yang, Y. Sun, and J. U. Guo, “Regulation of nonsense-mediated mRNA decay in neural development and disease,” *Journal of Molecular Cell Biology*, vol. 13, no. 4, pp. 269–281, Apr. 2021.

[146] M. Jung and E. K. Lee, “RNA–Binding Protein HuD as a Versatile Factor in Neuronal and Non–Neuronal Systems,” *Biology*, vol. 10, no. 5, Art. no. 5, May 2021.

[147] R. Schieweck et al., “Pumilio2 and Staufen2 selectively balance the synaptic proteome,” *Cell Reports*, vol. 35, no. 12, p. 109279, Jun. 2021.

[148] L. M. Bronicki and B. J. Jasmin, “Emerging complexity of the HuD/ELAVl4 gene; implications for neuronal development, function, and dysfunction,” *RNA*, vol. 19, no. 8, pp. 1019–1037, Aug. 2013.

[149] W. Akamatsu et al., “The RNA-binding protein HuD regulates neuronal cell identity and maturation,” *PNAS*, vol. 102, no. 12, pp. 4625–4630, Mar. 2005.

[150] N. Perrone-Bizzozero and F. Bolognani, “Role of HuD and other RNA-binding proteins in neural development and plasticity,” *Journal of Neuroscience Research*, vol. 68, no. 2, pp. 121–126, 2002.

[151] V. Hilgers, S. B. Lemke, and M. Levine, “ELAV mediates 3′ UTR extension in the *Drosophila* nervous system,” *Genes Dev.*, vol. 26, no. 20, pp. 2259–2264, Oct. 2012.

[152] A. A. Mirisis and T. J. Carew, “The ELAV family of RNA-binding proteins in synaptic plasticity and long-term memory,” *Neurobiology of Learning and Memory*, vol. 161, pp. 143–148, May 2019.

[153] Y. Saletore, S. Chen-Kiang, and C. E. Mason, “Novel RNA regulatory mechanisms revealed in the epitranscriptome,” *RNA Biology*, vol. 10, no. 3, pp. 342–346, Mar. 2013.

[154] A. K. Chokkalla, S. L. Mehta, and R. Vemuganti, “Epitranscriptomic Modifications Modulate Normal and Pathological Functions in CNS,” *Transl. Stroke Res.*, Jul. 2021.

[155] K. D. Meyer, Y. Saletore, P. Zumbo, O. Elemento, C. E. Mason, and S. R. Jaffrey, “Comprehensive Analysis of mRNA Methylation Reveals Enrichment in 3′ UTRs and near Stop Codons,” *Cell*, vol. 149, no. 7, pp. 1635–1646, Jun. 2012.

[156] M. Chang et al., “Region-specific RNA m^{6}A methylation represents a new layer of control in the gene regulatory network in the mouse brain,” *Open Biology*, vol. 7, no. 9, p. 170166.

[157] S. Schwartz et al., “Perturbation of m^{6}A Writers Reveals Two Distinct Classes of mRNA Methylation at Internal and 5′ Sites,” *Cell Reports*, vol. 8, no. 1, pp. 284–296, Jul. 2014.

[158] K.-J. Yoon et al., “Temporal Control of Mammalian Cortical Neurogenesis by m^{6}A Methylation,” Cell, vol. 171, no. 4, pp. 877-889.e17, Nov. 2017.

[159] J. Widagdo and V. Anggono, “The m^{6}A-epitranscriptomic signature in neurobiology: from neurodevelopment to brain plasticity,” *Journal of Neurochemistry*, vol. 0, no. ja, doi: 10.1111/jnc.14481.

[160] L. Li et al., “Fat mass and obesity-associated (FTO) protein regulates adult neurogenesis,” *Human Molecular Genetics*, vol. 26, no. 13, pp. 2398–2411, Jul. 2017.

[161] P. Zhou et al., “Arhgef2 regulates neural differentiation in the cerebral cortex through mRNA m*6*A-methylation of *Npdc1* and *Cend1*,” *iScience*, vol. 24, no. 6, p. 102645, Jun. 2021.

[162] J. Widagdo et al., “Experience-Dependent Accumulation of N^6-Methyladenosine in the Prefrontal Cortex Is Associated with Memory Processes in Mice,” *J. Neurosci.*, vol. 36, no. 25, pp. 6771–6777, Jun. 2016.

[163] B. J. Walters et al., “The Role of The RNA Demethylase FTO (Fat Mass and Obesity-Associated) and mRNA Methylation in Hippocampal Memory Formation,” *Neuropsychopharmacol*, vol. 42, no. 7, pp. 1502–1510, Jun. 2017.

[164] M. E. Hess et al., “The fat mass and obesity associated gene (Fto) regulates activity of the dopaminergic midbrain circuitry,” *Nat Neurosci*, vol. 16, no. 8, pp. 1042–1048, Aug. 2013.

[165] L. Wang, X. Liu, X. Luo, M. Zeng, L. Zuo, and K.-S. Wang, “Genetic Variants in the Fat Mass- and Obesity-Associated (FTO) Gene are Associated with Alcohol Dependence,” *J Mol Neurosci*, vol. 51, no. 2, pp. 416–424, Oct. 2013.

[166] Y.-L. Weng et al., “Epitranscriptomic m*6*A Regulation of Axon Regeneration in the Adult Mammalian Nervous System,” *Neuron*, vol. 97, no. 2, pp. 313-325.e6, Jan. 2018.

[167] C. E. Holt and E. M. Schuman, “The Central Dogma Decentralized: New Perspectives on RNA Function and Local Translation in Neurons,” *Neuron*, vol. 80, no. 3, pp. 648–657, Oct. 2013.

[168] J. L. Brechbiel and E. R. Gavis, “Spatial Regulation of nanos Is Required for Its Function in Dendrite Morphogenesis,” *Current Biology*, vol. 18, no. 10, pp. 745–750, May 2008.

[169] K. C. Martin and R. S. Zukin, “RNA Trafficking and Local Protein Synthesis in Dendrites: An Overview,” *J. Neurosci*., vol. 26, no. 27, pp. 7131–7134, Jul. 2006.

[170] J. D. Richter and E. Klann, “Making synaptic plasticity and memory last: mechanisms of translational regulation,” *Genes Dev*., vol. 23, no. 1, pp. 1–11, Jan. 2009.

[171] M. Doyle and M. A. Kiebler, “Mechanisms of dendritic mRNA transport and its role in synaptic tagging,” *The EMBO Journal*, vol. 30, no. 17, pp. 3540–3552, Aug. 2011.

[172] B. Ye, C. Petritsch, I. E. Clark, E. R. Gavis, L. Y. Jan, and Y. N. Jan, “*nanos* and *pumilio* Are Essential for Dendrite Morphogenesis in *Drosophila* Peripheral Neurons,” *Current Biology*, vol. 14, no. 4, pp. 314–321, Feb. 2004.

[173] E. C. Olesnicky, B. Bhogal, and E. R. Gavis, “Combinatorial use of translational co-factors for cell type-specific regulation during neuronal morphogenesis in *Drosophila*,” *Developmental Biology*, vol. 365, no. 1, pp. 208–218, May 2012.

[174] C. M. Loya, D. Van Vactor, and T. A. Fulga, “Understanding neuronal connectivity through the post-transcriptional toolkit,” *Genes Dev*, vol. 24, no. 7, pp. 625–635, Apr. 2010.

[175] H. Chiu, A. Alqadah, and C. Chang, “The role of microRNAs in regulating neuronal connectivity,” *Front Cell Neurosci*, vol. 7, p. 283, Jan. 2014.

[176] D. Colak, S.-J. Ji, B. T. Porse, and S. R. Jaffrey, “Regulation of Axon Guidance by Compartmentalized Nonsense-Mediated mRNA Decay,” *Cell*, vol. 153, no. 6, pp. 1252–1265, 2013.

[177] A. A. Long et al., “The nonsense-mediated decay pathway maintains synapse architecture and synaptic vesicle cycle efficacy,” *Journal of Cell Science*, vol. 123, no. 19, pp. 3303–3315, Oct. 2010.

[178] J. J. An, K. Gharami, G.-Y. Liao, N. H. Woo, A. G. Lau, and F. Vanevski, “Distinct Role of Long 3′ UTR *BDNF* mRNA in Spine Morphology and Synaptic Plasticity in Hippocampal Neurons,” Cell, vol. 21, pp. 175–187, 2008.

[179] M. Notaras et al., “UPF2 leads to degradation of dendritically targeted mRNAs to regulate synaptic plasticity and cognitive function,” *Mol Psychiatry*, vol. 25, no. 12, pp. 3360–3379, Dec. 2020.

[180] S. A. Swanger and G. J. Bassell, “Making and breaking synapses through local mRNA regulation,” *Current Opinion in Genetics & Development*, vol. 21, no. 4, pp. 414–421, Aug. 2011.

[181] N. C. M. Oliveira, É. M. Lins, K. B. Massirer, and M. H. Bengtson, “Translational Control during Mammalian Neocortex Development and Postembryonic Neuronal Function,” *Seminars in Cell & Developmental Biology*, vol. 114, pp. 36–46, Jun. 2021.

[182] K. Burak et al., “*MicroRNA-16* targets mRNA involved in neurite extension and branching in hippocampal neurons during presymptomatic prion disease,” *Neurobiol Dis*, vol. 112, pp. 1–13, Apr. 2018.

[183] E. Franzoni et al., "*miR-128* regulates neuronal migration, outgrowth and intrinsic excitability via the intellectual disability gene Phf6," *Elife*, vol. 4, Jan. 2015.

[184] Q. Xue et al., "*miR-9* and *miR-124* synergistically affect regulation of dendritic branching via the AKT/GSK3β pathway by targeting Rap2a," *Sci Rep*, vol. 6, p. 26781, May 2016.

[185] Y. Xu and C. C. Quinn, "Transition between synaptic branch formation and synaptogenesis is regulated by the *lin-4* microRNA," *Dev Biol*, vol. 420, no. 1, pp. 60–66, Dec. 2016.

[186] N. Hamada, H. Ito, I. Iwamoto, R. Morishita, H. Tabata, and K.-I. Nagata, "Role of the cytoplasmic isoform of *RBFOX1/A2BP1* in establishing the architecture of the developing cerebral cortex," *Mol Autism*, vol. 6, p. 56, 2015.

[187] E. C. Olesnicky, J. M. Bono, L. Bell, L. T. Schachtner, and M. C. Lybecker, "The RNA-binding protein Caper is required for sensory neuron development in *Drosophila melanogaster*," *Dev Dyn*, vol. 246, no. 8, pp. 610–624, Aug. 2017.

[188] J. L. Goldberg, "Intrinsic neuronal regulation of axon and dendrite growth," *Current Opinion in Neurobiology*, vol. 14, no. 5, pp. 551–557, Oct. 2004.

[189] J. Q. Lin, F. W. van Tartwijk, and C. E. Holt, "Axonal mRNA translation in neurological disorders," *RNA Biology*, vol. 18, no. 7, pp. 936–961, Jul. 2021.

[190] B. Bhogal, A. Plaza-Jennings, and E. R. Gavis, "Nanos-mediated repression of *hid* protects larval sensory neurons after a global switch in sensitivity to apoptotic signals," *Development*, vol. 143, no. 12, pp. 2147–2159, Jun. 2016.

[191] X. Xu, J. L. Brechbiel, and E. R. Gavis, "Dynein-Dependent Transport of *nanos* RNA in *Drosophila* Sensory Neurons Requires Rumpelstiltskin and the Germ Plasm Organizer Oskar," *J. Neurosci.*, vol. 33, no. 37, pp. 14791–14800, Sep. 2013.

[192] M. Misra et al., “A Genome-Wide Screen for Dendritically Localized RNAs Identifies Genes Required for Dendrite Morphogenesis,” *G3: Genes, Genomes, Genetics*, vol. 6, no. 8, pp. 2397–2405, Aug. 2016.

[193] C. Medioni, M. Ramialison, A. Ephrussi, and F. Besse, “Imp Promotes Axonal Remodeling by Regulating *profilin* mRNA during Brain Development,” *Current Biology*, vol. 24, no. 7, pp. 793–800, Mar. 2014.

[194] “Ythdf is a N^6-methyladenosine reader that modulates Fmr1 target mRNA selection and restricts axonal growth in *Drosophila*,” *The EMBO Journal*, vol. 40, no. 4, p. e104975, Feb. 2021.

[195] R. Roy et al., “Schizophrenia and autism associated mutations and disrupted m^6A signal by YTHDF1 cause defects in microtubule function and neurodevelopment,” *BioRxiv*, p. 2020.11.14.382556, Nov. 2020.

[196] T. Iijima, C. Hidaka, and Y. Iijima, “Spatio-temporal regulations and functions of neuronal alternative RNA splicing in developing and adult brains,” *Neuroscience Research*, vol. 109, pp. 1–8, Aug. 2016.

[197] F. Hossain, “RNA splicing in neuron physiology and neurodegenerative diseases,” *St. John’s University Theses and Dissertation*, 245, 2021.

[198] W. J. Lukiw, T. V. Andreeva, A. P. Grigorenko, and E. I. Rogaev, “Studying micro–RNA Function and Dysfunction in Alzheimer’s Disease,” *Front. Genet.*, vol. 0, 2013.

[199] E. M. Hollams, K. M. Giles, A. M. Thomson, and P. J. Leedman, “mRNA Stability and the Control of Gene Expression: Implications for Human Disease,” *Neurochem Res*, vol. 27, no. 10, pp. 957–980, Oct. 2002.

[200] M. Polymenidou, C. Lagier-Tourenne, K. R. Hutt, C. F. Bennett, D. W. Cleveland, and G. W. Yeo, “Misregulated RNA processing in amyotrophic lateral sclerosis,” *Brain Research*, vol. 1462, pp. 3–15, Jun. 2012.

[201] X.-L. Xu, Y. Li, F. Wang, and F.-B. Gao, “The Steady-State Level of the Nervous-System-Specific *MicroRNA-124a* Is Regulated by dFMR1 in *Drosophila*,” *J. Neurosci.,* vol. 28, no. 46, pp. 11883–11889, Nov. 2008.

[202] J. M. Long, B. Ray, and D. K. Lahiri, "*MicroRNA-339-5p* Down-regulates Protein Expression of β-Site Amyloid Precursor Protein-Cleaving Enzyme 1 (BACE1) in Human Primary Brain Cultures and Is Reduced in Brain Tissue Specimens of Alzheimer Disease Subjects," *Journal of Biological Chemistry*, vol. 289, no. 8, pp. 5184–5198, Feb. 2014.

[203] J. M. Long, B. Ray, and D. K. Lahiri, "*MicroRNA-153* Physiologically Inhibits Expression of Amyloid-β Precursor Protein in Cultured Human Fetal Brain Cells and Is Dysregulated in a Subset of Alzheimer Disease Patients," *Journal of Biological Chemistry*, vol. 287, no. 37, pp. 31298–31310, Sep. 2012.

[204] J. Kim et al., "*microRNA-33* Regulates ApoE Lipidation and Amyloid-β Metabolism in the Brain," *J. Neurosci.*, vol. 35, no. 44, pp. 14717–14726, Nov. 2015.

[205] "Alteration of the microRNA network during the progression of Alzheimer's disease," *EMBO Molecular Medicine*, vol. 5, no. 10, pp. 1613–1634, Oct. 2013.

[206] J. Banzhaf-Strathmann et al., "*Microrna-125b* induces tau hyperphosphorylation and cognitive deficits in Alzheimer's disease," *The EMBO Journal*, p. 201387576, 2014.

[207] S.-C. Ling, M. Polymenidou, and D. W. Cleveland, "Converging mechanisms in ALS and FTD: disrupted RNA and protein homeostasis," *Neuron*, vol. 3, no. 416–438, 2013.

[208] M. J. Strong, "The evidence for altered RNA metabolism in amyotrophic lateral sclerosis (ALS)," *Journal of the neurological sciences*, vol. 1, no. 1–12, 2010.

[209] O. Penagarikano, J. G. Mulle, and S. T. Warren, "The Pathophysiology of Fragile X Syndrome," *Annual Review of Genomics and Human Genetics*, vol. 8, no. 1, pp. 109–129, 2007.

[210] L. Pan, Y. Q. Zhang, E. Woodruff, and K. Broadie, "The *Drosophila Fragile-x* gene negatively regulates neuronal elaboration and synaptic differentiation," *Current Biology*, vol. 20, no. 1863–1870, 2004.

[211] C. L. Gatto and K. Broadie, “Temporal requirements of the fragile X mental retardation protein in the regulation of synaptic structure,” *Development*, vol. 135, no. 15, pp. 2637–2648, Aug. 2008.

[212] H. Zhou, M. Mangelsdorf, J. Liu, L. Zhu, and J. Y. Wu, “RNA-binding proteins in neurological diseases,” *Sci. China Life Sci.*, vol. 57, no. 4, pp. 432–444, Apr. 2014.

[213] A. C. Goldstrohm, T. M. T. Hall, and K. M. McKenney, “Post-transcriptional Regulatory Functions of Mammalian Pumilio Proteins,” *Trends in Genetics*, vol. 34, no. 12, pp. 972–990, Dec. 2018.

[214] L.-E. Jao, B. Appel, and S. R. Wente, “A zebrafish model of lethal congenital contracture syndrome 1 reveals Gle1 function in spinal neural precursor survival and motor axon arborization,” *Development*, vol. 139, no. 7, pp. 1316–1326, Apr. 2012.

[215] A. H. Corbett, “Post-transcriptional regulation of gene expression and human disease,” *Current Opinion in Cell Biology*, vol. 52, pp. 96–104, Jun. 2018.

[216] J. Blackinton et al., “Post-transcriptional regulation of mRNA associated with DJ-1 in sporadic Parkinson disease,” *Neuroscience Letters*, vol. 452, no. 1, pp. 8–11, Mar. 2009.

[217] C. Yang et al., “The role of m^6A modification in physiology and disease,” *Cell Death Dis*, vol. 11, no. 11, pp. 1–16, Nov. 2020.

[218] A. K. Chokkalla, S. L. Mehta, and R. Vemuganti, “Epitranscriptomic regulation by m^6A RNA methylation in brain development and diseases,” *J Cereb Blood Flow Metab*, vol. 40, no. 12, pp. 2331–2349, Dec. 2020.

[219] A. Bianco, M. Dienstbier, H. K. Salter, G. Gatto, and S. L. Bullock, “Bicaudal-D Regulates Fragile X Mental Retardation Protein Levels, Motility, and Function during Neuronal Morphogenesis,” *Current Biology*, vol. 20, no. 16, pp. 1487–1492, Aug. 2010.

[220] B. D. Auerbach, E. K. Osterweil, and M. F. Bear, “Mutations causing syndromic autism define an axis of synaptic pathophysiology,” *Nature*, vol. 480, no. 7375, pp. 63–68, Dec. 2011.

[221] A. Goikolea-Vives and H. B. Stolp, “Connecting the Neurobiology of Developmental Brain Injury: Neuronal Arborisation as a Regulator of Dysfunction and Potential Therapeutic Target,” *International Journal of Molecular Sciences*, vol. 22, no. 15, Art. no. 15, Jan. 2021.

[222] A. Handley, T. Schauer, A. G. and M. Ladurner, and C.E., “Designing cell-type-specific genome-wide experiments,” *Mol.Cell*, 58, 621-631, 2015.

[223] M. D. Cleary, “Uncovering cell type-specific complexities of gene expression and RNA metabolism by TU-tagging and EC-tagging,” *Wiley Interdisciplinary Reviews: Developmental Biology*, p. e315, Jan. 2018.

[224] Z. Josh Huang and H. Zeng, “Genetic Approaches to Neural Circuits in the Mouse,” *Annual Review of Neuroscience*, vol. 36, no. 1, pp. 183–215, 2013.

[225] T. Weber and R. Köster, “Genetic tools for multicolor imaging in zebrafish larvae,” *Methods*, vol. 62, no. 3, pp. 279–291, Aug. 2013.

[226] A. del Valle Rodríguez, D. Didiano, and C. Desplan, “Power tools for gene expression and clonal analysis in *Drosophila*,” Nature Methods, vol. 9, no. 1, pp. 47–55, Jan. 2012.

[227] L. Madisen et al., “Transgenic Mice for Intersectional Targeting of Neural Sensors and Effectors with High Specificity and Performance,” *Neuron*, vol. 85, no. 5, pp. 942–958, Mar. 2015.

[228] W. A. Sassen and R. W. Köster, “A molecular toolbox for genetic manipulation of zebrafish,” *Advances in Genomics and Genetics*, vol. 5, pp. 151–163, 2015.

[229] V. Mariano, T. Achsel, C. Bagni, and A. K. Kanellopoulos, “Modelling Learning and Memory in *Drosophila* to Understand Intellectual Disabilities,” *Neuroscience*, vol. 445, pp. 12–30, Oct. 2020.

[230] C. J. Evans, T. Liu, and U. Banerjee, “*Drosophila* hematopoiesis: Markers and methods for molecular genetic analysis,” *Methods*, vol. 68, no. 1, pp. 242–251, Jun. 2014.

[231] A. H. and P. Brand and N., “Targeted gene expression as a means of altering cell fates and generating dominant phenotypes,” *Development*, vol. 118, pp. 401–415, 1993.

[232] Q. U. Ain, J. Y. Chung, and Y.-H. Kim, “Current and future delivery systems for engineered nucleases: ZFN, TALEN and RGEN,” *Journal of Controlled Release*, vol. 205, pp. 120–127, May 2015.

[233] J. A. Doudna and E. Charpentier, “The new frontier of genome engineering with CRISPR-Cas9,” *Science*, vol. 346, no. 6213, Nov. 2014.

[234] Z. Wang, M. Gerstein, and M. Snyder, “RNA-Seq: a revolutionary tool for transcriptomics,” *Nature Reviews Genetics*, vol. 10, no. 1, Art. no. 1, Jan. 2009.

[235] S. K. Whitley, W. T. Horne, and J. K. Kolls, “Research Techniques Made Simple: Methodology and Clinical Applications of RNA Sequencing,” *Journal of Investigative Dermatology*, vol. 136, no. 8, pp. e77–e82, Aug. 2016.

[236] J. B. Moroney, A. Vasudev, A. Pertsemlidis, H. Zan, and P. Casali, “Integrative transcriptome and chromatin landscape analysis reveals distinct epigenetic regulations in human memory B cells,” *Nature Communications*, vol. 11, no. 1, Art. no. 1, Oct. 2020.

[237] Y. Ghavi-Helm et al., “Enhancer loops appear stable during development and are associated with paused polymerase,” *Nature*, vol. 512, no. 7512, Art. no. 7512, Aug. 2014.

[238] S. Bonn, R. P. Zinzen, A. Perez-Gonzalez, A. Riddell, A.-C. Gavin, and E. E. M. Furlong, “Cell type–specific chromatin immunoprecipitation from multicellular complex samples using BiTS-ChIP,” *Nature Protocols*, vol. 7, no. 5, Art. no. 5, May 2012.

[239] S. Bonn et al., “Tissue-specific analysis of chromatin state identifies temporal signatures of enhancer activity during embryonic development,” *Nature Genetics*, vol. 44, no. 2, Art. no. 2, Feb. 2012.

[240] T. K. Barth and A. Imhof, “Fast signals and slow marks: the dynamics of histone modifications,” *Trends in Biochemical Sciences*, vol. 35, no. 11, pp. 618–626, Nov. 2010.

[241] B. Delatte, R. Deplus, and F. Fuks, “Playing TETris with DNA modifications,” *The EMBO Journal*, vol. 33, no. 11, pp. 1198–1211, Jun. 2014.

[242] S. Farris, J. M. Ward, K. E. Carstens, M. Samadi, Y. Wang, and S. M. Dudek, “Hippocampal Subregions Express Distinct Dendritic Transcriptomes that Reveal Differences in Mitochondrial Function in CA2,” *Cell Reports*, vol. 29, no. 2, pp. 522-539.e6, Oct. 2019.

[243] K. H. Zivraj et al., Eds., “Subcellular profiling reveals distinct and developmentally regulated repertoire of growth cone mRNAs,” *The Journal of Neuroscience*, vol. 46, no. 15464–15478, 2010.

[244] Z. Ezzoukhry et al., “Combining laser capture microdissection and proteomics reveals an active translation machinery controlling invadosome formation,” *Nature Communications*, vol. 9, no. 1, Art. no. 1, May 2018.

[245] C. M. Hempel, K. Sugino, and S. B. Nelson, “A manual method for the purification of fluorescently labeled neurons from the mammalian brain,” *Nat Protoc*, vol. 2, no. 11, pp. 2924–2929, 2007.

[246] S. Loontiens et al., “Purification of high-quality RNA from a small number of fluorescence activated cell sorted zebrafish cells for RNA sequencing purposes,” *BMC Genomics*, vol. 20, no. 1, p. 228, Mar. 2019.

[247] V. Espina et al., “Laser-capture microdissection,” *Nat P*rotoc, vol. 1, no. 2, pp. 586–603, 2006.

[248] F. von Eggeling and F. Hoffmann, “Microdissection—An Essential Prerequisite for Spatial Cancer Omics,” *PROTEOMICS*, vol. 20, no. 17–18, p. 2000077, 2020.

[249] R. B. Deal and S. Henikoff, “A Simple Method for Gene Expression and Chromatin Profiling of Individual Cell Types within a Tissue,” *Developmental Cell*, vol. 18, no. 6, pp. 1030–1040, Jun. 2010.

[250] G. L. Henry, F. P. Davis, S. and E. Picard, and S.R., “Cell type-specific genomics of *Drosophila* neurons,” *Nucleic Acids Res*., 40, 9691-9704, 2012.

[251] S. Haenni et al., “Analysis of *C. elegans* intestinal gene expression and polyadenylation by fluorescence-activated nuclei sorting and 3’-end-seq,” *Nucleic Acids Res*, vol. 40, no. 13, pp. 6304–6318, Jul. 2012.

[252] G. M. Richardson, J. Lannigan, and I. G. Macara, “Does FACS perturb gene expression?” *Cytometry A*, vol. 87, no. 2, pp. 166–175, Feb. 2015.

[253] S. C. van den Brink et al., “Single-cell sequencing reveals dissociation-induced gene expression in tissue subpopulations,” *Nature Methods*, vol. 14, no. 10, pp. 935–936, Sep. 2017.

[254] B. W. Okaty, K. Sugino, and S. B. Nelson, “A quantitative comparison of cell-type-specific microarray gene expression profiling methods in the mouse brain,” *PLoS One*, vol. 6, no. 1, p. e16493, Jan. 2011.

[255] M. Singha, L. Spitalny, K. Nguyen, A. Vandewalle, and R. C. Spitale, “Chemical methods for measuring RNA expression with metabolic labeling,” *WIREs RNA*, e1650, Feb. 2021.

[256] J. D. Dougherty, “The Expanding Toolkit of Translating Ribosome Affinity Purification,” *J. Neurosci*., vol. 37, no. 50, pp. 12079–12087, Dec. 2017.

[257] E. Sanz, J. C. Bean, D. P. Carey, A. Quintana, and G. S. McKnight, “RiboTag: Ribosomal Tagging Strategy to Analyze Cell-Type-Specific mRNA Expression *In Vivo*,” *Current Protocols in Neuroscience*, vol. 88, no. 1, p. e77, 2019.

[258] W. C. Spencer et al., “A spatial and temporal map of *C. elegans* gene expression,” *Genome Res*., vol. 21, no. 2, pp. 325–341, Feb. 2011.

[259] M. He, Y. Liu, X. Wang, M. Q. Zhang, G. J. Hannon, and Z. J. Huang, “Cell-Type-Based Analysis of MicroRNA Profiles in the Mouse Brain,” *Neuron*, vol. 73, no. 1, pp. 35–48, Jan. 2012.

[260] S. Mili and J. A. Steitz, “Evidence for reassociation of RNA-binding proteins after cell lysis: Implications for the interpretation of immunoprecipitation analyses,” *RNA*, vol. 10, no. 11, pp. 1692–1694, Nov. 2004.

[261] K. J. Riley, T. A. Yario, and J. A. Steitz, “Association of Argonaute proteins and microRNAs can occur after cell lysis,” *RNA*, vol. 18, no. 9, pp. 1581–1585, Sep. 2012.

[262] M. Furlan, S. de Pretis, and M. Pelizzola, “Dynamics of transcriptional and post-transcriptional regulation,” *Briefings in Bioinformatics*, vol. 22, no. 4, Jul. 2021.

[263] M. T. Paulsen et al., “Use of Bru-Seq and BruChase-Seq for genome-wide assessment of the synthesis and stability of RNA,” *Methods*, vol. 67, no. 1, pp. 45–54, May 2014.

[264] M. D. Cleary, C. D. Meiering, E. Jan, R. Guymon, and J. C. Boothroyd, “Biosynthetic labeling of RNA with uracil phosphoribosyltransferase allows cell-specific microarray analysis of mRNA synthesis and decay,” *Nature Biotechnology*, vol. 23, no. 2, pp. 232–237, Feb. 2005.

[265] M. R. Miller, K. J. Robinson, M. D. Cleary, and C. Q. Doe, “TU-tagging: cell type–specific RNA isolation from intact complex tissues,” *Nature Methods*, vol. 6, no. 6, pp. 439–441, Jun. 2009.

[266] R. and C. Weng and S.M., “*Drosophila miR-124* regulates neuroblast proliferation through its target anachronism,” *Development*, vol. 139, pp. 1427–1434, 2012.

[267] A. Tallafuss et al., “Transcriptomes of post-mitotic neurons identify the usage of alternative pathways during adult and embryonic neuronal differentiation,” *BMC Genomics*, vol. 16, 2015.

[268] T. and N. Erickson and T., “Identification of sensory hair-cell transcripts by thiouracil-tagging in zebrafish,” *BMC Genomics*, vol. 16, p. 842, 2015.

[269] J. L. Rinn et al., “A dermal HOX transcriptional program regulates site-specific epidermal fate,” *Genes Dev*, vol. 22, pp. 303–307, 2008.

[270] L. Gay et al., “Mouse TU tagging: a chemical/genetic intersectional method for purifying cell type-specific nascent RNA,” *Genes Dev*, vol. 27, no. 1, pp. 98–115, Jan. 2013.

[271] C. Chatzi, Y. Zhang, R. Shen, G. L. Westbrook, and R. H. Goodman, “Transcriptional Profiling of Newly Generated Dentate Granule Cells Using TU Tagging Reveals Pattern Shifts in Gene Expression during Circuit Integration,” *eNeuro*, vol. 3, no. 1, Mar. 2016.

[272] A. C. Ghosh, M. Shimell, E. R. Leof, M. J. and O. ’Connor Haley, and M.B., UPRT, a suicide-gene therapy candidate in higher eukaryotes, is required for *Drosophila* larval growth and normal adult lifespan,” *Sci.Rep*., 5, 13176, 2015.

[273] R. Y. Hwang et al., “Nociceptive neurons protect *Drosophila* larvae from parasitoid wasps,” *Curr Biol*, vol. 17, no. 24, pp. 2105–2116, Dec. 2007.

[274] Y. Xiang, Q. Yuan, N. Vogt, L. L. Looger, L. Y. Jan, and Y. N. Jan, “Light-avoidance-mediating photoreceptors tile the *Drosophila* larval body wall,” *Nature*, vol. 468, no. 7326, pp. 921–926, Dec. 2010.

[275] S. Antonacci et al., “Conserved RNA-Binding Proteins Required for Dendrite Morphogenesis in *Caenorhabditis elegans* Sensory Neurons,” *G3 (Bethesda)*, vol. 5, no. 4, pp. 639–653, Feb. 2015.

[276] E. C. Olesnicky et al., “Extensive Use of RNA-Binding Proteins in *Drosophila* Sensory Neuron Dendrite Morphogenesis,” *G3 (Bethesda)*, vol. 4, no. 2, pp. 297–306, Dec. 2013.

[277] M. K. Lobo, S. L. Karsten, M. Gray, D. H. and Y. Geschwind, and X.W., “FACS-array profiling of striatal projection neuron subtypes in juvenile and adult mouse brains,” *Nat.Neurosci*., 9, 443-452, 2006.

[278] V. A. M. Vincent, J. J. DeVoss, H. S. Ryan, and G. M. Murphy, “Analysis of neuronal gene expression with laser capture microdissection,” *Journal of Neuroscience Research*, vol. 69, no. 5, pp. 578–586, 2002.

[279] D. Carter, R. G. Donald, D. and U. Roos, and B., “Expression, purification, and characterization of uracil phosphoribosyltransferase from *Toxoplasma gondii*,” *Mol. Biochem. Parasitol*, vol. 87, pp. 137–144, 1997.

[280] N. Hida et al., “EC-tagging allows cell type-specific RNA analysis,” *Nucleic Acids Res*, vol. 45, no. 15, pp. e138–e138, Sep. 2017.

[281] L. Dolken et al., “High-resolution gene expression profiling for simultaneous kinetic parameter analysis of RNA synthesis and,” 1972.

[282] M. Kenzelmann, S. Maertens, M. Hergenhahn, S. Kueffer, and A. Hotz-Wagenblatt, “Microarray analysis of newly synthesized RNA in cells and animals,” *Proc.Nat.Acad.Sci*., 104, 6164-6169, 2007.

[283] Z. Yang, H. J. and D. Edenberg, and R.L., “Isolation of mRNA from specific tissues of *Drosophila* by mRNA tagging,” in *Nucleic Acids Res*., 33, e148, 2005.

[284] M. Heiman et al., “A translational profiling approach for the molecular characterization of CNS cell types,” *Cell*, 135, 738-748, 2008.

[285] M.R. Miller, K.J. Robinson, M.D. Cleary & C.Q. Doe, “TU-tagging: cell type-specific RNA isolation from intact complex tissues,” *Nature Methods*, 6, 439-441, May 2009.

[286] A. Tallafuss, and P. Washbourne, “Temporally and spatially restricted gene expression profiling,” *Curr. Genomics*, vol. 15, pp. 278–292, 2014.

[287] E. E. Duffy, M. Rutenberg-Schoenberg, C. D. Stark, R. R. Kitchen, M. B. and S. Gerstein, “Tracking distinct RNA populations using efficient and reversible covalent chemistry,” *Mol.Cell*, 59, 858-866, 2015.

[288] D. Curanovic, M. Cohen, I. Singh, C. E. Slagle, C. S. and J. Leslie, and S.R., “Global profiling of stimulus-induced polyadenylation in cells using a poly(A) trap,” *Nat. Chem. Bio*, vol. 9, pp. 671–673, 2013.

[289] S. Nainar, S. Beasley, M. Fazio, M. Kubota, N. Dai, I. R. Correa, and Spitale, R.C, “Metabolic incorporation of azide functionality into cellular RNA,” *Chembiochem*, vol. 17, pp. 2149–2152, 2016.

[290] C. A. Mullen, M. and B. Kilstrup, and R.M., “Transfer of the bacterial gene for cytosine deaminase to mammalian cells confers lethal sensitivity to 5-fluorocytosine: a negative selection system,” *Proc.Nat.Acad.Sci*., 89, 33-37, 1992.

[291] T. Miyagi et al., “Gene therapy for prostate cancer using the cytosine deaminase/uracil phosphoribosyltransferase suicide system,” *The Journal of Gene Medicine*, vol. 5, no. 1, pp. 30–37, 2003.

[292] A. R. and P. Waldorf and A., “Mechanisms of action of 5-fluorocytosine,” *Antimicrob. Agents Chemother*, vol. 23, pp. 79–85, 1983.

[293] C. Y. and S. Jao and A., “Exploring RNA transcription and turnover *in vivo* by using click chemistry,” in *Proc.Nat.Acad.Sci*., 105, 15779-15784, 2008.

[294] H. Tani et al., “Genome-wide determination of RNA stability reveals hundreds of short-lived noncoding transcripts in mammals,” *Genome Res*, vol. 22, pp. 947–956, 2012.

[295] N. Hao *et al*., “Reciprocal regulation of the basic helix-loop-helix/Per-Arnt-Sim partner proteins, Arnt and Arnt2, during neuronal differentiation,” *Nucleic Acids Research*, vol. 41, no. 11, pp. 5626–5638, 2013.

[296] T. S. Chan, M. and G. Meuth, and H., “Pyrimidine excretion by cultured fibroblasts: effect of mutational deficiency in pyrimidine salvage enzymes,” *J. Cell Physiol*, vol. 83, pp. 263–266, 1974.

[297] H. Luan, N. C. Peabody, C. R. and W. Vinson, and B.H., “Refined spatial manipulation of neuronal function by combinatorial restriction of transgene expression,” *Neuron*, 52, 425-436, 2006.

[298] P. H. and M. Ear and S.W., “A general life-death selection strategy for dissecting protein functions,” *Nat. Methods*, vol. 6, pp. 813–816, 2009.

[299] J. R. Kroll, S. M. Lennox, O. Ogundeyi, J. Jeter, G. and T. Depasquale, and J.W., “A GAL4 driver resource for developmental and behavioral studies on the larval CNS of *Drosophila*,” *Cell Rep*, vol. 8, pp. 897–908, 2013.

[300] L. Manning et al., “A resource for manipulating gene expression and analyzing cis-regulatory modules in the *Drosophila* CNS,” *Cell Rep*, vol. 2, pp. 1002–1013, 2012.

[301] F. Friggi-Grelin, H. Coulom, M. Meller, D. Gomez, J. and B. Hirsh, and S., “Targeted gene expression in *Drosophila* dopaminergic cells using regulatory sequences from tyrosine hydroxylase,” *J. Neurobiol.*, 54,6 18-627, 2003.

[302] R. A. Schulz and C. Chromey, and Olson,E.N, “Expression of the D-MEF2 transcription in the *Drosophila* brain suggests a role in neuronal cell differentiation,” *Oncogene*, vol. 12, pp. 1827–1831, 1996.

[303] J. A. Ainsley et al., “Enhanced locomotion caused by loss of the *Drosophila* DEG/ENaC protein Pickpocket1,” *Curr. Biol*, vol. 13, pp. 1557–1563, 2003.

[304] J. B. Brown et al., “Diversity and dynamics of the *Drosophila* transcriptome,” *Nature*, 512, 393-399, 2014.

[305] O. and K. Kann and R., “Mitochondria and neuronal activity,” *Am. J. Physiol. Cell Physiol*, vol. 292, pp. 641–657, 2007.

[306] R. L. Davis, “Mushroom bodies and *Drosophila* learning,” *Neuron*, 11, 1-14, 1993.

[307] A. Crocker, X. J. Guan, C. T. and M. Murphy, and M., “Cell-type-specific transcriptome analysis in the *Drosophila* mushroom body reveals memory-related changes in gene expression,” *Cell Rep*, vol. 15, pp. 1580–1596, 2016.

[308] M. Kobayashi et al., “Differential microarray analysis of *Drosophila* mushroom body transcripts using chemical ablation,” *Proc.Nat.Acad.Sci.*, 103, 14417-14422, 2006.

[309] F. Schnorrer et al., “Systematic genetic analysis of muscle morphogenesis and function in *Drosophila*,” *Nature*, vol. 464, no. 7286, Art. no. 7286, Mar. 2010.

[310] B. Silva, N. I. Goles, R. and C. Varas, and J.M., “Serotonin receptors expressed in *Drosophila* mushroom bodies differentially modulate larval locomotion,” *PLoS One*, Feb 2014.

[311] M. Selcho, D. Pauls, K. A. Han, R. F. and T. Stocker, and A. S, “The role of dopamine in *Drosophila* larval classical olfactory conditioning,” in *PLoS One*, 4, e5897, 2009.

[312] S. EL-KHOLY, F. STEPHANO, Y. LI, A. BHANDARI, C. and R. O. E. D. E. R. FINK, and T., “Expression analysis of octopamine and tyramine receptors in *Drosophila*,” *Cell and Tissue Research*, vol. 361, no. 3, pp. 669–684, 2015.

[313] E. S. BROOKS et al., “A putative vesicular transporter expressed in *Drosophila* mushroom bodies that mediates sexual behavior may define a neurotransmitter system,” *Neuron*, vol. 72, no. 2, pp. 316–329, 2011.

[314] A. Noveen, A. and H. Daniel, and V., “Early development of the *Drosophila* mushroom body: the roles of eyeless and dachshund,” *Development*, vol. 127, pp. 3475–3488, 2000.

[315] T. Awasaki et al., “The *Drosophila* trio plays an essential role in patterning of axons by regulating their directional extension,” *Neuron*, 26(1), 119-131, Apr 2000.

[316] D. Pauls, M. Selcho, N. Gendre, R. F. and T. Stocker, and A.S., “*Drosophila* larvae establish appetitive olfactory memories via mushroom body neurons of embryonic origin,” *J. Neurosci*, vol. 30, pp. 10655–10666, 2010.

[317] A. C. and W. Keene and S., “*Drosophila* olfactory memory: single genes to complex neural circuits,” *Nat. Rev.* Neurosci, vol. 8, pp. 341–354, 2007.

[318] G. Udolph, “Notch signaling and the generation of cell diversity in *Drosophila* neuroblast lineages,” *Adv. Exp. Med Biol*, vol. 727, pp. 47–60, 2012.

[319] S. Yoshikawa, R. D. McKinnon, M. and T. Kokel, and J.B., “Wnt-mediated axon guidance via the *Drosophila* Derailed receptor,” *Nature*, 422, 583-588, 2003.

[320] P. Hayward, T. and A. Kalmar, and A.M., "Wnt/Notch signalling and information processing during development," *Development*, vol. 135, pp. 411–424, 2008.

[321] L. Zhong, R. Y. Hwang, and W. D. Tracey, "Pickpocket is a DEG/ENaC protein required for mechanical nociception in *Drosophila* larvae," *Curr Biol*, vol. 20, no. 5, pp. 429–434, Mar. 2010.

[322] H. K. Inagaki, and Anderson,D.J, "Visualizing neuromodulation *in vivo*: TANGO-mapping of dopamine signaling reveals appetite control of sugar sensing," *Cell*, 148, 583-595. 2012.

[323] S. L. Lai, M. R. Miller, and C.Q. Doe, "The Snail family member Worniu is continuously required in neuroblasts to prevent Elav-induced premature differentiation," *Dev. Cell*, 23, 849-857, Oct 2012.

[324] R. Yagi, Y. Mabuchi, M. Mizunami, and N. K. Tanaka, "Convergence of multimodal sensory pathways to the mushroom body calyx in *Drosophila melanogaster*," Scientific Reports, vol. 6, no. 1, Art. no. 1, Jul. 2016.

[325] P. Kielkowski, R. and H. Pohl, "Synthesis of acetylene linked double-nucleobase nucleos(t)ide building blocks and polymerase construction of DNA containing cytosines in the major groove," *J. Org. Chem.*, 76, 9, 3457-3462, 2011.

[326] Y. Liang, J. P. and W. Pitteloud, and S. F, "Hydrogermylation of 5-ethynyluracil nucleosides: formation of 5-(2-germylvinyl)uracil and 5-(2-germylacetyl)uracil nucleosides," *J. Org. Chem.*, 78, 11, 5761-5767, 2013.

[327] I. Ghosh, A. D. and R. Hamilton, and L. Regan, "Antiparallel leucine zipper-directed protein reassembly: application to the green fluorescent protein," *J. Org. Chem.*, 122, 23, 5658-5659, 2000.

[328] W. Huang, B. T. and L. Sherman, and R.A., "Systematic and integrative analysis of large gene lists using DAVID bioinformatics resources," *Nat. Protoc*, vol. 4, pp. 44–57, 2009.

[329] O. Yildirim, "Isolation of nascent transcripts with click chemistry," *Curr. Protoc. Mol. Biol*, vol. 111, pp. 4–24, 2015.

[330] R. C. Spitale et al., “Structural imprints in vivo decode RNA regulatory mechanisms,” *Nature*, 519, 486-490, Mar. 2015.

[331] E. I. Boyle et al., “GO:TermFinder - open-source software for accessing Gene Ontology information and finding significantly enriched Gene Ontology terms associated with a list of genes,” *Bioinformatics*, vol. 20, pp. 3710–3715, 2004.

[332] M. Y. Aboukilila, J. D. Sami, J. Wang, W. England, R. C. Spitale, and M. D. Cleary, “Identification of novel regulators of dendrite arborization using cell type-specific RNA metabolic labeling,” *PLOS ONE*, vol. 15, no. 12, p. e0240386, Dec. 2020.

[333] F. Gao, J. E. Brenman, L. Y. Jan, and Y. N. Han, “Genes regulating dendritic outgrowth, branching, and routing in *Drosophila*,” *Genes & Development*, vol. 13, no. 19, pp. 2549–2561, 1999.

[334] Y. Hattori et al., “Sensory-Neuron Subtype-Specific Transcriptional Programs Controlling Dendrite Morphogenesis: Genome-wide Analysis of Abrupt and Knot/Collier,” *Developmental Cell*, vol. 27, no. 5, pp. 530–544, Dec. 2013.

[335] S. Nainar et al., “An optimized chemical-genetic method for cell-specific metabolic labeling of RNA,” *Nature Methods*, vol. 17, no. 3, Art. no. 3, Mar. 2020.

[336] J. Tomorsky, L. DeBlander, C. G. Kentros, C. Q. Doe, and C. M. Niell, “TU-Tagging: A Method for Identifying Layer-Enriched Neuronal Genes in Developing Mouse Visual Cortex,” *eNeuro*, vol. 4, no. 5, Oct. 2017.

[337] T. Lence et al., “m^6A modulates neuronal functions and sex determination in *Drosophila*,” *Nature*, vol. 540, no. 7632, Art. no. 7632, Dec. 2016.

[338] F. Juge, S. Zaessinger, C. Temme, E. Wahle, and M. Simonelig, “Control of poly(A) polymerase level is essential to cytoplasmic polyadenylation and early development in *Drosophila*,” *The EMBO Journal*, vol. 21, no. 23, pp. 6603–6613, Dec. 2002.

[339] F. Besse, S. L. de Quinto, V. Marchand, A. Trucco, and A. Ephrussi, "*Drosophila* PTB promotes formation of high-order RNP particles and represses oskar translation," *Genes Dev*., vol. 23, no. 2, pp. 195–207, Jan. 2009.

[340] W. B. Grueber, L. Y. Jan, and Y. N. Jan, "Different Levels of the Homeodomain Protein Cut Regulate Distinct Dendrite Branching Patterns of *Drosophila* Multidendritic Neurons," *Cell*, vol. 112, no. 6, pp. 805–818, Mar. 2003.

[341] L. Kan et al., "The m^6A pathway facilitates sex determination in *Drosophila*," *Nature Communications*, vol. 8, no. 1, Art. no. 1, Jul. 2017.

[342] M. I. Love, W. Huber, and S. Anders, "Moderated estimation of fold change and dispersion for RNA-seq data with DESeq2," *Genome Biol*, vol. 15, no. 12, p. 550, Dec. 2014.

[343] E. L. Zajaczkowski et al., "Bioorthogonal metabolic labelling of nascent RNA in neurons improves the sensitivity of transcriptome-wide profiling," *ACS Chemical Neuroscience*, Jun. 2018.

[344] E. C. Olesnicky and D. J. Killian, "The cytoplasmic polyadenylation element binding protein (CPEB), Orb, is important for dendrite development and neuron fate specification in *Drosophila melanogaster*," *Gene*, vol. 738, p. 144473, May 2020.

[345] S. Farris, Y. Wang, J. M. Ward, and S. M. Dudek, "Optimized Method for Robust Transcriptome Profiling of Minute Tissues Using Laser Capture Microdissection and Low-Input RNA-Seq," *Front. Mol. Neurosci*., vol. 0, 2017.

[346] J. Fee, M. Aboukilila, and M. Cleary, "Progenitor-derived ribosomal RNA supports protein synthesis in *Drosophila* neurons," Jul. 2021 (*under review*), preprint available at DOI: 10.22541/au.162523356.62057193/v1

[347] J. Cui, N. shen, Z. Lu, G. Xu, Y. Wang, and B. Jin, "Analysis and comprehensive comparison of PacBio and nanopore-based RNA sequencing of the *Arabidopsis transcriptome*," *Plant Methods*, vol. 16, no. 1, p. 85, Jun. 2020.

[348] K. C. Maier, S. Gressel, P. Cramer, and B. Schwalb, “Native molecule sequencing by nano-ID reveals synthesis and stability of RNA isoforms,” *Genome Res.*, vol. 30, no. 9, pp. 1332–1344, Sep. 2020.

[349] H. L. Drexler, K. Choquet, and L. S. Churchman, “Splicing Kinetics and Coordination Revealed by Direct Nascent RNA Sequencing through Nanopores,” *Molecular Cell*, vol. 77, no. 5, pp. 985-998.e8, Mar. 2020.

[350] B. Linder, A. V. Grozhik, A. O. Olarerin-George, C. Meydan, C. E. Mason, and S. R. Jaffrey, “Single-nucleotide-resolution mapping of m*6*A and m*6*Am throughout the transcriptome,” *Nat Methods*, vol. 12, no. 8, pp. 767–772, Aug. 2015.

[351] V. Pelechano, W. Wei, and L. M. Steinmetz, “Widespread Co-translational RNA Decay Reveals Ribosome Dynamics,” *Cell*, vol. 161, no. 6, pp. 1400–1412, Jun. 2015.